01 Jan 1976

Evaluation of the results of gravity and load tests of c and z purlin roof systems

Teoman Peköz

EVALUATION OF THE RESULTS OF GRAVITY LOAD TESTS OF C AND Z PURLIN ROOF SYSTEMS

by

TEOMAN PEKÖZ, Ph.D.
Structural Engineer

for

THE METAL BUILDING MANUFACTURERS ASSOCIATION
and
THE AMERICAN IRON AND STEEL INSTITUTE

January 1976

TEOMAN PEKÖZ, Ph.D.
Structural Engineer

501 The Parkway
Ithaca, N.Y. 14850

EVALUATION OF THE RESULTS OF GRAVITY LOAD TESTS OF C AND Z PURLIN ROOF SYSTEMS

by

TEOMAN PEKÖZ, Ph.D.
Structural Engineer

for

THE METAL BUILDING MANUFACTURERS ASSOCIATION
and
THE AMERICAN IRON AND STEEL INSTITUTE

January 1976

501 The Parkway *Ithaca, N.Y. 14850*

CCFSS LIBRARY Pekoz, Teoman EVALUATION OF THE
22 3 * 143 RESULTS OF GRAVITY LOAD TESTS OF
c1 C AND Z PURLIN ROOF SYSTEMS

ACKNOWLEDGEMENTS

The preparation of this report and the tests evaluated herein were jointly sponsored by the Metal Building Manufacturers Association and the American Iron and Steel Institute. The author wishes to acknowledge the help of the A.I.S.I.-M.B.M.A. Task group members.

1. INTRODUCTION

The objective of this report is to discuss and interpret the results of two tests on roof purlin assemblies conducted at the Wiss, Janney, Elstner and Associates, Inc. Laboratories.

The results of these two tests are reported in Ref. 1 which will be referred to as "the test report" hereinafter. These tests were conducted as the second phase of the testing program to study the validity and the adequacy of a computer program prepared by the author (Ref. 2). The test conducted in the first phase of this program are described in Ref. 3. The results of the first phase are evaluated and interpreted in Ref. 4. For a general discussion of the behavior the reader is referred to Ref. 4 and the references listed in Ref. 4.

In the first phase, the roof systems were subjected to simulated uplift loading, whereas the second phase involved simulated gravity loading.

In addition to the full scale purlin assembly tests, tests were conducted by Mr. J. H. Peterson of Inryco and the author to determine the rotational restraint parameter F. These tests and their results are also presented in this report.

the case of gravity loading, the bearing of the roof panel on the purlins as well as the relative rotation has to be simulated.

As discussed in Appendix A, reasonable lower limits for the values of F were found to be 0.06 and 0.085 in-lb/in/rad for the Z and C-purlin assemblies, respectively. These values were used in the analyses presented in this report. In addition, values of F equal to 0.09 and 0.120 in-lb/in/rad were used for the Z and C-purlins, respectively, to study the sensitivity of the end results to the value of F. The results of these analyses summarized in Table II will be discussed briefly in Section 3 below.

2.2 ROOF PANEL SHEAR RIGIDITY Q

The reader is referred to References 3 and 4 for a general discussion concerning the shear rigidity. In particular, Sections 3 and 4.1 of Ref. 4 present information on the determination and values of Q.

In agreement with the conclusions of Ref. 4, for Z-purlins, Q was assumed to be 152 k. for the end spans, and 192 k. for the center spans. The value of 152 k. was determined in Test No. 3 illustrated in Fig. 69 of Ref. 3. This test setup was deemed to be more representative of the conditions in an end span where there is no connection at the end between the roof panel and an edge beam (such as a rake channel). The value of 192 k. was found in Test No. 2 illustrated in Fig. 69 of Ref. 3. This setup is expected to simulate the continuity of the roof panels over an intermediate support.

For C-purlins, a large value of Q such as 1000 K. was used as discussed at the end of Section 3 of Ref. 4.

2.3 MATERIAL PROPERTIES

As given in Section 6 of Ref. 3, average yield stress of Z-purlin material is 55.5 ksi. The yield stress of the end span C-purlins is 40.0 ksi. The yield stress of the center span C-purlins is 47.5 ksi.

2.4 END MOMENT COEFFICIENTS FOR PURLINS

As discussed in Refs. 2 and 4, the computer program makes use of the end moment coefficients to account for continuity of the purlins over interior supports. End moment coefficients -0.105 and -0.108 were computed for Z- and C-purlins, respectively, on the basis of a continuous beam analysis doubling the moment of inertia where the purlins are nested or lapped. These values were used in the computer analysis.

The load cells were placed under two of the supports to measure the reactions. The ratios of the reactions are given in Tables 1 and 2 of Ref. 1 for Z- and C-purlins, respectively. It might be noted that the locations for the sensors 67 and 68 of Table 1 appear to be interchanged in Sheet No. 3 of Ref. 1.

It is seen in the tables in question that the ratio, r, of the interior reaction, R_I, to the exterior reaction, R_E, varies considerably depending upon the intensity of loading. The moment coefficient implied by the ratio r can be calculated as follows:

$$wL = 2(R_E + R_I) \qquad 2.1$$

where w is the load per foot of purlin

L is the total of the three span lengths of each purlin (two end and one center spans)

By definition

$$r = \frac{R_I}{R_E} \qquad 2.2$$

and

$$M = Cw\ell^2 \qquad 2.3$$

where M is the interior support moment for an end span

ℓ is the span length of the span for which M is computed

C is the support moment coefficient

Substituting Eq. 2.2 into 2.1

$$R_E = \frac{wL}{2}\,\frac{1}{1+r} \qquad 2.4$$

The support moment is

$$M = \frac{w\ell^2}{2} - R_E\ell \qquad 2.5$$

Using Eqs. 2.3, 2.4 and 2.5, an expression for C can be obtained

$$C = \frac{1}{2}\left[1 - \frac{L}{\ell}\,\frac{1}{1+r}\right] \qquad 2.6$$

For the Z-purlins tested, L = 74.75' and ℓ = 24.875'. A table of C versus r can be made as follows:

r	C
2.30	0.0447
2.35	0.0515
2.40	0.0581
2.50	0.0707
2.75	0.0993

An inspection of Tables 1 and 2 of Ref. 1 leads one to the conclusion that a value of r = 2.35 and hence C = 0.0515 are reasonable average values. These values were used in the analyses that will be described below for both Z- and C-purlins.

Further discussion of the support reactions and the end moment coefficients is given in Section 3.1.

3. PURLIN-ROOF PANEL ASSEMBLY TESTS

In this section the results of the purlin-roof panel assembly tests will be discussed and compared with the analytically predicted results.

The locations of the stress and deflection measuring devices are given in Figs. 1a, 1b for Z-purlins and in Figs. 16a, 16b for C-purlins. Figures 2a through 15b give the results on Z-purlins and Figs. 17a through 26b give results on C-purlins.

In the figures presenting the results, the test observations are shown as test points joined by solid lines. These figures are taken from Ref. 1. The computed predictions are superposed on the test results as dashed or dot-dashed lines. In the figures presenting stress data yield stress of the particular purlin material is shown by dotted vertical lines.

The computations for each case were carried out on the basis of full continuity of the purlins over the support and on the basis of the support reactions measured by means of the load cells. The measured support reactions (for r = 2.35 as defined in Eq. 2.2) lead to a moment coefficient of -0.0515

over the interior supports. The figures with "a" designation (such as Fig. 2a) present the results of computations based on full continuity, whereas figures with "b" designation (such as Fig. 2b) contain the results of computations based on r = 2.35.

3.1 REACTIONS AND MOMENT COEFFICIENTS

As described earlier, the reactions were measured at two of the supports by means of load cells. The pressure under the test setup was measured by means of a water manometer. The pressure was also computed on the basis of load cell readings. The pressures computed in these two different ways are tabulated in Tables 1 and 2 of Ref. 1. In these tables it is seen that the difference between the two pressures determined is up to 22.2% (of the pressure determined by the manometer) for the Z-purlin test and up to 18.3% for the C-purlin test during early cycling of the load. In the final cycle of loading the differences were up to 12.3 and 15.6% for the Z- and the C-purlin tests.

In Ref. 1, all the plots were drawn on the basis of pressures computed from the values of reactions determined by load cells. Therefore, the test plots do include whatever (experimental) error might be present in the load cell values.

As discussed in Section 2.4, on the basis of the load cell readings given in Tables 1 and 2 of Ref. 1, an average value of the ratio (r) of the interior reaction to the exterior reaction is seen to be about 2.35. This value of r leads to an end moment coefficient of -0.0515. As will be discussed below, the

observed deflection and stress values seem to indicate a higher value of the end moment coefficient and hence a higher value of the ratio r.

A simple calculation made on the basis of Section 2.4 indicates that the value of the end moment coefficient is quite sensitive to the value of the reactions. For example, if there is an error of

$$100 \times [(2.5 - 2.35)/2.35] = 6.4\%$$

in the value of r, then the resulting error in the end moment coefficient is

$$100 \times [(0.0707 - 0.0515)/0.0515] = 37.3\%.$$

Therefore, on the basis of the correlation between the manometer and the load cell readings and on the basis of the above calculation, it appears that an intermediate value of the end moment coefficient between 2.35 and 2.75 is quite possible.

An indication of the value of the end moment coefficient and the ratio r can be obtained from the relative angular displacements of the purlins at the intermediate supports. Since the deformation of the purlins around the supports is quite complex, the relative angular rotation of the purlins with respect to each other can only be determined in an approximate manner from the sensors that were placed at the purlin ends. These sensors were numbered 77-78, 79-80, 81-82, 87-88, 89-90, 99-100 in the Z-purlin test and 60-61, 62-63, 64-65,

70-71, 72-73, 82-82 in the C-purlin test. The relative angular rotation θ_i in radians can be found by dividing the difference of the readings of each pair of sensors by the distance between the sensors.

The relative rotation θ_i is assumed to take place under load. The sensor readings are quite small and are not in precise agreement at each similar location they were used. As mentioned above, the readings are to obtain only an approximate estimate of the value of θ_i. Therefore, some simplifying assumptions will be made in the derivation of the expressions for various parameters in terms of θ_i. It will be assumed that the center spans and the end spans are equal in length. The purlins will be assumed to be of equal moment of inertia throughout; namely, the effect of the double section will be ignored (leading to a 5% error in the case of Z-purlins). It will also be assumed that the end moment is determined by the beam type deflections; namely the effect of twisting will be ignored.

The end moment for partial continuity due to relative rotation θ_i can be written as

$$M_{op} = \frac{W\ell}{10} - \frac{12EI\theta_i}{10L} \qquad (3.1)$$

where I is the moment of inertia

ℓ is the span length

W is the total load on the span in question

For full continuity, $\theta_i = 0$ and the above equation leads to the correct expression of $M_o = W\ell/10$.

The interior support reaction R_I and the exterior support reaction R_E can be written as follows:

$$R_I = W + M_{op}/\ell \tag{3.2}$$

$$R_E = W/2 - M_{op}/\ell \tag{3.3}$$

Thus the ratio r can be written as

$$r = R_I/R_E \tag{3.4}$$

$$= (1 + \beta)/(0.5 - \beta) \tag{3.5}$$

where

$$\beta = M_{op}/WL \tag{3.6}$$

β can also be written in terms of θ_i as

$$\beta = 0.1 - \alpha \tag{3.7}$$

where

$$\alpha = 1.2\ EI\theta_i/W\ell^2 \tag{3.8}$$

Thus r can be written in terms of α as

$$r = (1.1 - \alpha)/(0.4 + \alpha) \tag{3.9}$$

For the Z-purlin test for a load of 58 psf the following are the values of various parameters:

$W = 4.64$ k.

$I = 10.27$ in^4

$\ell = 300$ in.

Thus

$$\alpha = 0.8853\ \theta_i$$

Similarly, using the above equations θ_i can be expressed in terms of r as

$$\theta_i = (1.1 - 0.4r)/[0.8853(r + 1)]$$

Using the expression for r in terms of α and hence θ_i and using the values of θ_i obtained from the sensor readings as described above, the following table can be made. The values are for the Z-purlin test for a load of 58 psf.

Sensor	θ_i (rad)	r
99-100	0.0110	2.66
81-82	0.0034	2.72
87-88	0.0036	2.72
79-80	0.0050	2.71
77-78	0.0075	2.69

For a value of r = 2.35, θ_i = 0.054 rad. which is not in the range of values of θ_i that were measured.

For the C-purlin test the following values of θ_i can be computed for a load of 57.2

Sensor	θ_i (rad)
60-61	0.008
62-63	0.004
64-65	0.007
70-71	0.011
72-73	0.006
82-82	0.005

The expressions for the C-purlin test become quite complicated due to the fact that the center and the end span purlins have different moments of inertia. If, for purposes of general

comparison, the Z-purlin expressions are assumed to be valid for C-purlin tests, then if r = 2.35, θ_i = 0.054 rad as before. The values of θ_i observed above are much smaller than the value of θ_i for r = 2.35. Therefore a value of r close to 2.75 or the fully continuous case is expected for C-purlins as well.

Further comments on the values of r will be made while evaluating the test results relating to the deflections and the stresses.

3.2 DEFLECTIONS AND TWIST ANGLES

As stated in Ref. 1, the vertical deflections were measured optically by means of a level and scales placed at the points where deflections were desired. The deflections measured in this manner are expected to be quite reliable.

The horizontal deflections and the twist angles were measured by means of electrical potentiometers mounted upon stands and contacting the purlins at the tip of the plunger. Due to the nature of the loading the potentiometers and their stands were under the test assembly and hence were not visible. Throughout the tests, at various load increments the test assembly has contacted the potentiometer stands. As will be discussed below, this could have impaired the accuracy of the readings. Furthermore, the contact and the friction between the tip of the plungers and the purlins might have contributed to some inaccuracies.

3.2.1 VERTICAL DEFLECTIONS

The vertical deflections are plotted in Figs. 2 through 4 for the Z-purlin test and in Figs. 17 through 20 for the C-purlin test.

The predicted curves given in figures designated as "a" (such as 2a) where full continuity was assumed with those designated as "b" (such as 2b) where partial continuity with r = 2.35 was assumed are to be compared. It is seen that the observed curves fall between the two predictions. The observed curves are quite close to the curves drawn based on the assumption of full continuity. The observed results for the C-purlins are closer to the predicted results based on full continuity than those for the Z-purlins. This leads to the conclusion that the C-purlins were closer to being fully continuous than the Z-purlins were.

For the center spans the assumption of full continuity leads to the prediction of upward deflections at midspan. The observed downward deflection is due to partial continuity.

The above discussion supports the conclusion regarding the moment coefficients and r presented in Section 3.1 above.

3.2.2 LATERAL DEFLECTIONS AND TWIST ANGLES

As discussed in the beginning of this section (Section 3.2), difficulties were experienced in measuring lateral deflections and twist angles.

The observed and the predicted results are presented in Tables V and VI for Z- and C-purlins, respectively. The

following conclusions can be drawn from an inspection of the observed results.

In general, the values obtained for the same loading in different load cycles vary very significantly and quite often by an order of magnitude. Sometimes even the direction of the deflection is changed. For example, in Table V-A for lateral deflections in the Z-purlin test, sensors 71-72 indicate a value 0.1066 in. during the first load cycle at 10.4 psf loading. The same sensors indicate a value of 0.0153 in. during the third load cycle at 10.4 psf loading.

Again in general the sensors at four similar points (such as 10 feet from the end support of each of the four end spans) in the same load cycle and at the same load give results that differ significantly and quite often by an order of magnitude. For example, again in Table V-A at load step no. 18 at a load of 42.1 psf, the four pairs of sensors at similar locations indicate values of 0.1201, 0.0373, 0.0194 and 0.0524.

In view of the above general observations regarding the reliability of the experimental results, it is not possible to make a meaningful comparison of the observed and the predicted values.

3.3 STRESSES

The observed and the computed stresses are plotted in Figs. 5 through 15 for Z-purlins and in Figs. 21 through 27 for C-purlins. As in the case of deflections the test points are joined by solid lines and the computed results are shown by

dashed and dot-dashed lines. The yield stresses for the purlin in question are shown as dotted vertical lines. Again as in the case of deflections, stresses computed on the basis of full continuity are plotted in figures designated "a", whereas the stresses computed on the basis of r = 2.35 are given in figures designated "b".

The stresses were measured at points about 1/2 in. away from the tips of the stiffening lips or at some distance from the end of the rounded portion of the corners (at 1/2 in. from the web of the section as shown in Figs. 1 and 16). The stresses are computed on the basis of sharp corners and at the corners and at the tips of stiffening lips. The stresses at the points where strain gages were applied were obtained by an approximate interpolation from the stresses at the corners and the tips.

Each figure is designated by a three letter code immediately following the figure number. As explained in Tables III and IV this designation indicates the general location of the section. The particular location is designated by the location numbers which are shown in Figs. 1a and 16a for Z- and C-purlins, respectively.

It should be noted that stresses in excess of the yield stress of the material plotted for the test results are not, in general, possible. They should be interpreted as the observed strain multiplied by the modulus of elasticity. The computed results were based on unlimited elasticity. The yield stress indicated by the dotted lines should be assumed to be the limiting values of the stresses.

3.3.1 STRESSES AT 10 FT. FROM THE END SUPPORT OF THE END SPANS

The stresses at 10 ft. from the end support of the end spans are given in Figs. 5 through 8 for the Z-purlins and in Figs. 21 through 23 for the C-purlins.

For both types of purlins, it is seen that the stresses computed on the basis of full continuity agree well within the test results. An excellent correlation is expected if partial continuity with an r value between 2.6 to 2.7 were used. An estimate of the r value most pertinent can be made by comparing the curves for r = 2.75 (full continuity) and r = 2.35. It is seen in some of the figures that as the load increases lowered values of r would lead to an exact correlation; this seems to support the possibility of the angular rotation of the two lapped purlins relative to each other under loading and hence lowering of the value of r.

In the plots for the Z-purlins, it is seen that at the last load increment when readings were taken, the stresses were very close to but below the yield stress of the material. Extrapolating the results of the last few load increments to the load increment aimed at but not reached, it is seen that yielding was expected. In particular at locations 11 and 19 (Figs. 7 and 8) yielding of the purlins must have taken place at failure.

In the plots for the C-purlins, at almost every section at the location being discussed yielding was reached at two or more load increments before the last load increment. It is seen that

the C-purlins had considerable load carrying capacity above the yield load.

3.3.2 STRESSES NEAR THE LAPPED REGION IN THE END SPAN

The stresses at a half inch away from the lapped region in the end spans are plotted in Figs. 9 and 10 for the Z-purlin test and in Figs. 24 and 25 for the C-purlin test.

Observations similar to those made in Section 3.3.1 can also be made here. In the case of the C-purlins, it is seen that yielding has started at the location described in Section 3.3.1 and subsequently yielding took place in the section discussed here.

3.3.3 STRESSES AT AN INTERMEDIATE SUPPORT

The stresses at an intermediate support were measured in the Z-purlin test. They are plotted in Figs. 11 and 12. Sensor No. 8 in Fig. 11 appears to be defective.

The computer program (Ref. 2) determines the stresses for a single section over the support. Since there are two purlins over the support, the values determined by the computer program of Ref. 2 were divided by two. General conclusions similar to those made in Section 3.3.1 may also be drawn here except the fact that at this location the stresses were not near yield stress of the material.

3.3.4 STRESSES NEAR THE LAPPED REGION IN THE CENTER SPAN

The stresses at a half inch away from the lapped region in the center spans are given in Figs. 13 and 14 for the Z-purlins and in Fig. 27 for the C-purlins.

In these figures it is seen that an analysis that assumes close to full continuity would lead to either very close or conservative correlation with the test results depending upon the point in the cross-section where the stress is determined.

3.3.5 STRESSES AT MIDSPAN OF CENTER SPAN

The stresses at midspan of center spans are plotted in Fig. 15 for Z-purlins and in Fig. 26 for C-purlins.

In these figures it is seen that an analysis that assumes close to full continuity would lead to results in fairly good agreement with the test results.

3.4 STRAP FORCES

The Z-purlins are connected to the supporting frame on one flange and the roof panels are connected to the purlins on the other flange. Thus the loading being applied by the roof panels has a moment about the point of connection of the purlin to the supporting frame. In the actual roof systems this moment may be balanced by the details of construction. In the test setup the moment in question had to be balanced at the support points by 16 gage steel straps (2 in. wide) as shown in Figs. 1 and 16.

This problem is minor or nonexistent in C-purlins. The load applied by the roof panels is either in line or close to being in line with the reaction between the purlins and the supporting frame.

The forces in the steel straps were measured by means of strain gages applied on each face of the straps. The use of

pairs of strain gages eliminates the stresses due to bending and gives a reading of the average axial strains in the straps.

In the Z-purlin test, the strain gage (or sensor) pairs 59-60 and 65-66 were applied to the straps at the end supports and the pairs 61-62 and 63-64 were at the intermediate supports.

The following table gives some of the axial forces computed from the strain values given in Appendix A of Ref. 1.

Test Increment No.	Load (psf)	Axial Force (lbs)			
Sensor No.		59-60	61-62	63-64	65-66
17	36	162	1204	607	270
21	58	306	2376	1084	675

As can be observed in the above, the force in the straps varies considerably (compare 2376 and 1084 for the intermediate support straps and 306 and 675 for the end support straps). The ratios of the strap forces for the two load increments also vary (for example 1084/607 = 1.79 and 675/270 = 2.5).

The vertical components of the forces for the 58 psf loadings, namely, 306 lbs, 2376 lbs, 1084 lbs and 675 lbs can be found by geometry to be 45 lbs, 348 lbs, 154 lbs and 99 lbs, respectively. The interior and exterior support reactions (R_I and R_E) can be found on the basis of r = 2.65 and ignoring the effect of strap forces.

Load (psf)	R_E (lbs)	R_I (lbs)
36	1187	3146
58	1913	5069

It is seen in the above table that the vertical components of the strap forces are rather small compared to the expected reactions.

A table for the strap forces in the C-purlin test can be prepared in the same manner as above.

Sensor No.	Test Increment No.	Load (psf)	Axial Force (lbs)			
			41-42	43-44	45-46	47-48
	64	41.6	22	11	7	-
	67	57.2	31	5	-25	-
	73	57.2	7	5	-14	11
	76	72.8	-7	-40	-302	5

In the above table it is seen that the strap forces are quite small and hence inconsequential for the C-purlins.

3.6 SENSITIVITY OF THE COMPUTED RESULTS TO THE VALUE OF F

In the computations discussed above a reasonable lower limit for vlaues of F were used. In a separate series of analyses, in order to study the sensitivity of the results to the value of F, higher values (1.5 and 1.4 times the lower limit values) were used for Z- and C-purlins. A comparison of the results for the lower and the higher values of F is presented in Table II.

It is seen in Table II that the results on C-purlins are more sensitive to the value of F. The vertical deflections are not affected by the value of F. The value of the twist angle is the most affected result. The stresses are influenced to a

rather small degree by a variation in the value of F. Therefore, the use of a conservative value of F would not, in terms of stresses, lead to results that are too conservative.

3.7 FAILURE MODES AND PREDICTION OF FAILURE

As stated in the test report (Ref. 1), in the Z-purlin test a series of roof panel buckles were observed at 33.36 psf. However, the load could be increased in excess of 58 psf. Though the purlins reached yielding, overall collapse of the purlins did not take place. The buckling of the roof panels might have introduced some additional membrane forces on the purlins. These membrane forces might have influenced the behavior of the roof system. A study of the stress plots indicate that the first yielding took place at 10 feet from the end supports (as discussed in Section 3.3.1). The ultimate condition was caused by the extensive buckling of the roof panels.

The correlation of the observed and the computed stresses and the vertical deflections have served to verify the validity of the theory and the computer program used. The test, however, did not show what post-yielding reserve load carrying capacity, if any, the Z-purlins have.

In the C-purlin test the initial yielding took place again at 10 feet from the exterior support of the end spans (as discussed in Section 3.3). The collapse load was significantly higher than the initial yield load. The correlation between the predicted and the observed vertical deflections and stresses is quite satisfactory. However, more work needs to be done to

determine the inelastic reserve load carrying capacity of purlins.

4. RECOMMENDED FUTURE STUDIES

A list of recommended future studies was given in Ref. 4. Some of those recommendations are strongly supported by the findings of the present study. These are:

a. Continuity of Purlins over a Nested or Back-to-Back Lapped Connection

In both the uplift and gravity loading tests to date less than full continuity has been observed over the intermediate support. The degree of continuity plays an important role in determining the stresses and vertical deflections.

Because of the complex nature a full scale test setup and the complexity of the behavior of a lapped joint, this problem would best be studied on a smaller scale using segments of the actual purlins.

b. Ultimate Behavior (Failure Loads) of C- and Z-Purlins

In the gravity loading tests, the C-purlins appeared to have significant post yielding reserve strength. Such information could not be obtained for Z-purlins. In the uplift tests of Refs. 3 and 4, collapse occurred before yielding as a result of local buckling. Though the computer program of Ref. 2 gives good estimate of the behavior up to initial yielding, more work is needed to be able to determine the ultimate load carrying capacity.

Again this problem can be studied without resorting to full scale testing. Tests on a small scale would be satisfactory. The results of a recent study at Cornell University under the direction of the author shall be useful in this study. The additional work will be on the influence of the interaction of the flexural and torsional stresses on the ultimate behavior.

c. Allowable Lateral Deflection and Twist Angle

Criteria for the allowable values of the lateral deflections and twist angles, similar to the existing criteria for vertical deflection, need to be considered by the industry. Based on the actual field experiences of the manufacturers, a criteria can be established as to what magnitude of these distortions are undesirable.

d. Load and Distortion Capacity of Purlin-to-Roof-Panel Connections

This recommendation was essential for uplift loading. The pull-over failure implied in this study is not, of course, critical in the case of gravity loading.

5. SUMMARY AND CONCLUSIONS

A test setup for determining F for the case of gravity loading was developed and used.

With proper consideration of the continuity over an interior support, the test results for stresses and vertical deflections are in good general agreement with the computed

results. The magnitudes of the observed twist angles and lateral deflections appear unreliable in accuracy and hence could not be compared with the test results.

The recommended future studies include the extent of continuity over an interior support and the ultimate load carrying capacity of C- and Z-sections.

REFERENCES

1. Guedelhoefer, O. C. and Linehan, P. W., "Gravity Load Tests of C and Z Purlin Roof Systems", Wiss, Janney, Elstner and Associates Report, Northbrook, Illinois, July 14, 1975.

2. Peköz, T., "Diaphragm Braced Channel and Z-Section Purlins", Report, 501 The Parkway, Ithaca, N.Y., September 30, 1973.

3. Peköz, T., "Continuous Purlin Tests", Report, Department of Structural Engineering, Cornell University, Ithaca, N.Y., November, 1974.

4. Peköz, T., "Evaluation of the Results of Continuous Purlin Tests", Report, 501 The Parkway, Ithaca, N.Y., January 1975.

APPENDIX A

DETERMINATION OF ROTATIONAL RESTRAINT F FOR THE CASE OF GRAVITY LOADING

A1. TEST SETUP

The test setup is illustrated in Fig. A1. The purlin was welded to a hot rolled channel and to a base at frequent intervals to minimize the distortion of the purlin web and the distortion of the angle between the lower flange and the web. The hot rolled channel was also welded at frequent intervals to a rigid base which was a massive block of pig iron.

The deflections were measured by means of dial gages at three points on each side. These points were at the midpoints of the valleys.

Loading was by means of cast iron bricks each weighing 26 lbs. They were placed along the direction of the purlins on the (narrow) crests of the panels. The balanced load of two bricks per foot corresponds to a uniform gravity load of (2×26/5 =) 10.4 psf if the purlins are spaced 5 feet apart.

A2. TEST PROCEDURE

The following test procedure was used:

1. Take zero readings of the dial gages with $P_1 = P_2 = 3\times26 =$ 78 lbs (refer to Fig. A1).
2. Add one brick on one side, thus, $P_1 = 78$ lbs and $P_2 = 4\times26 =$ 104 lbs. and take dial gage readings. (In the tests conducted, the readings for the dial gages on the larger load side were taken).

3. Remove the extra brick added in Step 2. Take zero readings of the dial gages.
4. Add one brick opposite the side with the additional brick in Step 2. Thus with P_1 = 104 lbs and P_2 = 78 lbs, take dial gage readings.

A3. COMPUTATION

The average of the deflections observed in Steps 1 and 2 and the average of the deflections observed in steps 3 and 4 are used to compute two different values of the rotational restraint factor F. The rotational restraint F can be defined as

$$F = \frac{\bar{M}}{\theta} \tag{A.1}$$

where $\bar{M}$ is the twisting moment per unit length of purlin in the case of full scale roof assembly and the moment due to the unbalanced load in the case of the test setup of this appendix. For the case of the loading and the setup used in this investigation $\bar{M}$ can be written as

$$\bar{M} = \frac{|P_2-P_1|\ell}{1000w} \tag{A.2}$$

where $|P_2-P_1|$ is the absolute value of P_2-P_1. P_2 and P_1 are in lbs and are shown in Fig. A1 (26 lbs in the tests conducted)

ℓ is the moment arm of the unbalanced load $|P_2-P_1|$ in inches (12 in. in the tests conducted)

w is the total width of the panel subjected to the unbalanced load in inches (36 in. in the tests

conducted). It is expected that the distance between the end screws and the ends of the panel (in the direction of the purlin) is one-half the spacing of the screws.

1000 is used to convert the units of $\bar{M}$ into k-in/in.

For the tests conducted $\bar{M}$ is equal to 0.0867 k-in/in.

In Eq. A1, θ is the angle of rotation of the roof panel and can be computed from the average deflections δ as

$$\theta = \frac{\delta}{\ell_1} \tag{A.3}$$

where ℓ_1 is the distance to the dial gages from the screws (12 in. in the tests conducted).

A4. RESULTS AND DISCUSSION

Tests were conducted by the author on Z-purlin-roof panel assemblies using the setup and the procedure described above. The value of F obtained appears to be very sensitive to the distortions of the web. Without the web support recommended here, the distortion of the web becomes much more severe than that would be expected in an actual roof system. The value of F was also sensitive to the location of the screws on the flange. This is expected to be the primary reason for obtaining two significantly different values of F (0.16 and 0.06 k-in/in-rad) depending on whether P_1 or P_2 is greater (Fig. A1). The lower value is thought to be a reasonable lower limit for F and is used in the evaluation of the Z-purlin test.

Using the same procedures, Mr. J. H. Peterson of Inryco has conducted tests on C-purlin-roof panel assemblies. He has obtained a lower limit of F = 0.085 k-in/in/rad. It may be noted that the roof panels used by him were those used in the C-purlin test. Different roof panels were used in C- and Z-purlin tests.

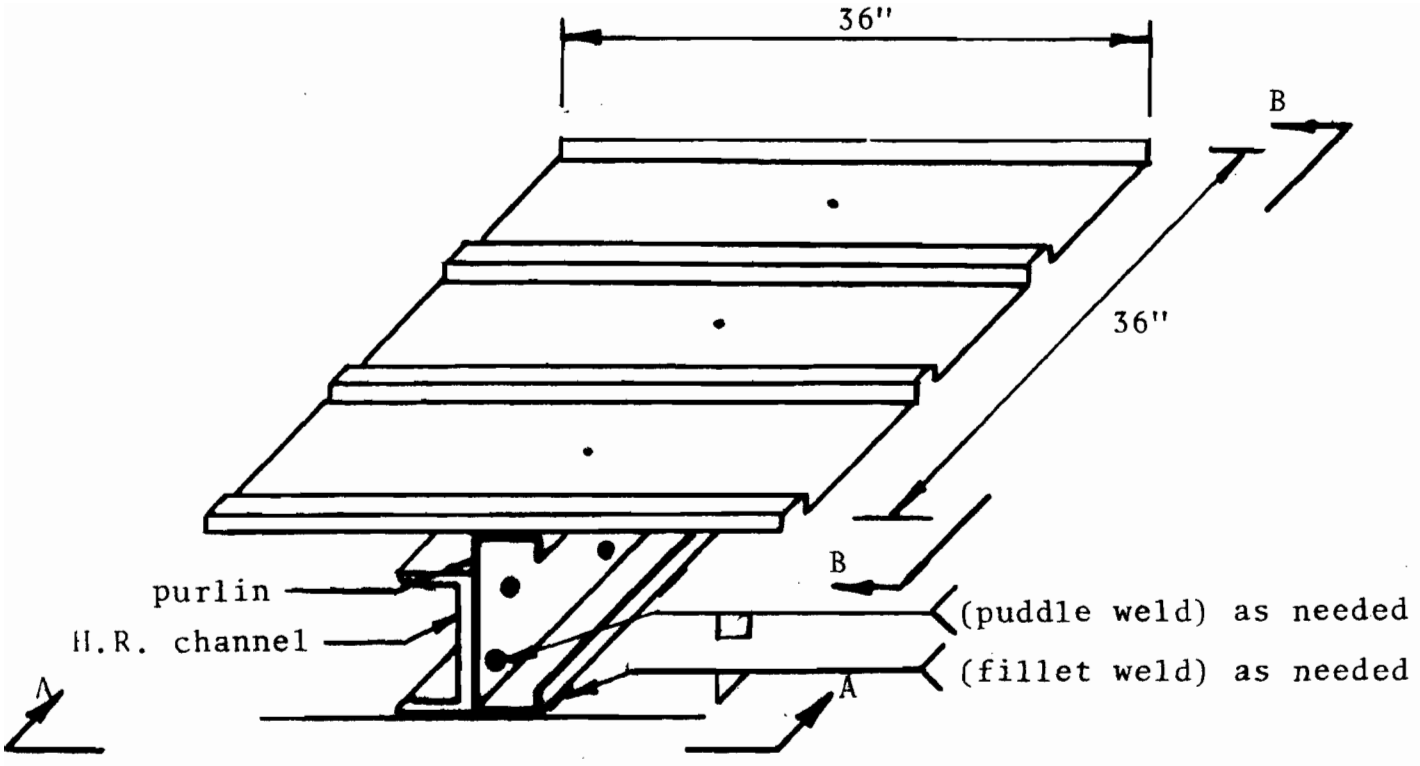

Overall view of the test setup

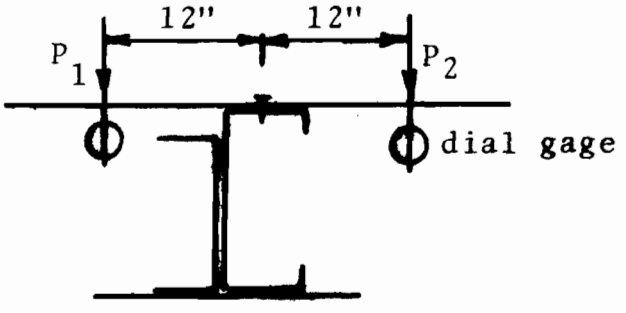

(Note: P_1 and P_2 are uniformly distributed)

View A-A

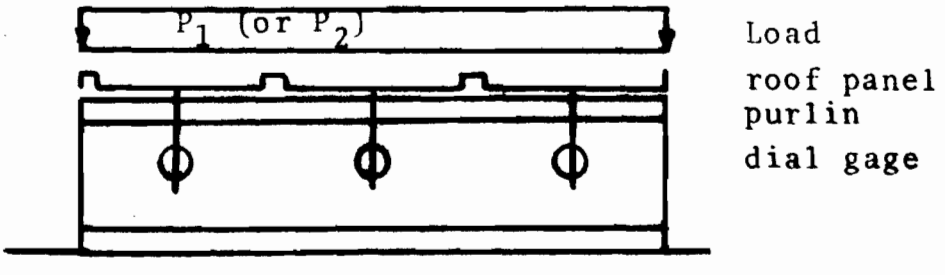

View B-B

Fig. A1 Test setup to determine F. (Gravity Load)

TABLE I

SUMMARY OF PARAMETERS
OF ANALYSIS USED

Purlin Type	Location	F in-lb/in/rad	Q k.	Screw in.	COEFL	COEFR
Z	End Span	0.06	152.0	0.875	0.0	-0.105
"	" "	"	"	"	"	-0.0515
"	" "	0.09*	"	"	"	-0.105
"	" "	"	"	"	"	-0.0515
"	Center Span	0.06	192.0	"	-0.105	-0.105
"	" "	"	"	"	-0.0515	-0.0515
"	" "	0.09*	"	"	-0.105	-0.105
"	" "	"	"	"	-0.0515	-0.0515
C	End Span	0.085	1000.0	1.375	0.0	-0.108
"	" "	"	"	"	"	-0.0515
"		0.120*	"	"		-0.108
"		"	"	"		-0.0515
"	Center Span	0.085	"	"	-0.108	-0.108
"	" "	"	"	"	"	-0.0515
"	" "	0.120*	"	"	"	-0.108
"	" "	"	"	"	"	-0.0515

* not plotted but used in Table II.

TABLE II

SENSITIVITY TO THE VALUE OF F
Expressed as % Difference*

Section	Location	Parameter		
		PHI (max)	U (max)	STRM (max)
Z	End Span	21	3	<1
Z	Center Span	22	4	<1
C	End Span	22	22	8
C	Center Span	25	25	4

* % Difference = $[(P_2 - P_1)/P_1] \times 100$

where P is the parameter in question

P_1 is P computed for F = 0.06 in-lb/in/rad if section is Z or P computed for F = 0.085 in-lb/in/rad if section is C

P_2 is P computed for F = 0.09 in-lb/in/rad if section is Z or P computed for F = 0.12 in-lb/in/rad if section is C

For purposes of this table, full continuity end moment coefficients were used.

TABLE III

Z-PURLIN TEST
FIGURE, LOCATION DESIGNATIONS

Fig. No.	Location Designation[1]	Location No.[2]	Sensor Nos.[2]
5	ZEM	1	1-3
6	"	9	25-27
7	"	11	30-32
8	"	19	56-58
9	ZEL	2	4-7
10	"	8	23-24
11	ZIS	3	8-9
12	"	7	21-22
13	ZCL	4	10-13
14	"	17	17-20
15	ZCM	5	14-16

1. ZEM - Z-purlin, end span, 10 ft. from end support
   ZEL - Z-purlin, end span, just outside the lapped portion
   ZIS - Z-purlin, at intermediate support
   ZCL - Z-purlin, just outside the lapped portion, center span
   ZCM - Z-purlin, center span mid-span

2. As given in Fig. 1a.

TABLE IV

C-PURLIN TEST
FIGURE, LOCATION DESIGNATIONS

Fig. No.	Location Designation[1]	Location No.[2]	Sensor Nos.[2]
21	CEM	1	1-5
22	"	6	23-27
23	"	9	18-22
24	CEL	2	6-8, 49
25	"	5	29-31
26	CCM	3	36-40
27	CCL	4	32-35

1. CEM - C-purlin, end span, 10 ft. from end support
   CEL - C-purlin, end span, just outside the lapped portion
   CCM - C-purlin, center span, mid-span
   CCL - C-purlin, just outside the lapped portion, center span

2. As given in Fig. 16a.

TABLE V-A

Z-PURLIN TEST

LATERAL DEFLECTIONS

AT 10 FEET FROM THE END SUPPORTS OF THE END SPANS

Sensor No.	TEST NO.	LOAD PSF.	Observed 71-72	93-94	73-74	95-96	Computed F = 0.06 in-lb/in/rad	F = 0.09 in-lb/in/rad
2		5.2	0.0784	0.0433	-0.0744	-0.0470		
3		10.4	0.1066	0.0526	-0.0930	-0.0517		
5		5.2	0.0882	0.0401	-0.0827	-0.0434		
6		15.6	0.1362	0.0522	-0.1071	-0.0443		
7		20.8	0.1582	0.1051	-0.1118	-0.0906		
8		26.0	0.2686	0.7114	-0.1876	-0.6801		
11		5.2	0.0074	0.0059	-0.0054	0.0857	0.04	0.03
12		10.4	0.0153	0.0041	-0.0044	-0.0051		
13		15.6	0.0252	0.0020	0.0044	0.0040		
14		20.8	0.0342	-0.0044	0.0113	0.0127	0.13	0.10
15		26.0	0.0508	-0.0061	0.0150	0.0270		
16		31.2	0.0716	0.0235	0.0196	0.0104		
17		36.4	0.0979	0.0269	0.0167	0.0201		
18		42.1	0.1201	0.0373	0.0194	0.0524		
19		47.3	0.1363	0.0392	0.0468	0.0867	0.23	0.19
20		55.1	0.1582	0.0000	0.1192	0.0000		
21		58.2	0.1647	0.0000	0.0000	0.0000	0.29	0.25

TABLE V-B

Z-PURLIN TEST
TWIST ANGLES
AT 10 FEET FROM THE END SUPPORTS OF THE END SPANS

Sensor No.	TEST NO.	LOAD PSF.	Observed ANGLE DEG. 71-72	Observed ANGLE DEG. 93-94	Observed ANGLE DEG. 73-74	Observed ANGLE DEG. 95-96	Computed F = 0.06 in-lb/in/rad	Computed F = 0.09 in-lb/in/rad
2		5.2	0.10	-0.10	0.09	0.02		
3		10.4	0.39	0.02	0.02	0.09		
5		5.2	0.02	-0.08	0.07	0.05		
6		15.6	0.54	0.15	-0.02	0.10		
7		20.8	0.84	0.06	-0.03	0.37		
8		26.0	1.03	-1.63	0.19	2.59		
11		5.2	0.23	0.02	-0.15	3.99	-0.19	-0.14
12		10.4	0.49	0.15	-0.19	-0.04		
13		15.6	0.76	0.21	-0.22	0.04		
14		20.8	0.95	0.28	-0.23	0.05	-0.55	-0.42
15		26.0	1.24	0.28	-0.17	0.10		
16		31.2	1.46	0.14	-0.11	0.53		
17		36.4	1.52	0.08	0.07	0.81		
18		42.1	1.73	-0.17	0.45	1.12	-0.69	-0.54
19		47.3	1.77	-0.28	1.00	0.95		
20		55.1	2.18	0.00	1.62	0.00		
21		58.2	2.22	0.00	0.00	0.00	-0.55	-0.44

TABLE V-C

Z-PURLIN TEST
TWIST ANGLES
MIDSPAN OF CENTER SPAN

Sensor No.	TEST NO.	LOAD PSF.	Observed ANGLE DEG. B5-B6	Observed ANGLE DEG. B3-B4	Computed F = 0.06 in-lb/in/rad	Computed F = 0.09 in-lb/in/rad
	2	5.2	-0.34	0.65		
	3	10.4	-0.84	1.09		
	5	5.2	-0.34	0.50		
	6	15.6	-1.25	1.58		
	7	20.8	-1.64	2.24		
	8	26.0	-1.32	4.06		
	11	5.2	-0.52	0.71	-0.14	-0.11
	12	10.4	-1.02	1.28		
	13	15.6	-1.33	1.82		
	14	20.8	-1.63	2.31		
	15	26.0	-1.96	2.87	-0.49	-0.39
	16	31.2	-2.16	3.32		
	17	36.4	-2.38	3.83		
	18	42.1	-2.66	4.60		
	19	47.3	-2.77	4.86	-0.85	-0.67
	20	55.1	-2.87	5.61		
	21	58.2	-3.24	5.68	-1.02	-0.80

TABLE V-D

Z-PURLIN TEST
LATERAL DEFLECTIONS
MIDSPAN OF CENTER SPAN

Sensor No.	TEST NO.	LOAD PSF.	Observed 85 86	Observed 83-84	Computed F = 0.06 in-lb/in/rad
	2	5.2	-0.1171	0.1256	
	3	10.4	-0.1768	0.1954	
	5	5.2	-0.1063	0.1175	
	6	15.6	-0.2127	0.2418	
	7	20.8	-0.2847	0.3333	
	8	26.0	-0.6792	0.6398	
	11	5.2	-0.0524	0.0636	0.03
	12	10.4	-0.0911	0.1145	
	13	15.6	-0.1210	0.1579	
	14	20.8	-0.1404	0.1933	0.11
	15	26.0	-0.1571	0.2322	
	16	31.2	-0.1735	0.2635	
	17	36.4	-0.1876	0.2966	
	18	42.1	-0.2079	0.3466	0.21
	19	47.3	-0.2281	0.3886	
	20	55.1	-0.2537	0.4585	
	21	58.2	-0.3087	0.5073	0.28

TABLE VI-A

C-PURLIN TEST
LATERAL DEFLECTIONS
AT 10 FEET FROM THE END SUPPORTS OF THE END SPANS

Sensor No.	TEST NO.	LOAD PSF.	Observed 76-77	54-55	78-79	56-57	Computed F = 0.085 in-lb/in/rad	F = 0.120 in-lb/in/rad
	52	5.2	-0.0462	-0.0474	-0.0466	-0.0493		
	53	10.4	-0.0866	-0.0951	-0.0829	-0.0997		
	54	15.6	-0.1201	-0.1372	-0.1164	-0.1367		
	55	20.8	-0.1648	-0.1912	-0.1518	-0.1840		
	56	26.0	-0.2168	-0.2412	-0.2337	-0.2398		
	57	31.2	-0.2539	-0.2823	-0.2745	-0.3049		
	59	10.4	-0.0860	-0.0824	-0.0650	-0.0897	-0.23	-0.18
	60	20.8	-0.1647	-0.1586	-0.1217	-0.1602		
	61	26.0	0.2986	-0.1879	-0.1356	-0.1663	-0.55	-0.42
	62	31.2	-0.2554	-0.2327	-0.1989	-0.2417		
	63	36.9	-0.3412	-0.2925	-0.2627	-0.3248		
	64	41.6	-0.4277	-0.3320	-0.3346	-0.4620		
	65	47.3	-0.4890	-0.3680	-0.3862	-0.8457	-0.94	-0.73
	66	52.5	-0.5347	-0.3949	-0.4328	-0.9411		
	67	57.7	-0.4896	-0.4194	-0.4564	-1.0253	-1.12	-0.87
	69	31.2	0.0000	0.0000	0.0000	0.0000		
	70	41.6	0.0000	0.0000	0.0000	0.0000		
	71	46.8	0.0000	0.0000	0.0000	0.0000		
	72	52.0	0.0000	0.0000	0.0000	0.0000		
	73	57.2	0.0000	0.0000	0.0000	0.0000		
	74	63.4	0.0000	0.0000	0.0000	0.0000		
	75	68.6	0.0000	0.0000	0.0000	0.0000		
	76	72.8	0.0000	0.0000	0.0000	0.0000		

TABLE VI-B

C-PURLIN TEST
TWIST ANGLES
AT 10 FEET FROM THE END SUPPORTS OF THE END SPANS

Sensor No.	TEST NO.	LOAD PSF.	Observed ANGLE DEG. 76-77	Observed ANGLE DEG. 54-55	Observed ANGLE DEG. 78-79	Observed ANGLE DEG. 56-57	Computed F = 0.085 in-lb/in/rad	Computed F = 0.120 in-lb/in/rad
	52	5.2	-0.87	-1.18	-1.12	-1.16		
	53	10.4	-1.54	-2.13	-1.95	-2.06		
	54	15.6	-2.15	-2.78	-2.67	-2.81		
	55	20.8	-2.91	-3.51	-3.63	-3.69		
	56	26.0	-3.81	-4.12	-4.74	-5.18		
	57	31.2	-4.37	-4.60	-6.76	-7.07		
	59	10.4	-1.61	-1.84	-1.78	-2.04	3.91	3.00
	60	20.8	-3.06	-2.94	-3.40	-3.57		
	61	26.0	-3.49	-3.29	-3.81	-4.60	9.27	7.18
	62	31.2	-4.06	-4.04	-5.58	-6.45		
	63	36.9	-5.52	-4.73	-7.74	-8.51		
	64	41.6	-7.60	-5.30	-8.96	-12.73		
	65	47.3	-10.15	-6.18	-9.06	-24.43	16.04	12.50
	66	52.5	-10.88	-6.45	-9.08	-24.32		
	67	57.7	-10.27	-6.84	-8.91	-24.17	19.25	15.02
	69	31.2	0.00	0.00	0.00	0.00		
	70	41.6	0.00	0.00	0.00	0.00		
	71	46.8	0.00	0.00	0.00	0.00		
	72	52.0	0.00	0.00	0.00	0.00		
	73	57.2	0.00	0.00	0.00	0.00		
	74	63.4	0.00	0.00	0.00	0.00		
	75	68.6	0.00	0.00	0.00	0.00		
	76	72.8	0.00	0.00	0.00	0.00		

TABLE VI-C

C-PURLIN TEST
LATERAL DEFLECTIONS
MIDSPAN OF CENTER SPAN

Sensor No.	TEST NO.	LOAD PSF.	Observed 66-67	Observed 68-69	Computed F = 0.085 in-lb/in/rad
	52	5.2	0.0489	0.0807	
	53	10.4	0.0840	0.1442	
	54	15.6	0.1319	0.1936	
	55	20.8	0.1752	0.2430	
	56	26.0	0.2325	0.2952	
	57	31.2	0.2658	0.3273	
	59	10.4	0.0772	0.1316	-0.24
	60	20.8	0.1743	0.2347	
	61	26.0	0.2057	0.2645	-0.61
	62	31.2	0.2564	0.3139	
	63	36.9	0.2973	0.3602	
	64	41.6	0.3385	0.4056	
	65	47.3	0.3646	0.4277	-1.12
	66	52.5	0.3925	0.4630	
	67	57.7	0.4001	0.4868	-1.38
	69	31.2	0.2535	0.3355	
	70	41.6	0.3209	0.4116	
	71	46.8	0.3368	0.4366	
	72	52.0	0.3664	0.4697	
	73	57.2	0.3828	0.5027	
	74	63.4	0.4204	0.5636	
	75	68.6	0.4373	0.6838	
	76	72.8	0.4551	0.7208	

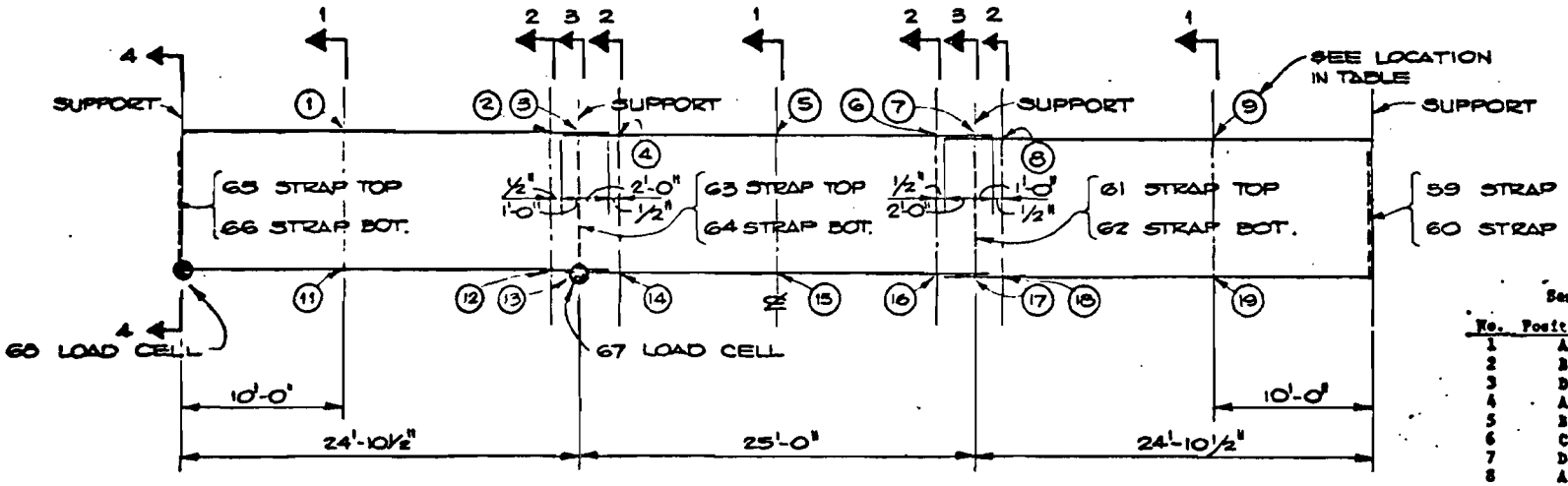

PLAN VIEW OF 'Z' PURLIN TEST

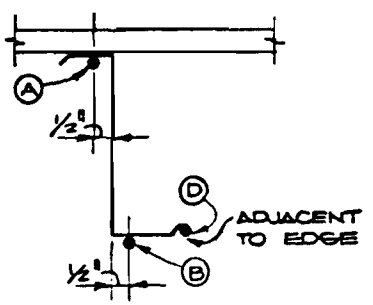

SECTION 1

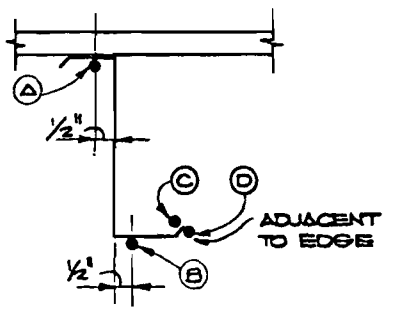

SECTION 2

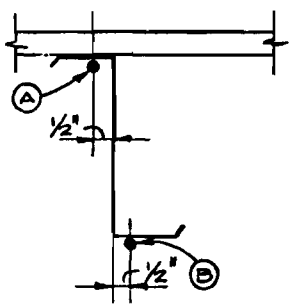

SECTION 3

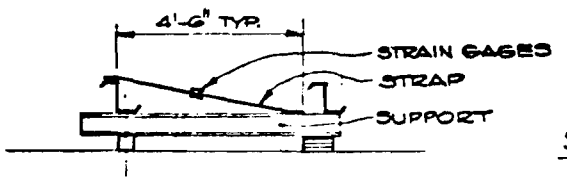

SECTION 4

Sensor No.	Position	Location	Sensor No.	Position	Location
1	A	1	30	A	11
2	B	1	31	B	11
3	D	1	32	D	11
4	A	2	33	A	12
5	B	2	34	B	12
6	C	2	35	C	12
7	D	2	36	D	12
8	A	3	37	A	13
9	B	3	38	B	13
10	A	4	39	A	14
11	B	4	40	B	14
12	C	4	41	C	14
13	D	4	42	D	14
14	A	5	43	A	15
15	B	5	44	B	15
16	C	5	45	D	15
17	A	6	46	A	16
18	B	6	47	B	16
19	C	6	48	C	16
20	D	6	49	D	16
21	A	7	50	A	17
22	B	7	51	B	17
23	C	8	52	A	18
24	D	8	53	B	18
25	A	9	54	C	18
26	B	9	55	D	18
27	D	9	56	A	19
28	B	8	57	B	19
29	A	8	58	D	19

NOTE: LOCATION OF SENSOR Nº 59 THRU Nº 68 IS SHOWN IN PLAN

LOCATION FOR ARRAY POINTS 1 TO 68

WISS, JANNEY, ELSTNER AND ASSOCIATES
CONSULTING & RESEARCH ENGINEERS
330 PFINGSTEN ROAD, NORTHBROOK, ILL. 60062

DATE:	STRAIN GAGE LOCATIONS Z' PURLIN TEST	SHEET NUMBER 3
DRAWN BY: R M		
CHECKED BY: O C G	CLIENT: MBMA	74565
SCALE: N T S.		

Fig. 1a

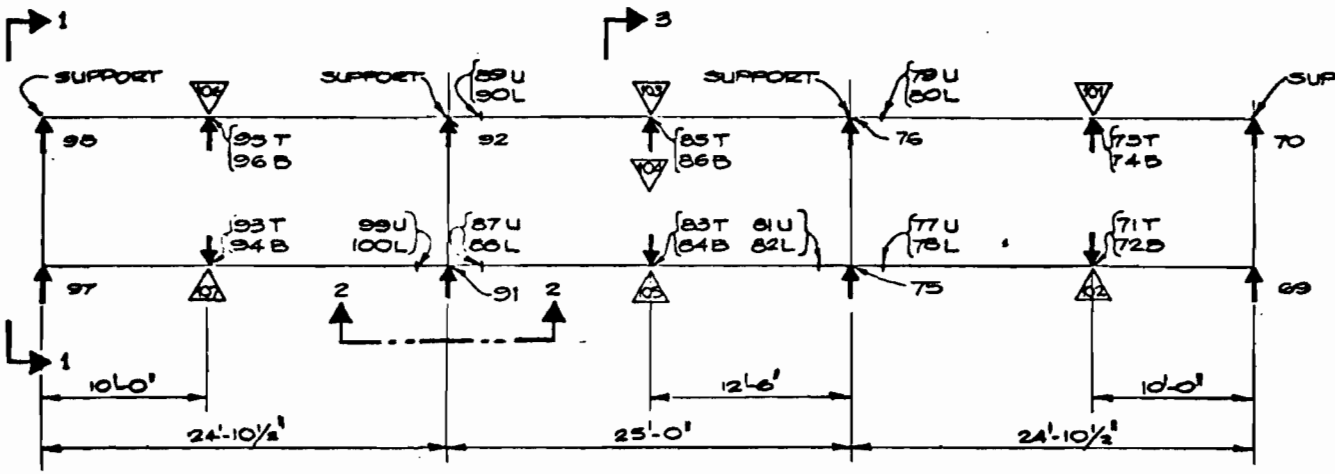

PLAN VIEW OF 'Z' PURLIN TEST

Sensor No.	Dimension A (in.)	Dimension B	Sensor No.	Dimension A (in.)	Dimension B
69	5.50	-	85T	4.50	-
70	5.50	-	86B	-	1.00
71T	5.50	-	87U	6.375	-
72B	-	1.50	88L	-	2.50
73T	4.75	-	89U	5.625	-
74B	-	1.375	90L	-	1.75
75	5.750	-	91	5.50	-
76	7.00	-	92	5.625	-
77U	6.00	-	93T	5.50	-
78L	-	2.00	94B	-	2.00
79U	5.625	-	95T	5.125	-
80L	-	2.00	96B	-	1.625
81U	5.50	-	97	6.00	-
82L	-	2.00	98	5.25	-
83T	5.00	-	99U	5.75	-
84B	-	1.375	100L	-	2.25

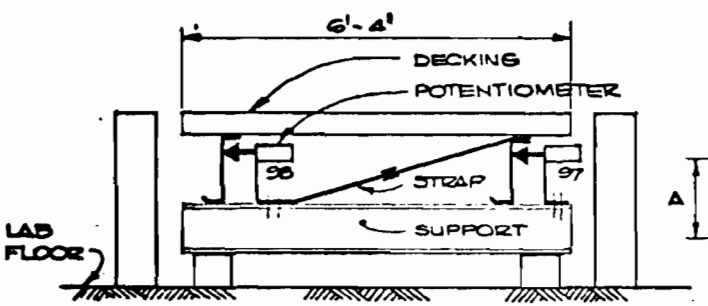

SECTION 1
TYPICAL SUPPORT HORIZONTAL MOTION MONITOR

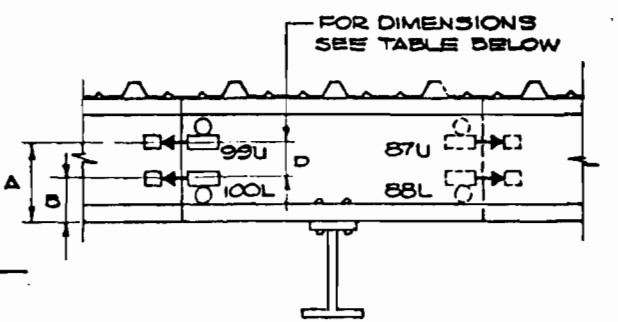

SECTION 2
TYPICAL SUPPORT

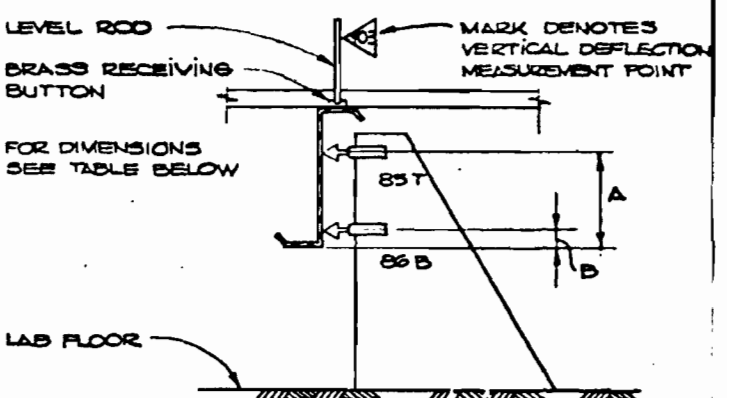

SECTION 3
TYPICAL HORIZONTAL MOTION AND ROTATION INSTRUM.

WISS, JANNEY, ELSTNER AND ASSOCIATES
CONSULTING & RESEARCH ENGINEERS
330 PFINGSTEN ROAD, NORTHBROOK, ILL. 60062

DATE:	DISPLACEMENT INSTRUMENT Z PURLIN TEST	SHEET NUMBER 4
DRAWN BY: R.M.		
CHECKED BY: O.C.E.	CLIENT: MBMA	74565
SCALE: N.T.S.		

Fig. 1b

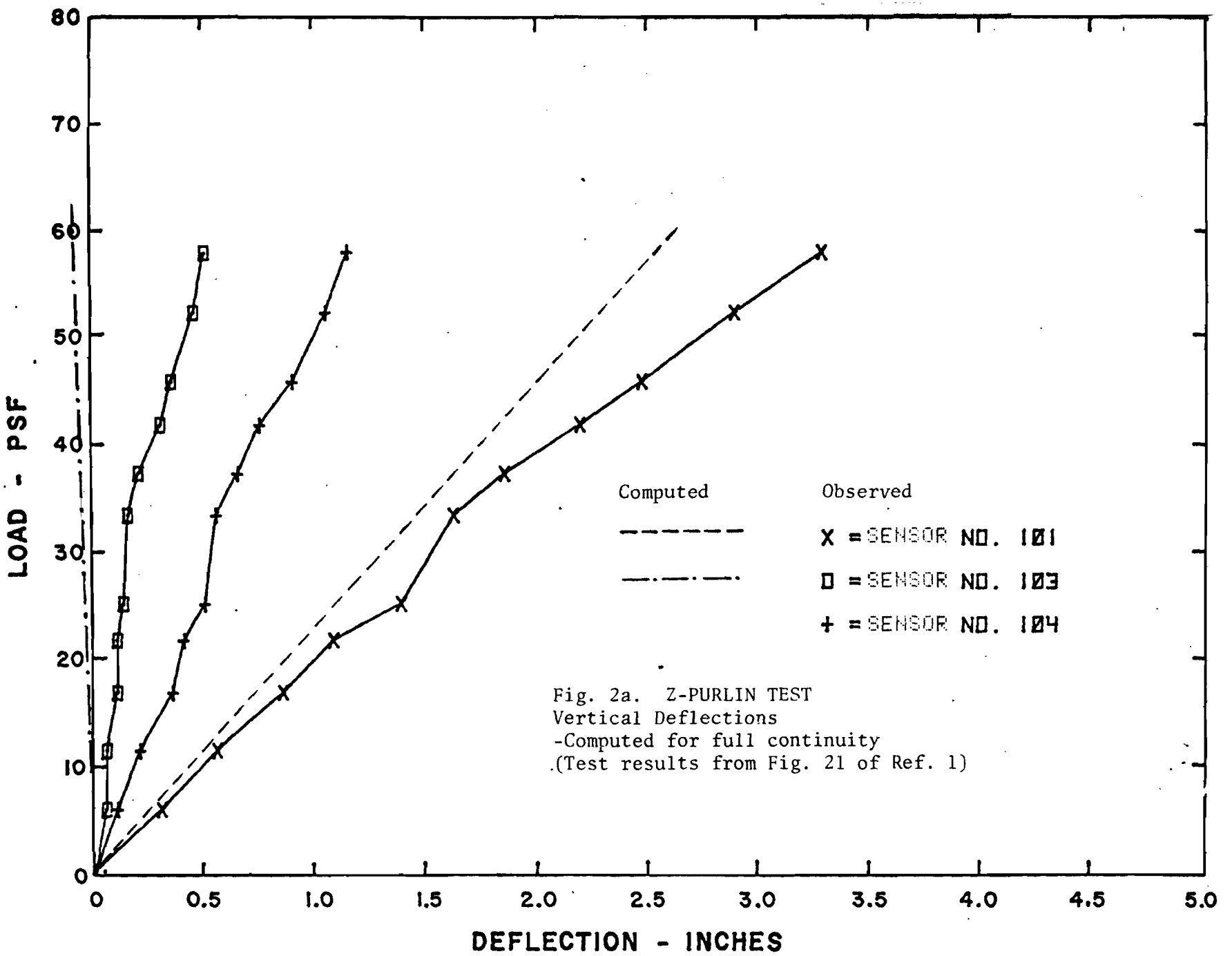

Fig. 2a. Z-PURLIN TEST
Vertical Deflections
-Computed for full continuity
.(Test results from Fig. 21 of Ref. 1)

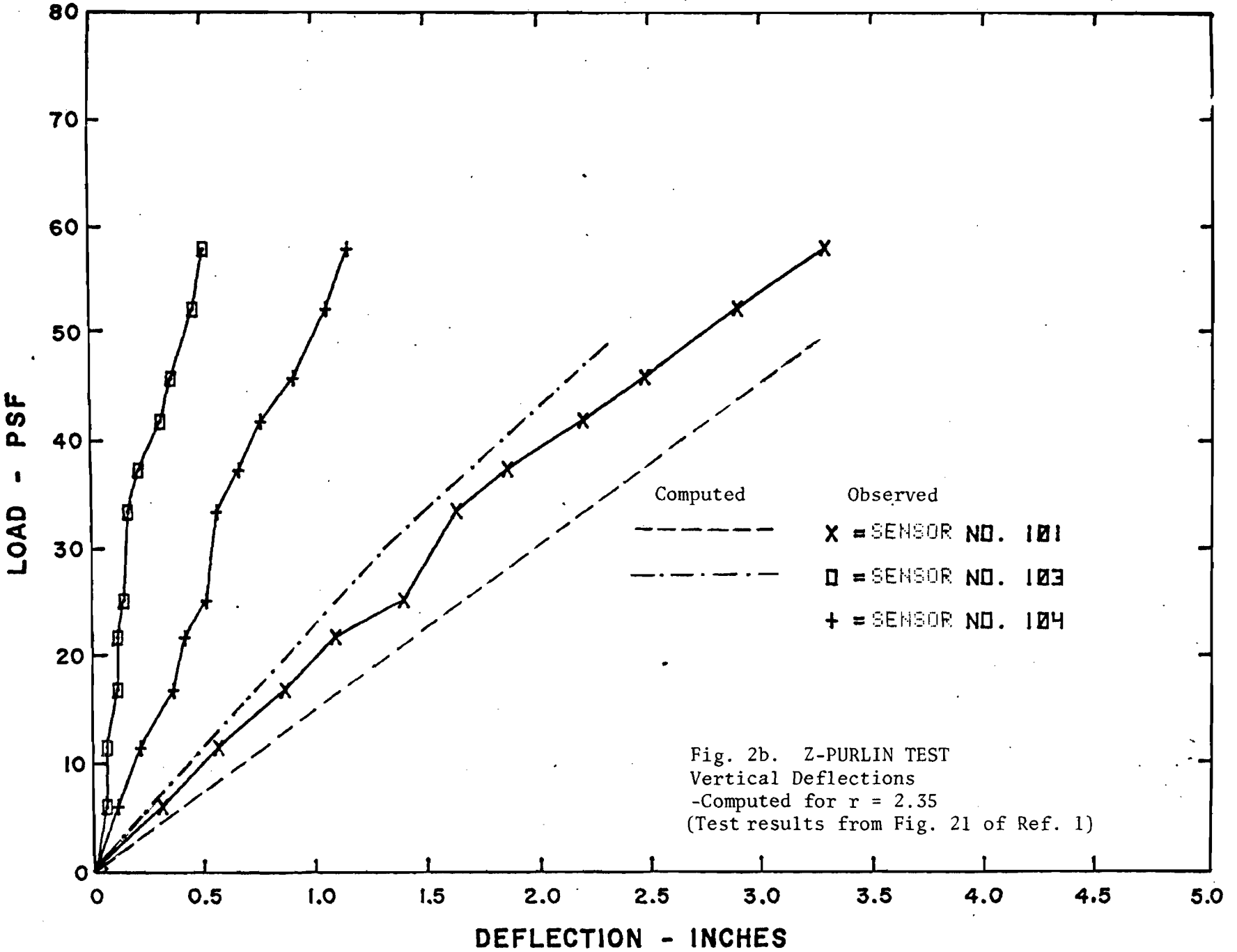

Fig. 2b. Z-PURLIN TEST
Vertical Deflections
-Computed for r = 2.35
(Test results from Fig. 21 of Ref. 1)

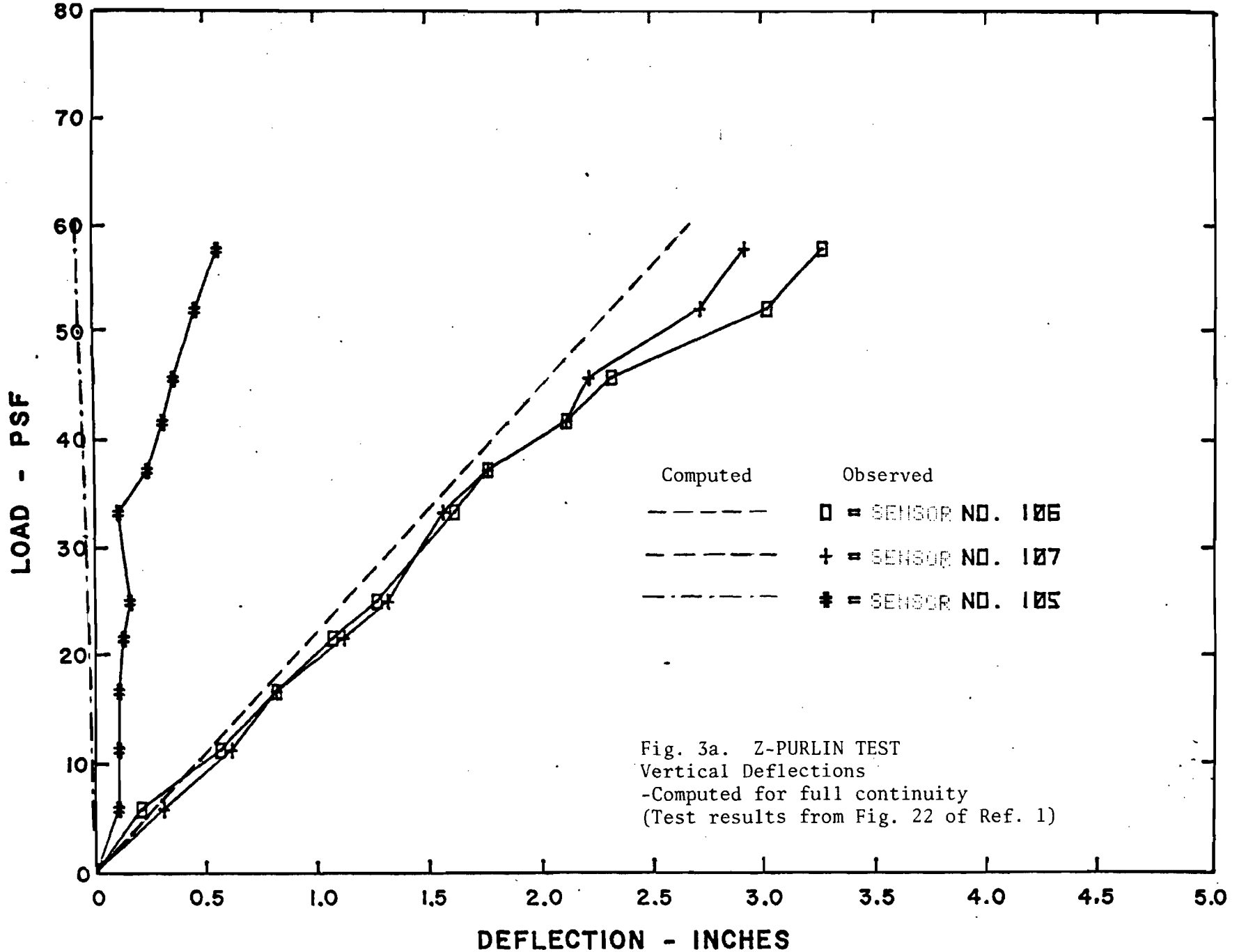

Fig. 3a. Z-PURLIN TEST
Vertical Deflections
-Computed for full continuity
(Test results from Fig. 22 of Ref. 1)

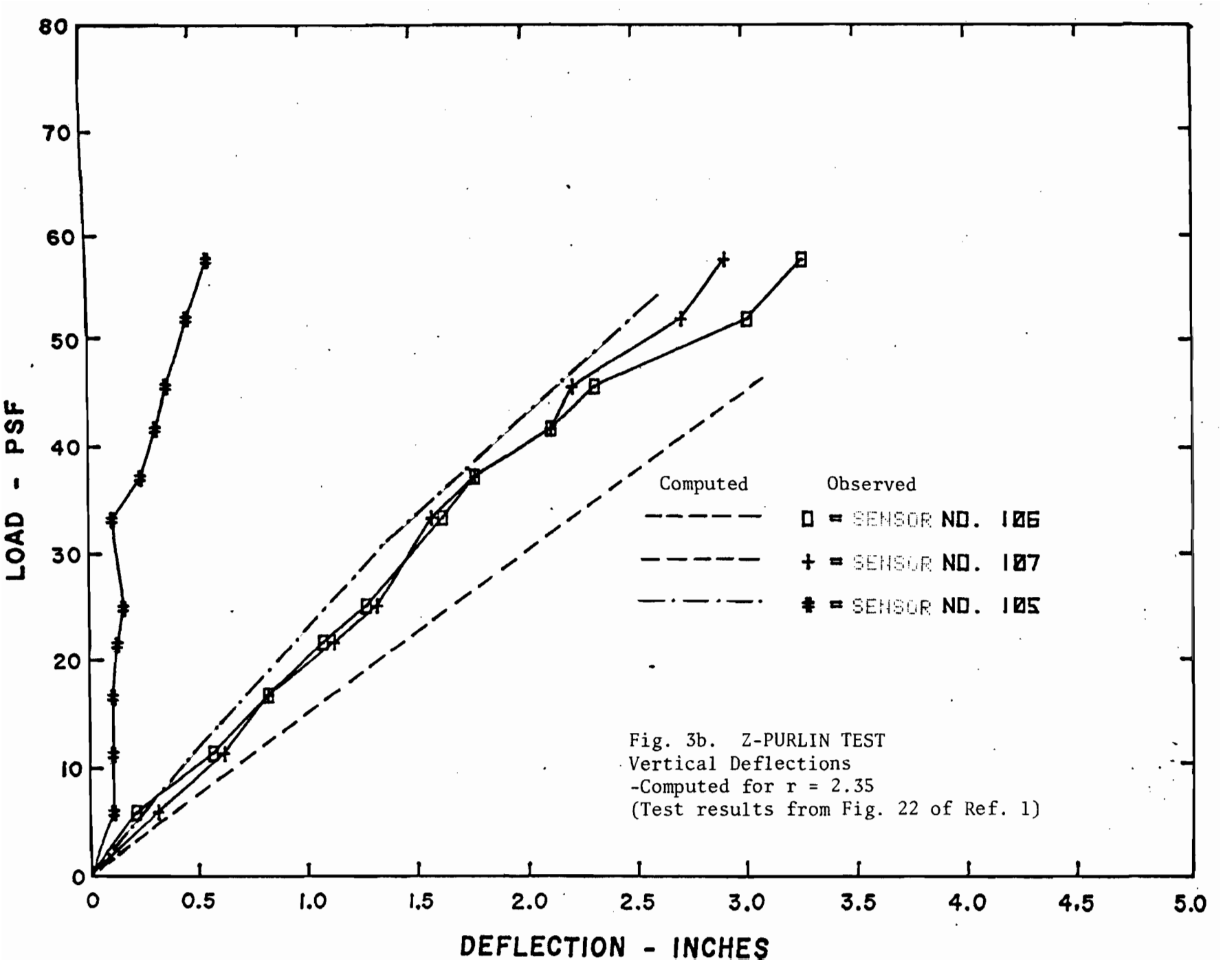

Fig. 3b. Z-PURLIN TEST
Vertical Deflections
-Computed for r = 2.35
(Test results from Fig. 22 of Ref. 1)

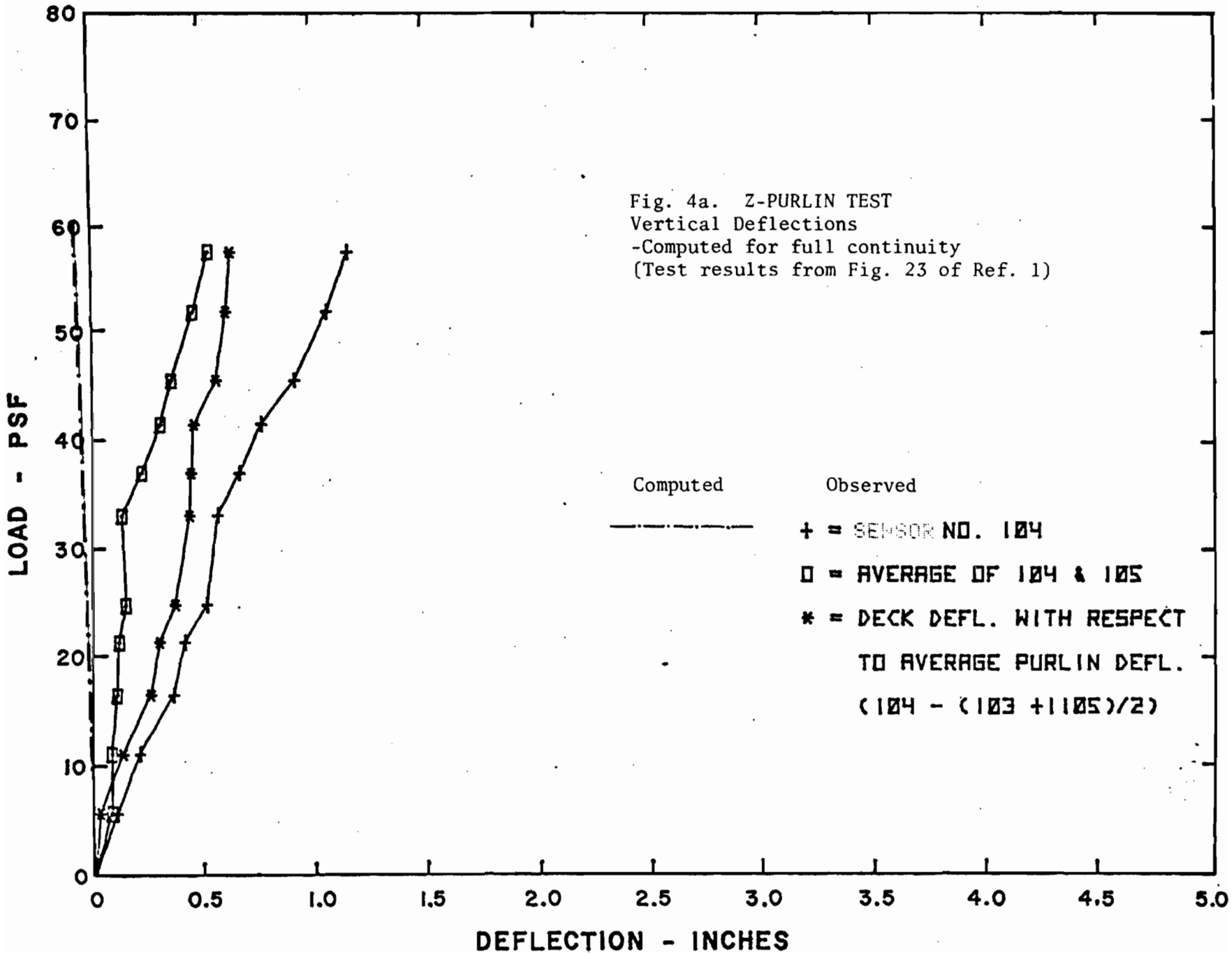

Fig. 4a. Z-PURLIN TEST
Vertical Deflections
-Computed for full continuity
(Test results from Fig. 23 of Ref. 1)

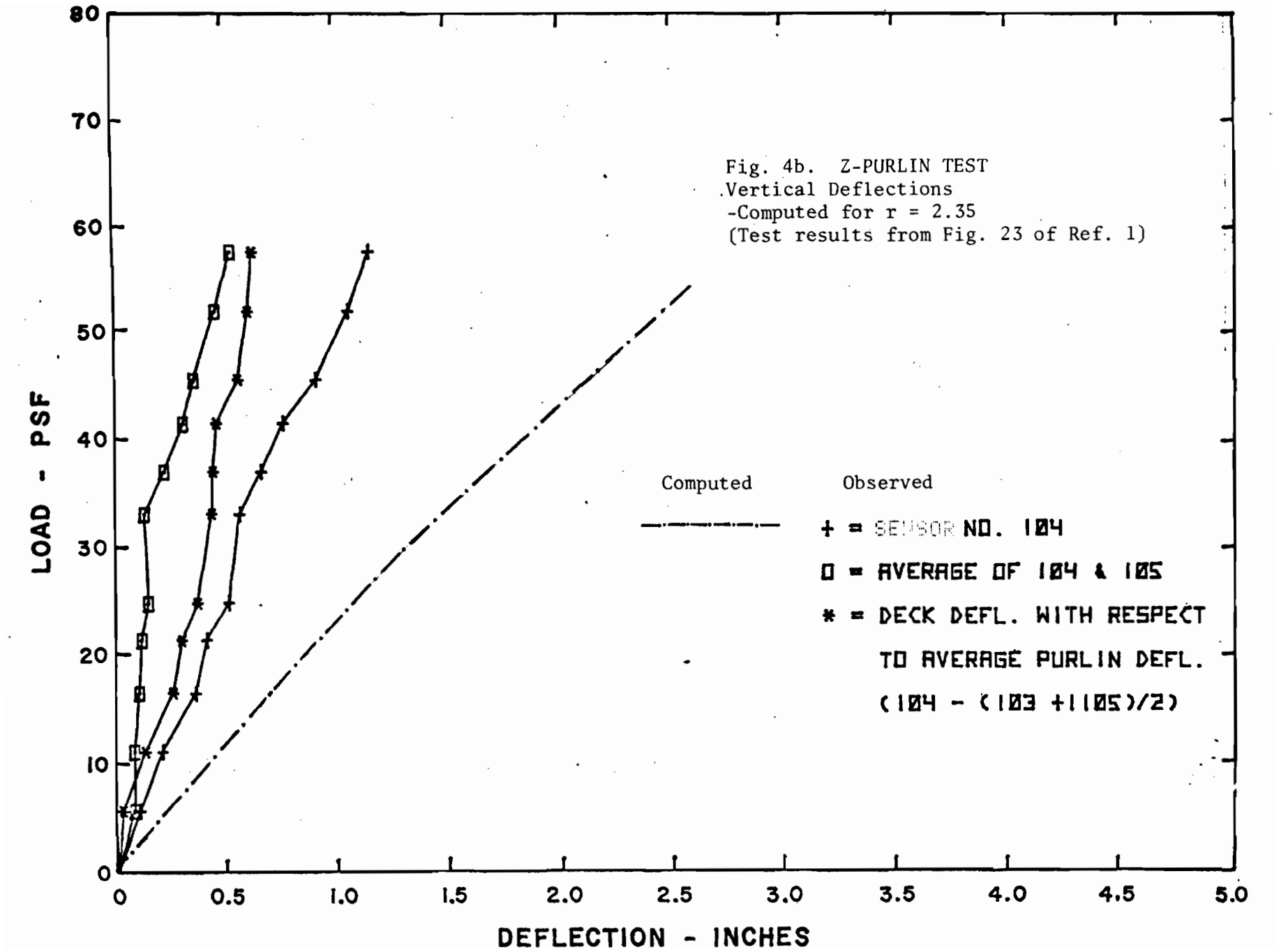

Fig. 4b. Z-PURLIN TEST
Vertical Deflections
-Computed for r = 2.35
(Test results from Fig. 23 of Ref. 1)

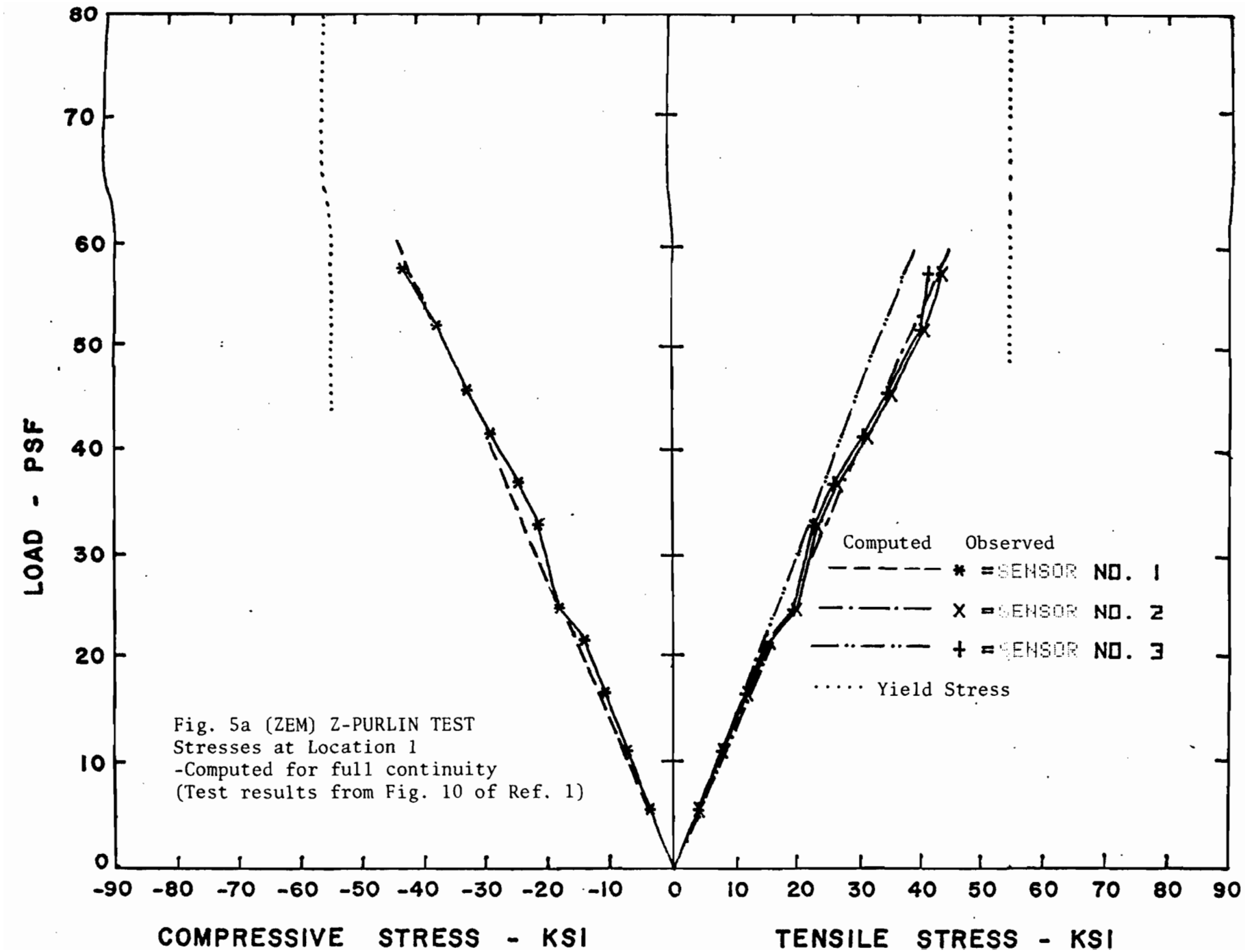

Fig. 5a (ZEM) Z-PURLIN TEST
Stresses at Location 1
-Computed for full continuity
(Test results from Fig. 10 of Ref. 1)

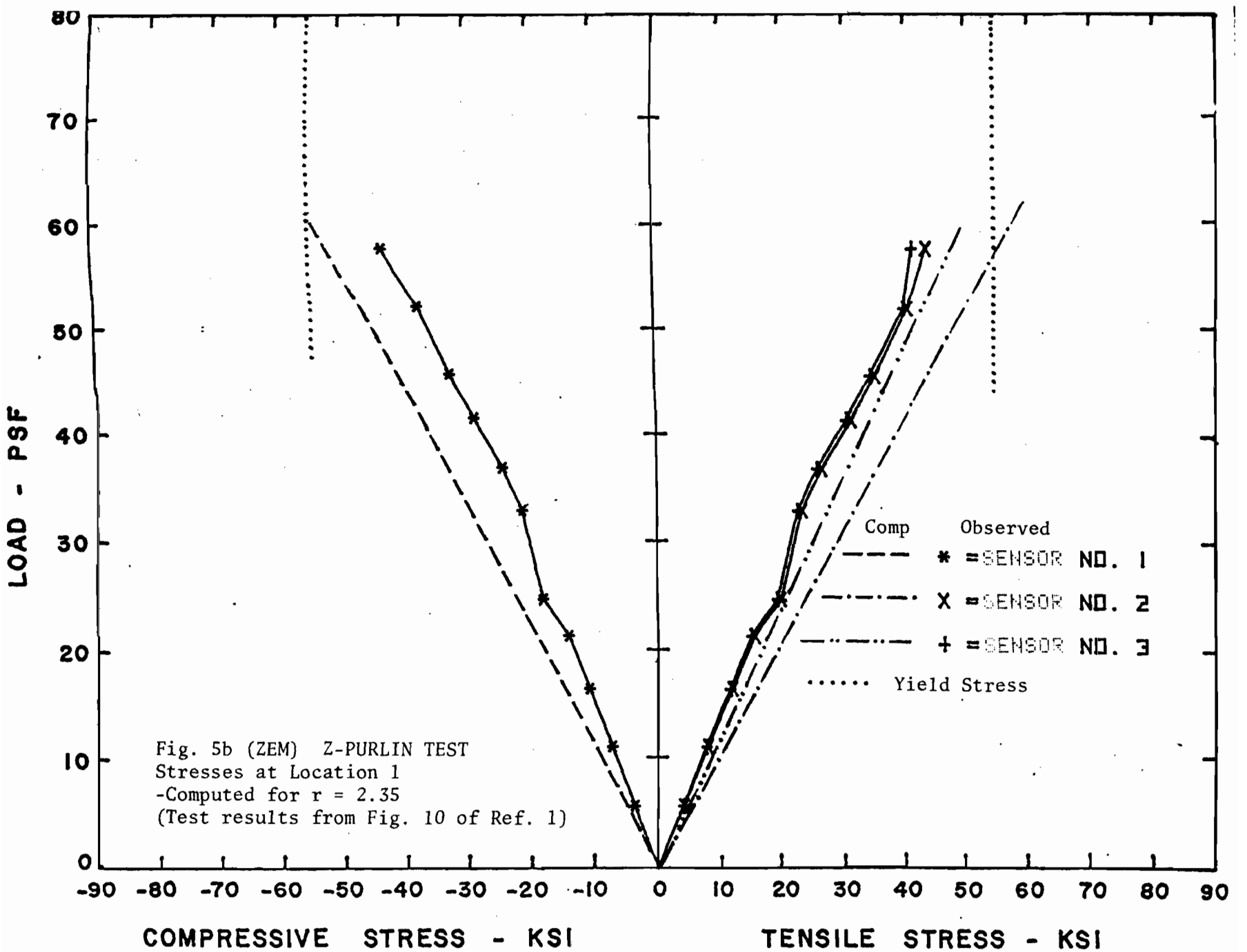

Fig. 5b (ZEM) Z-PURLIN TEST
Stresses at Location 1
-Computed for r = 2.35
(Test results from Fig. 10 of Ref. 1)

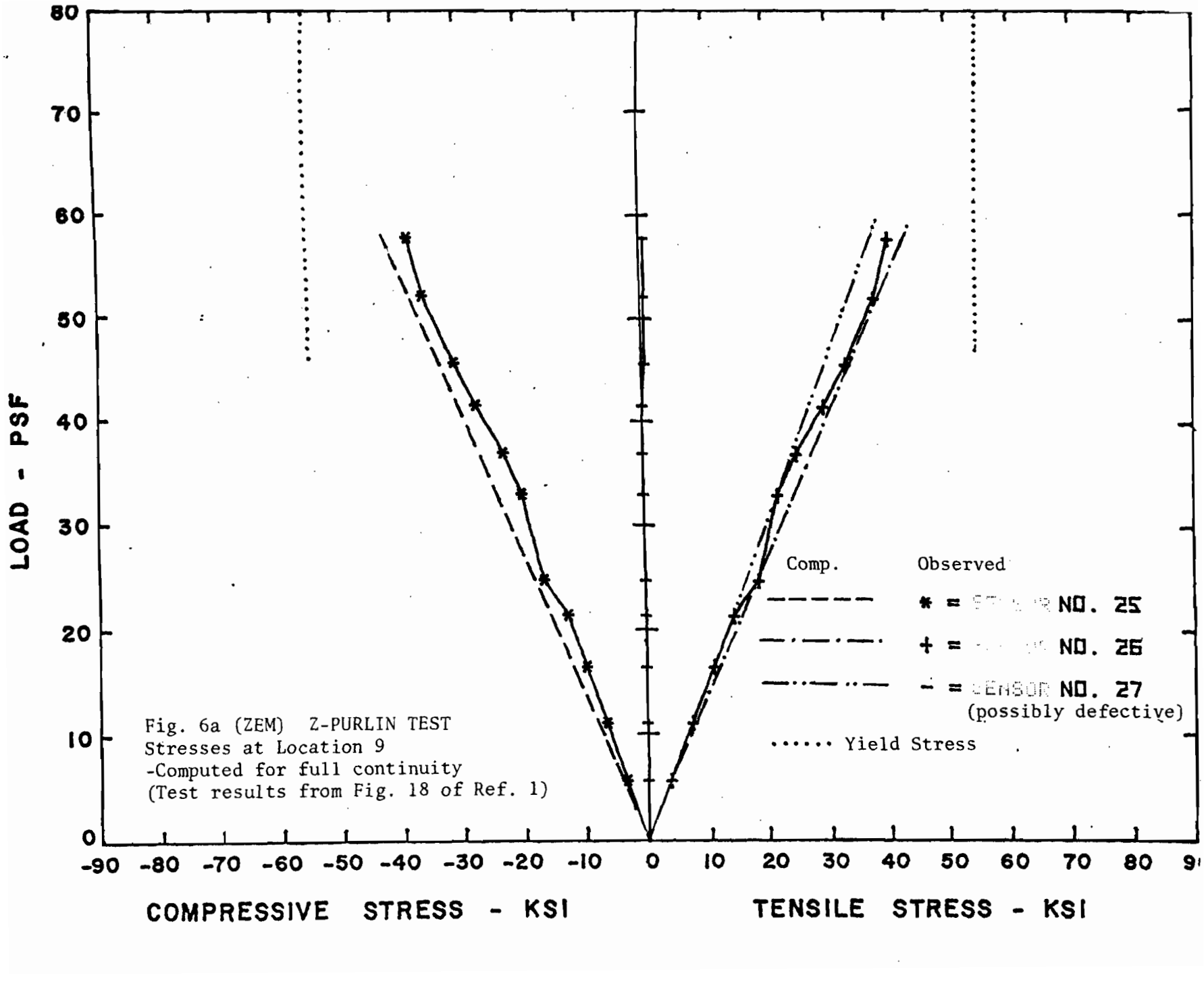
LOAD - PSF
80
70
60
50
40
30
20
10
0
-90 -80 -70 -60 -50 -40 -30 -20 -10 0 10 20 30 40 50 60 70 80 9
COMPRESSIVE STRESS - KSI
TENSILE STRESS - KSI
Comp.
Observed
* = NO. 25
+ = NO. 26
– = NO. 27
(possibly defective)
Yield Stress
Fig. 6a (ZEM) Z-PURLIN TEST
Stresses at Location 9
-Computed for full continuity
(Test results from Fig. 18 of Ref. 1)

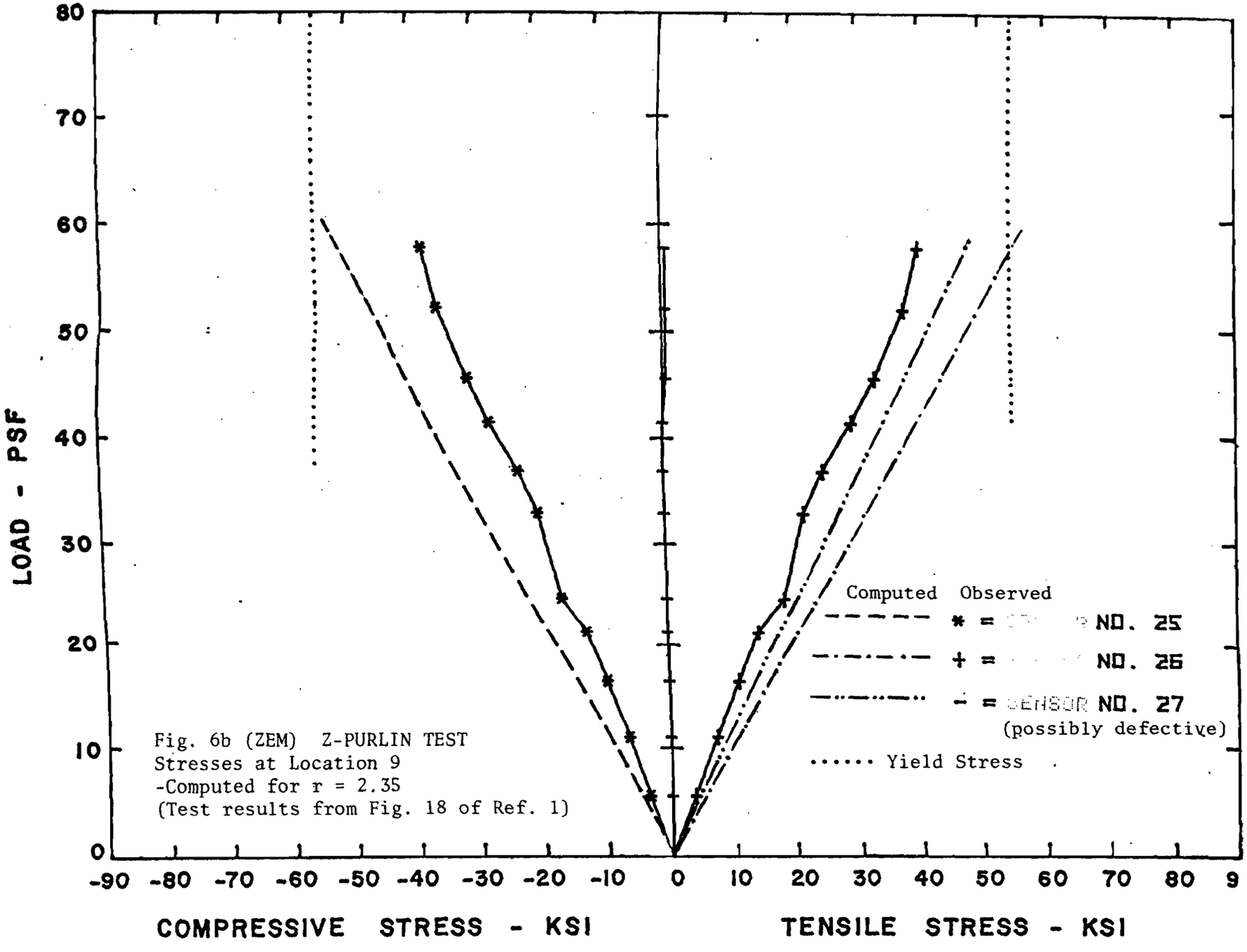

Fig. 6b (ZEM) Z-PURLIN TEST
Stresses at Location 9
-Computed for r = 2.35
(Test results from Fig. 18 of Ref. 1)

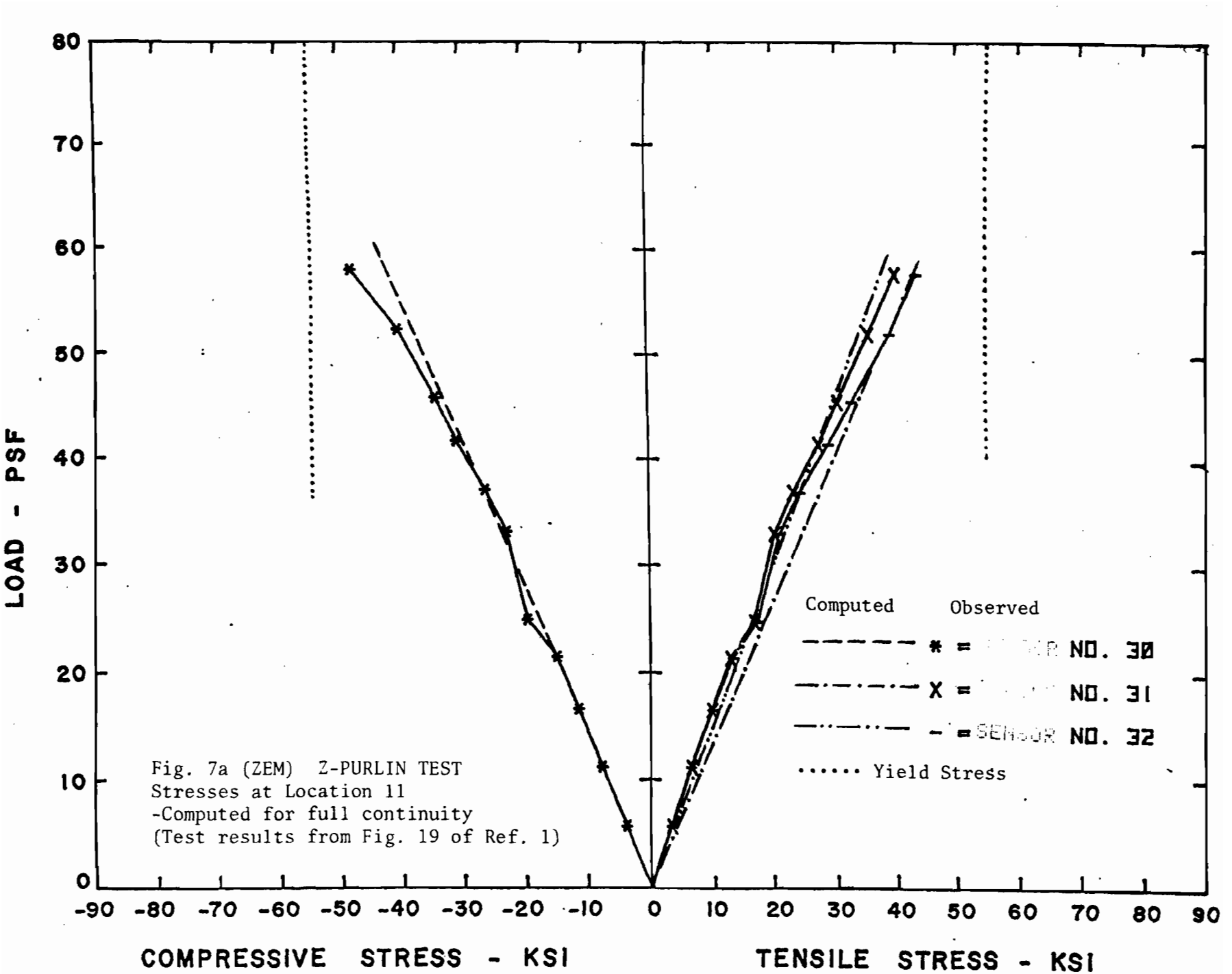

Fig. 7a (ZEM) Z-PURLIN TEST
Stresses at Location 11
-Computed for full continuity
(Test results from Fig. 19 of Ref. 1)

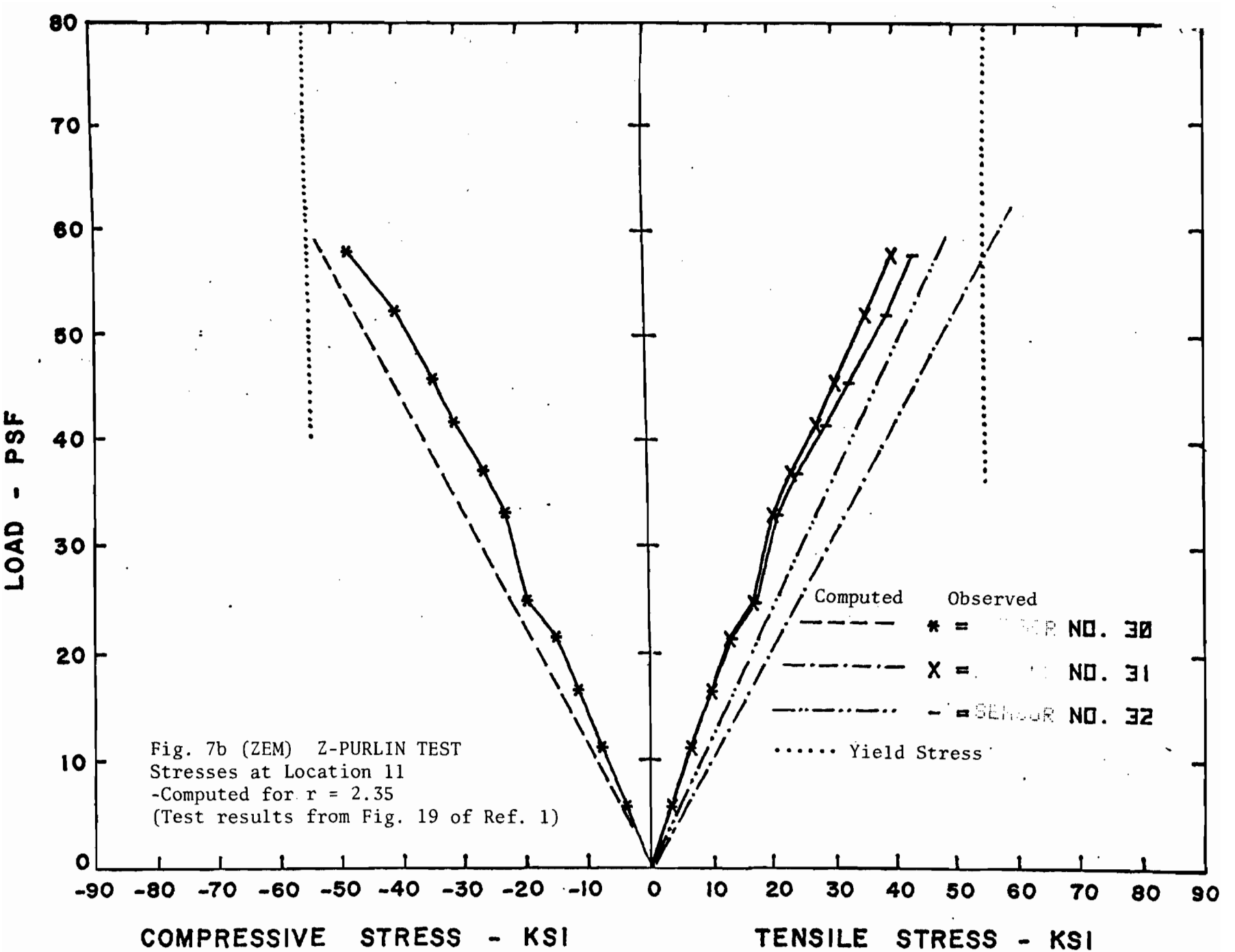

Fig. 7b (ZEM) Z-PURLIN TEST
Stresses at Location 11
-Computed for r = 2.35
(Test results from Fig. 19 of Ref. 1)

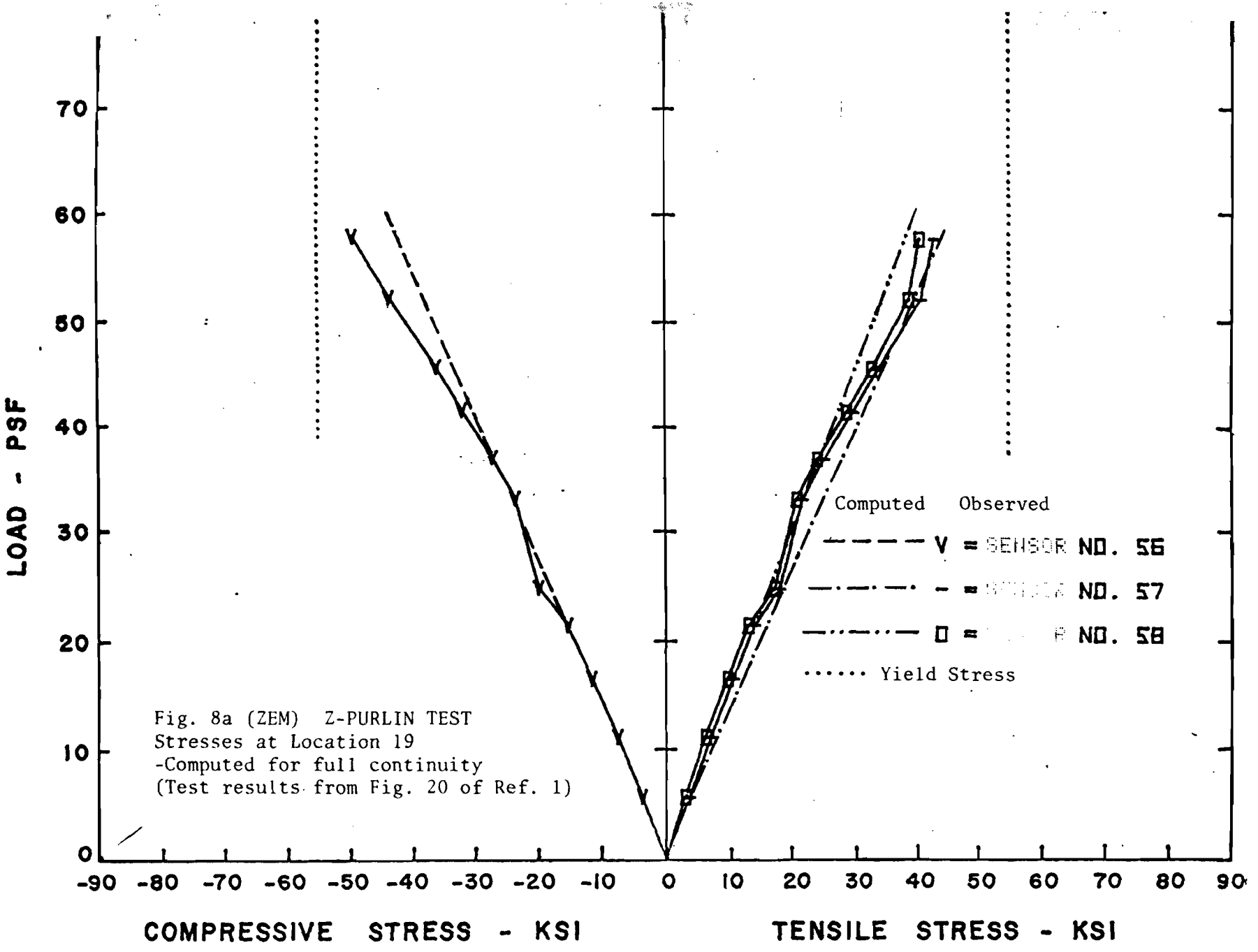

Fig. 8a (ZEM) Z-PURLIN TEST
Stresses at Location 19
-Computed for full continuity
(Test results from Fig. 20 of Ref. 1)

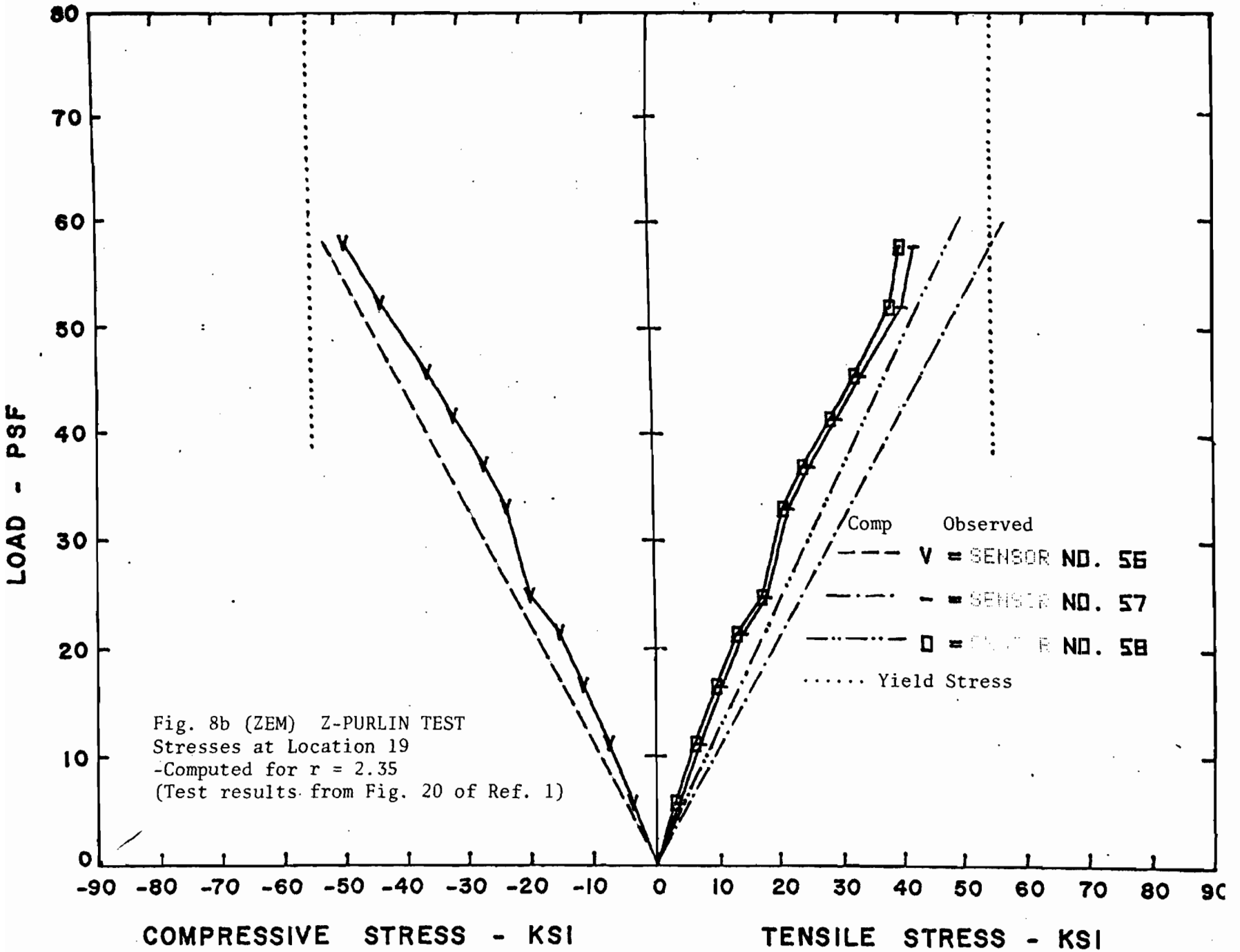

Fig. 8b (ZEM) Z-PURLIN TEST
Stresses at Location 19
-Computed for r = 2.35
(Test results from Fig. 20 of Ref. 1)

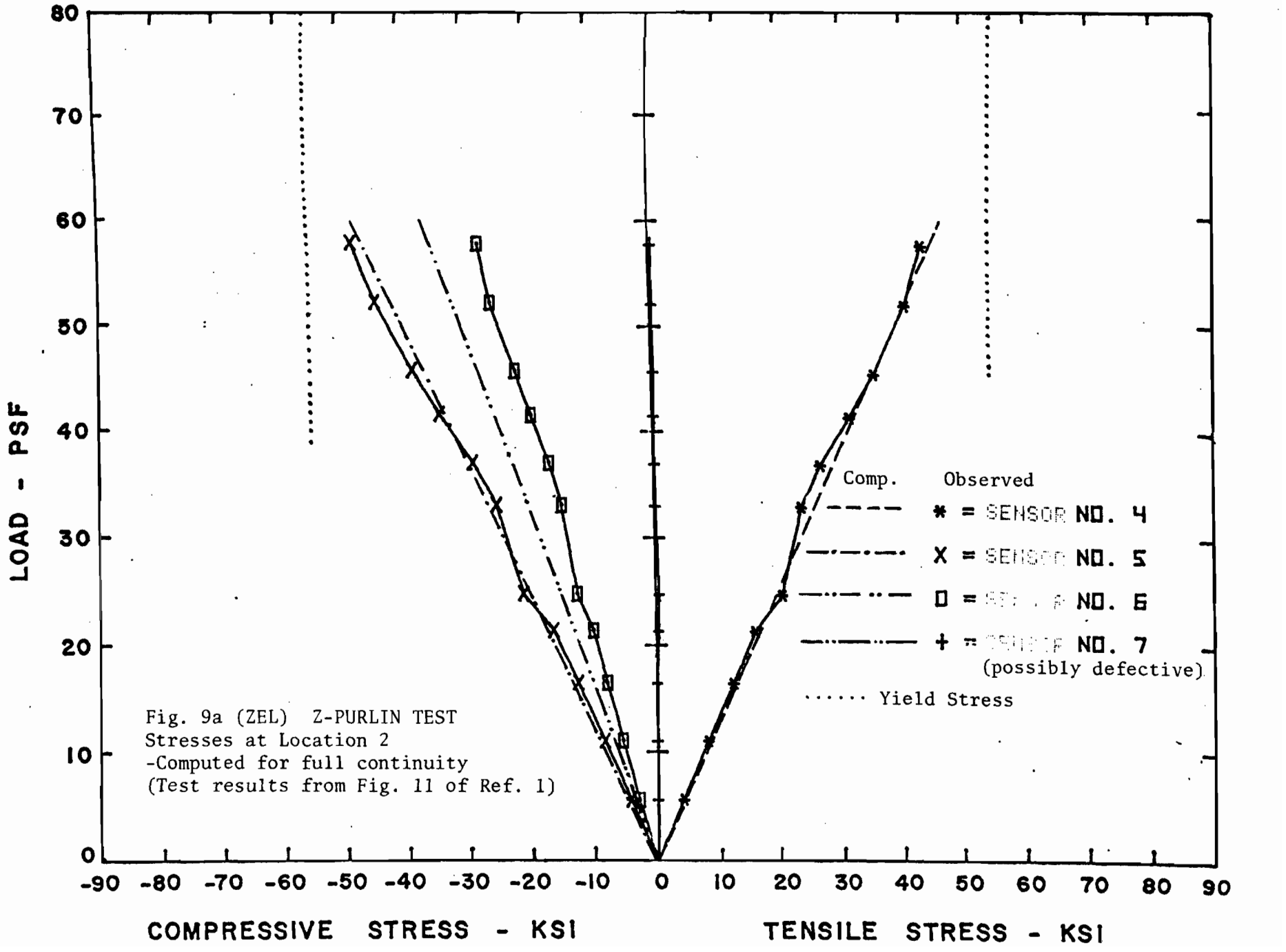

Fig. 9a (ZEL) Z-PURLIN TEST
Stresses at Location 2
-Computed for full continuity
(Test results from Fig. 11 of Ref. 1)

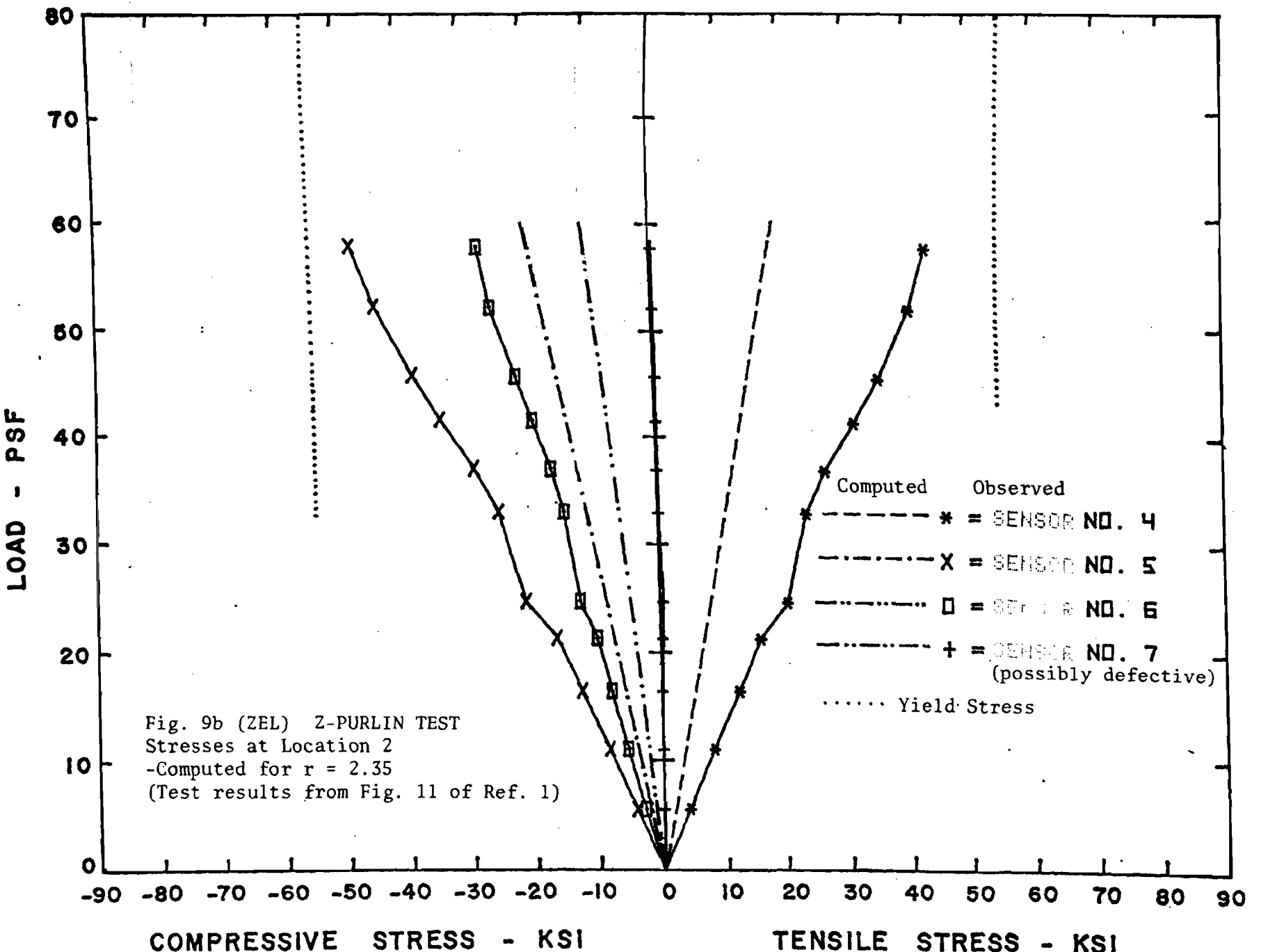

Fig. 9b (ZEL) Z-PURLIN TEST
Stresses at Location 2
-Computed for r = 2.35
(Test results from Fig. 11 of Ref. 1)

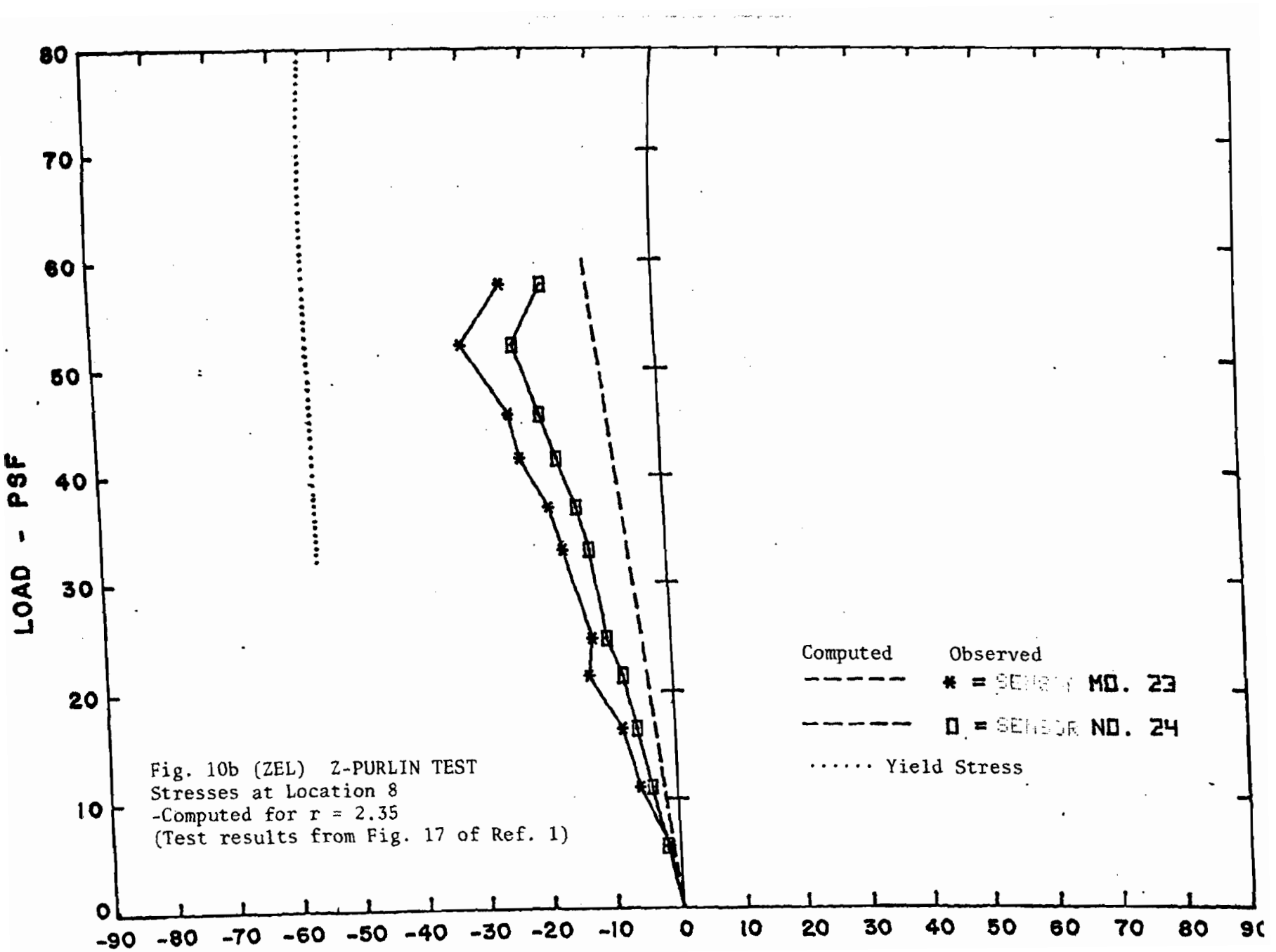

Fig. 10b (ZEL) Z-PURLIN TEST
Stresses at Location 8
-Computed for r = 2.35
(Test results from Fig. 17 of Ref. 1)

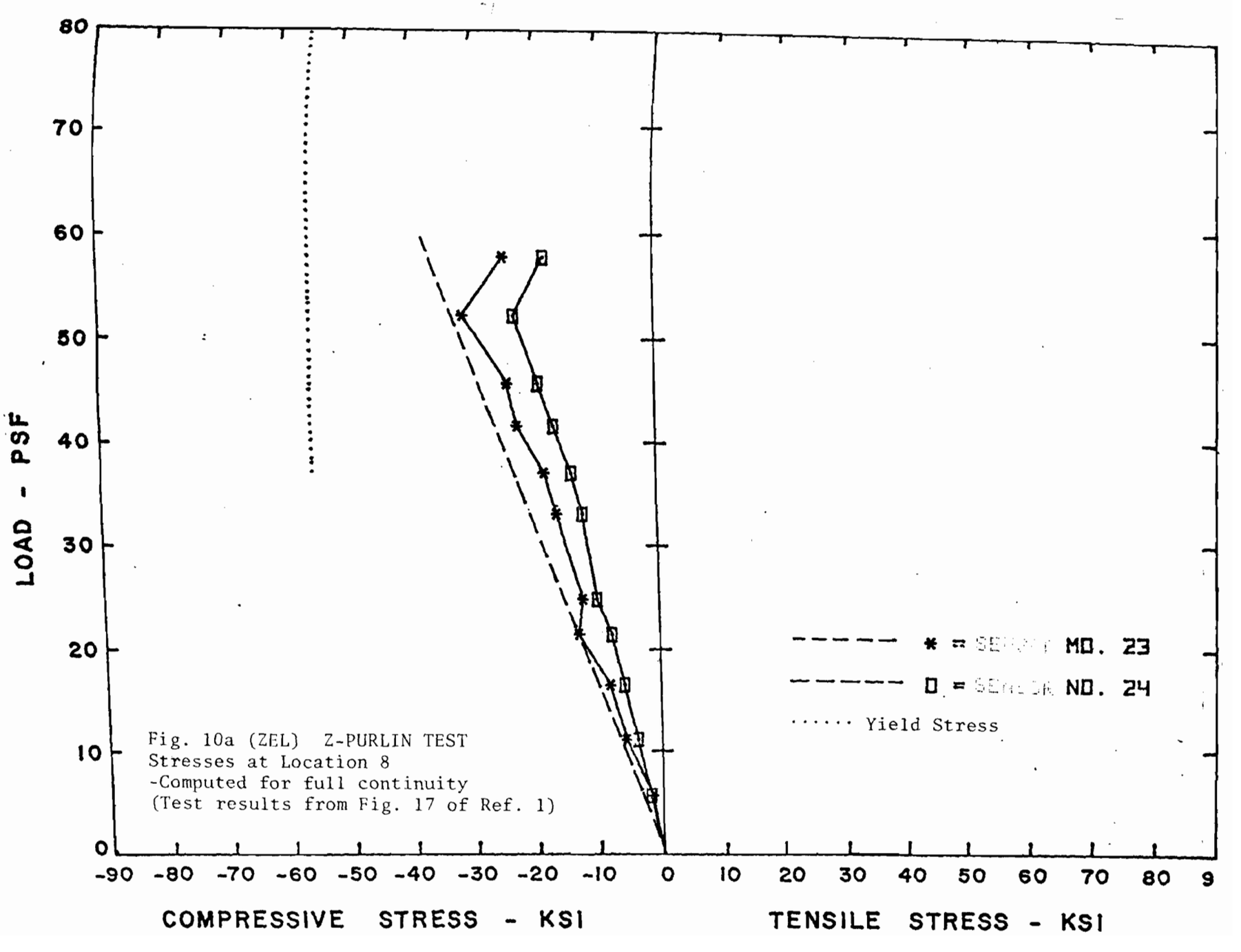

Fig. 10a (ZEL) Z-PURLIN TEST
Stresses at Location 8
-Computed for full continuity
(Test results from Fig. 17 of Ref. 1)

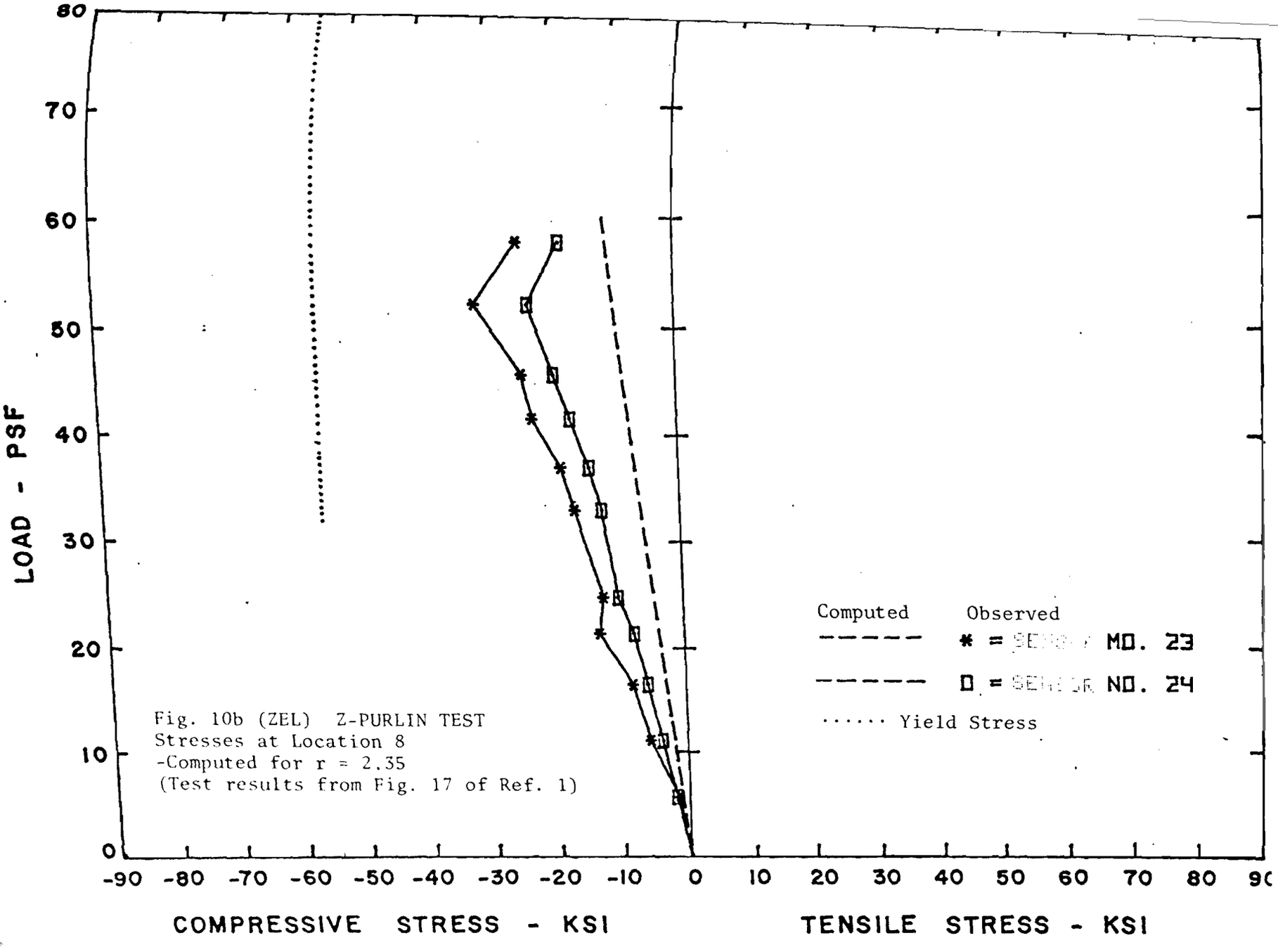

Fig. 10b (ZEL) Z-PURLIN TEST
Stresses at Location 8
-Computed for r = 2.35
(Test results from Fig. 17 of Ref. 1)

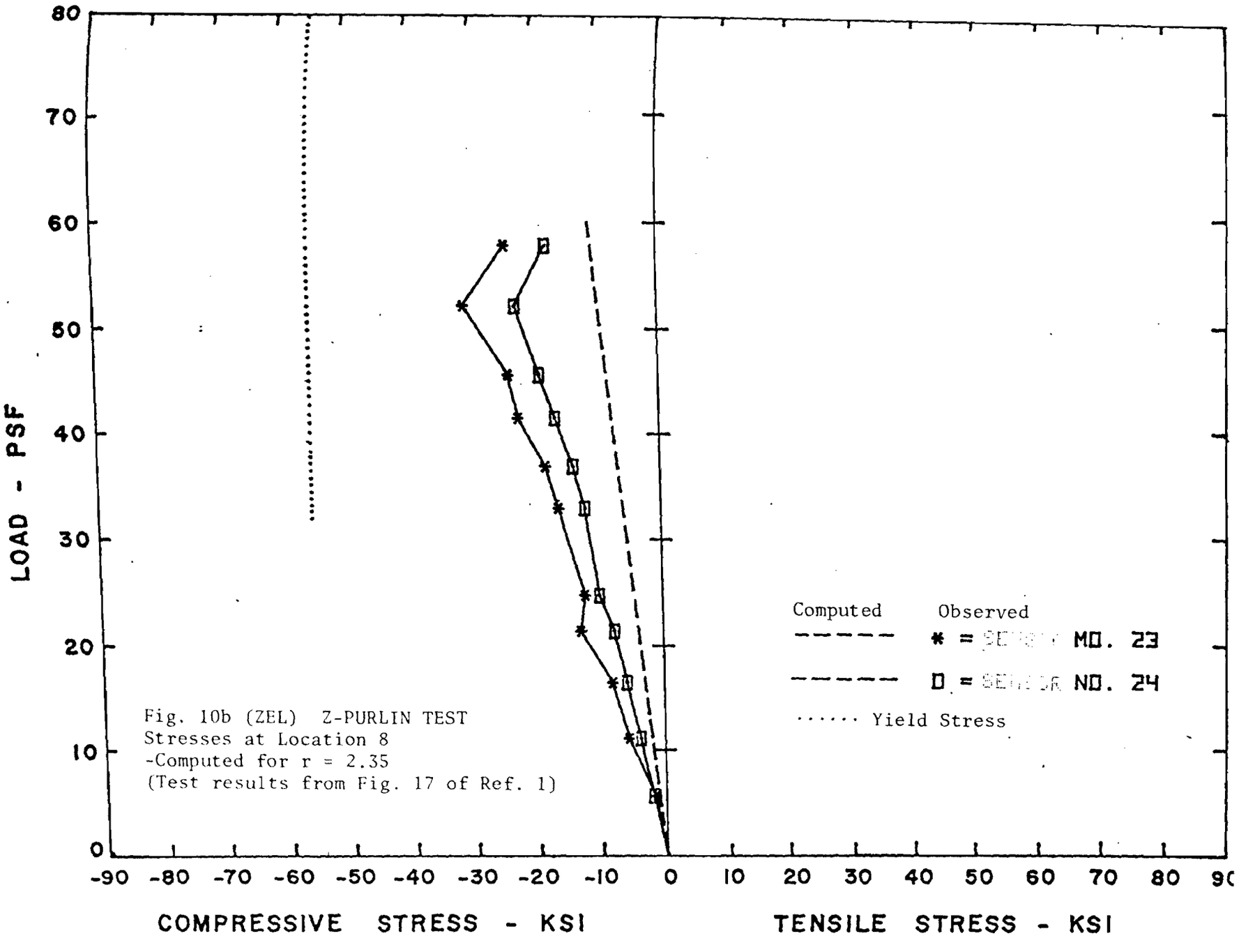

Fig. 10b (ZEL) Z-PURLIN TEST
Stresses at Location 8
-Computed for r = 2.35
(Test results from Fig. 17 of Ref. 1)

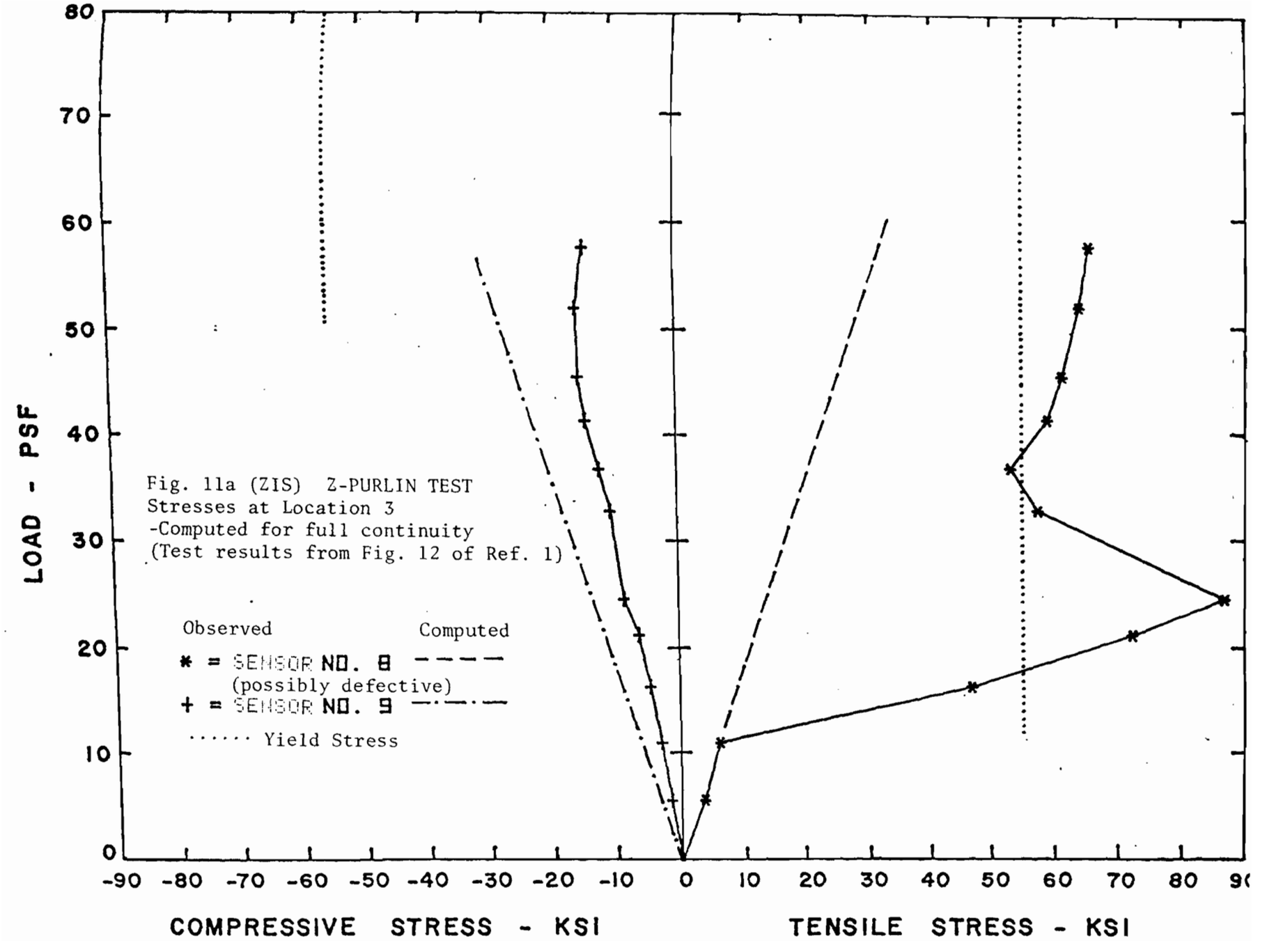

Fig. 11a (ZIS) Z-PURLIN TEST
Stresses at Location 3
-Computed for full continuity
(Test results from Fig. 12 of Ref. 1)

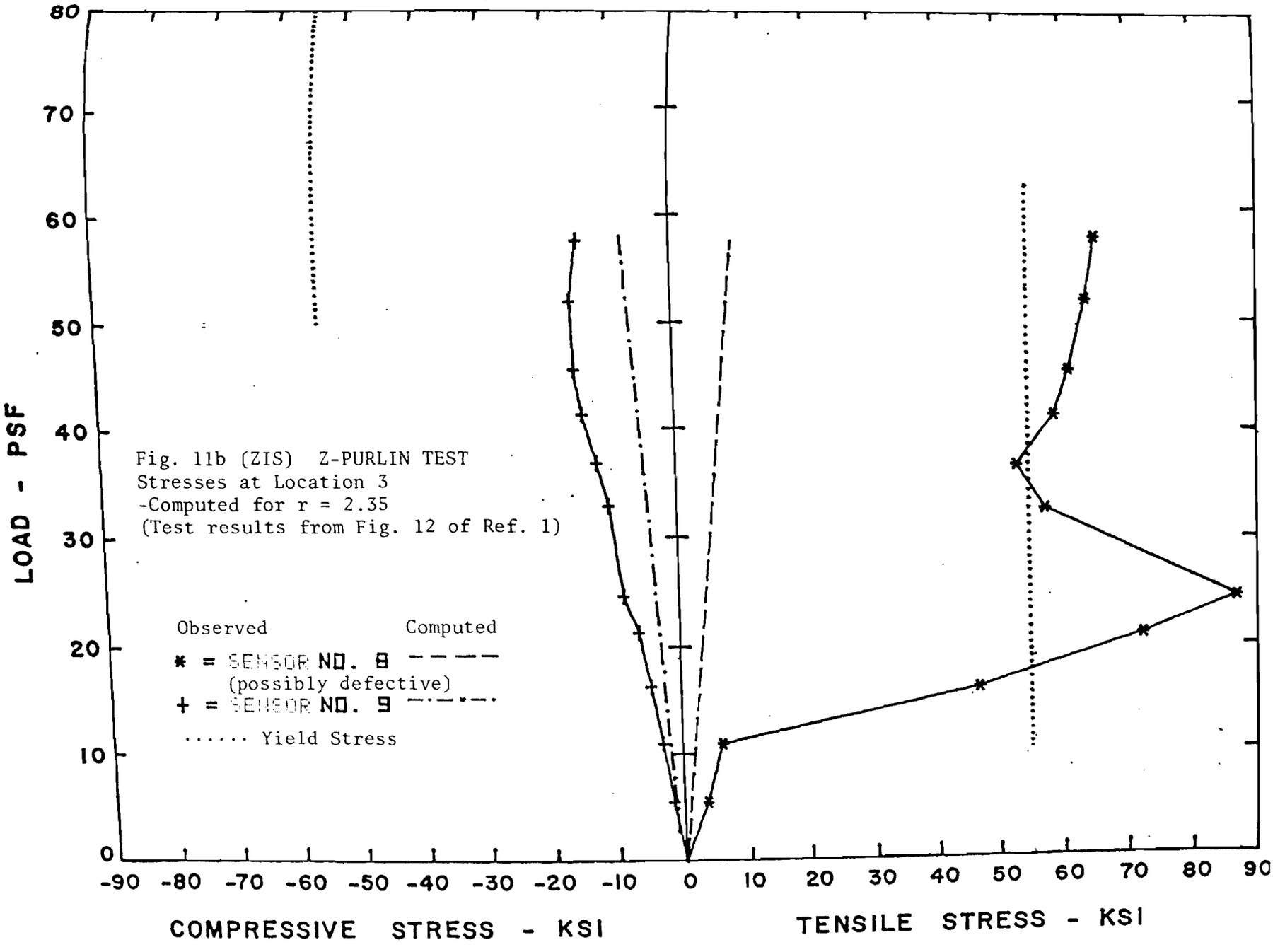

Fig. 11b (ZIS) Z-PURLIN TEST
Stresses at Location 3
-Computed for r = 2.35
(Test results from Fig. 12 of Ref. 1)

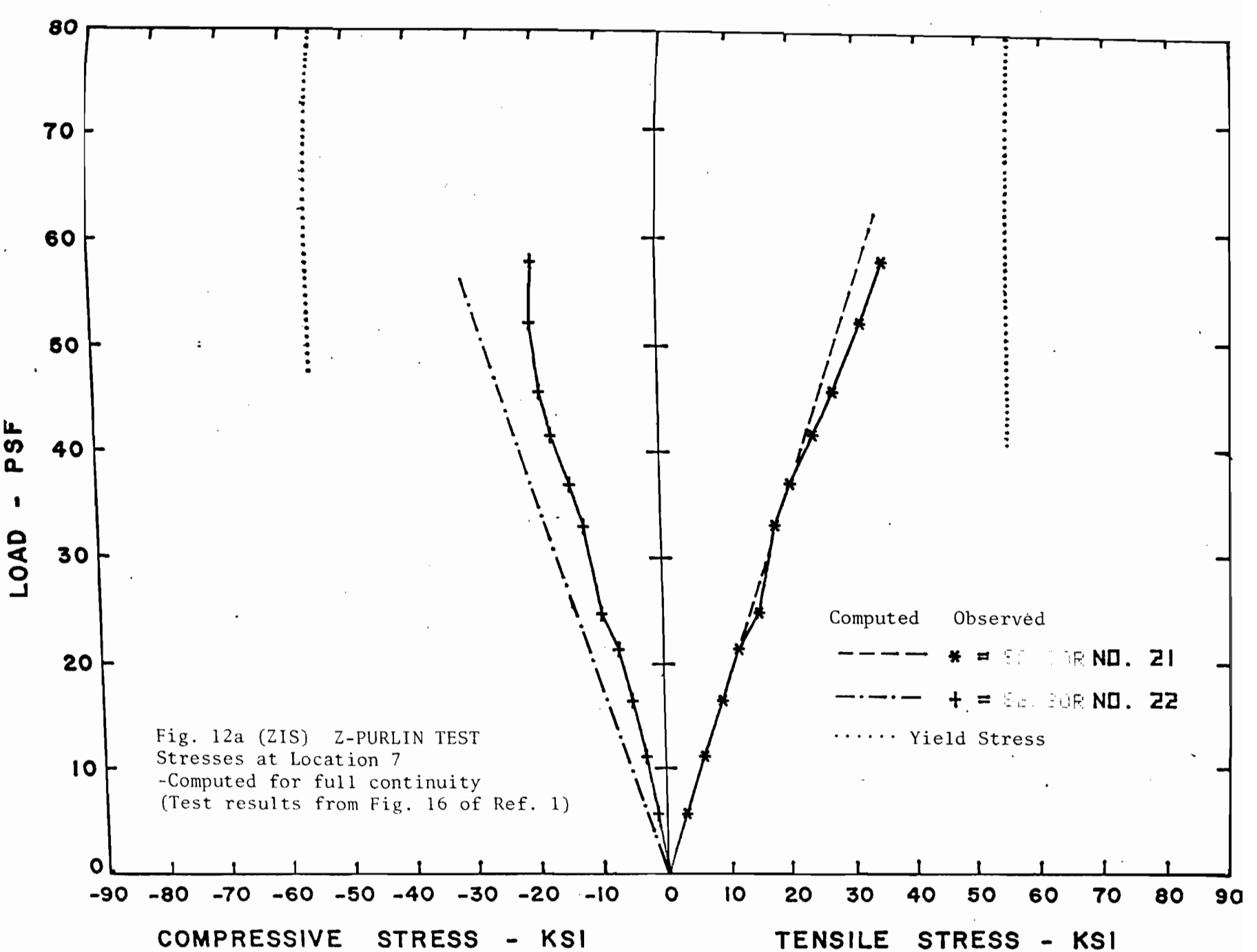

Fig. 12a (ZIS) Z-PURLIN TEST
Stresses at Location 7
-Computed for full continuity
(Test results from Fig. 16 of Ref. 1)

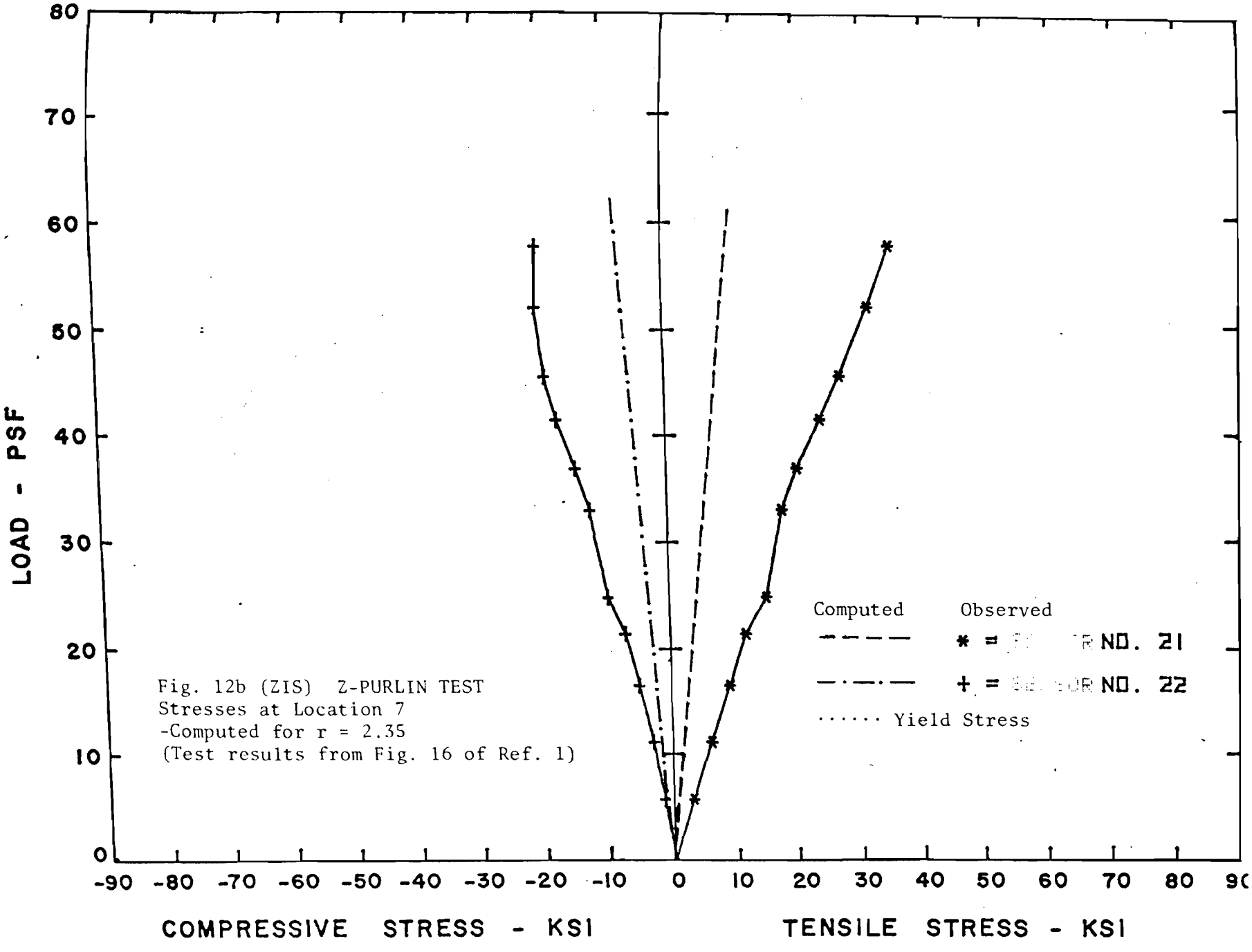

Fig. 12b (ZIS) Z-PURLIN TEST
Stresses at Location 7
-Computed for r = 2.35
(Test results from Fig. 16 of Ref. 1)

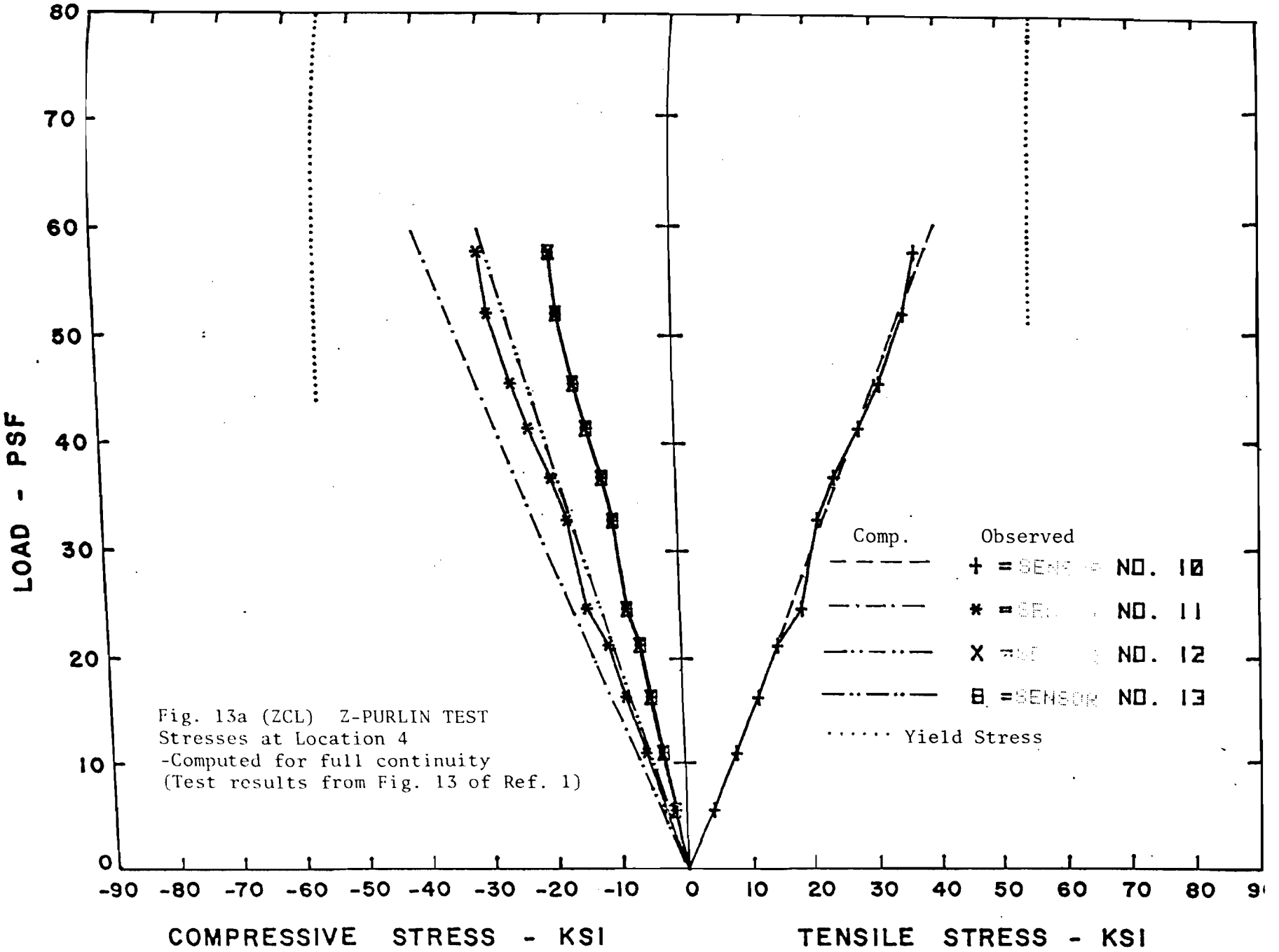

Fig. 13a (ZCL) Z-PURLIN TEST
Stresses at Location 4
-Computed for full continuity
(Test results from Fig. 13 of Ref. 1)

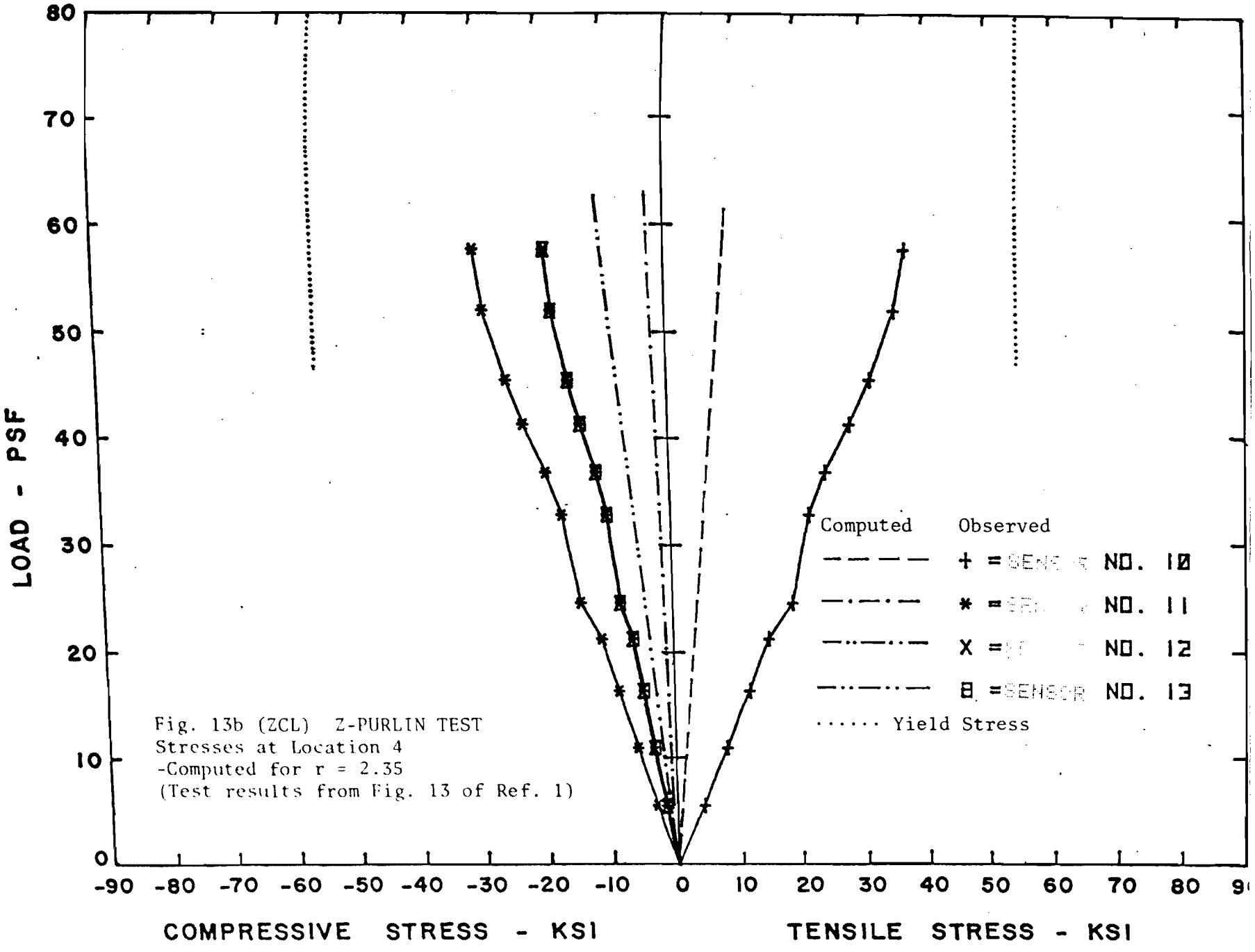

Fig. 13b (ZCL) Z-PURLIN TEST
Stresses at Location 4
-Computed for r = 2.35
(Test results from Fig. 13 of Ref. 1)

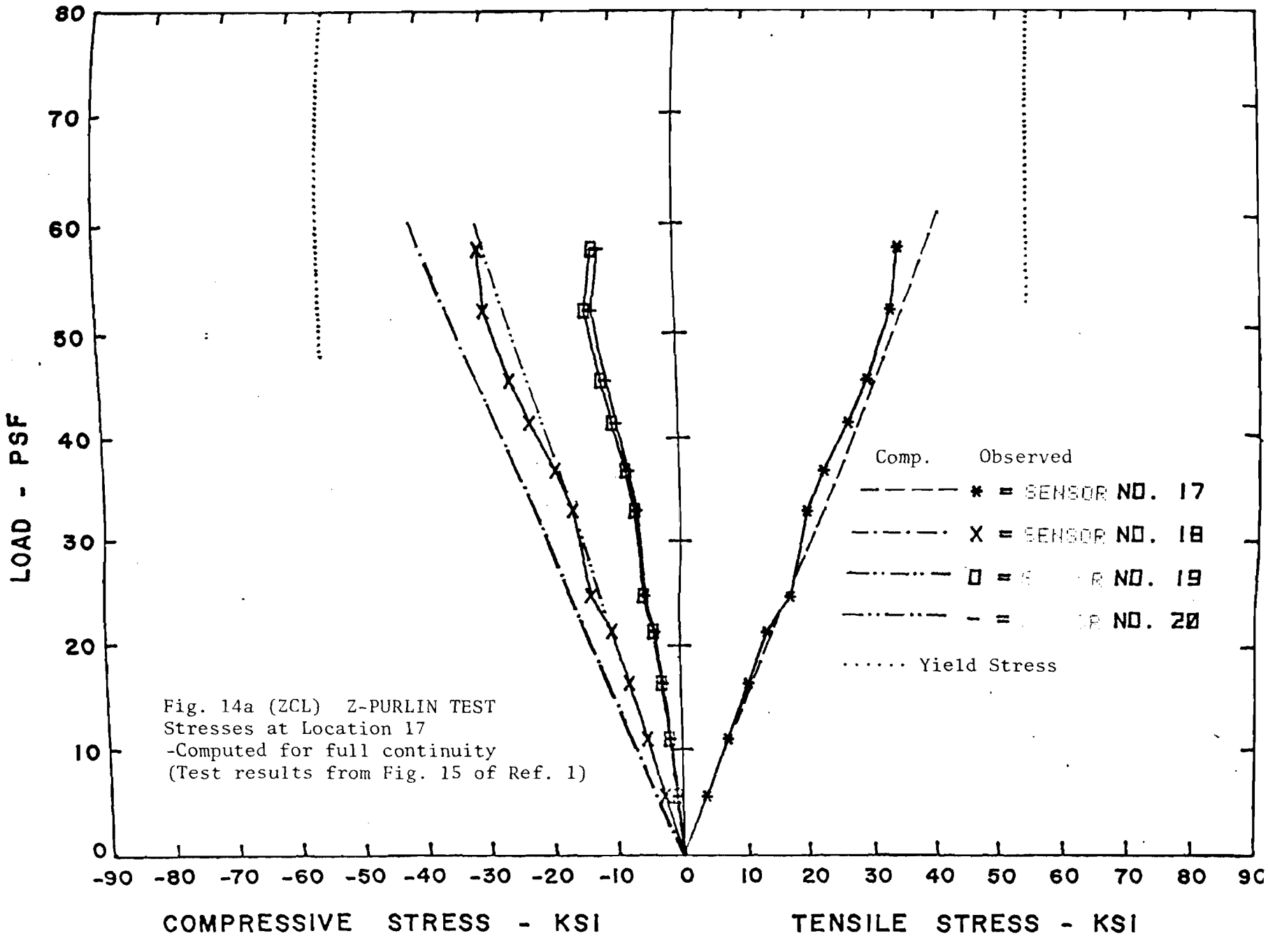

Fig. 14a (ZCL) Z-PURLIN TEST
Stresses at Location 17
-Computed for full continuity
(Test results from Fig. 15 of Ref. 1)

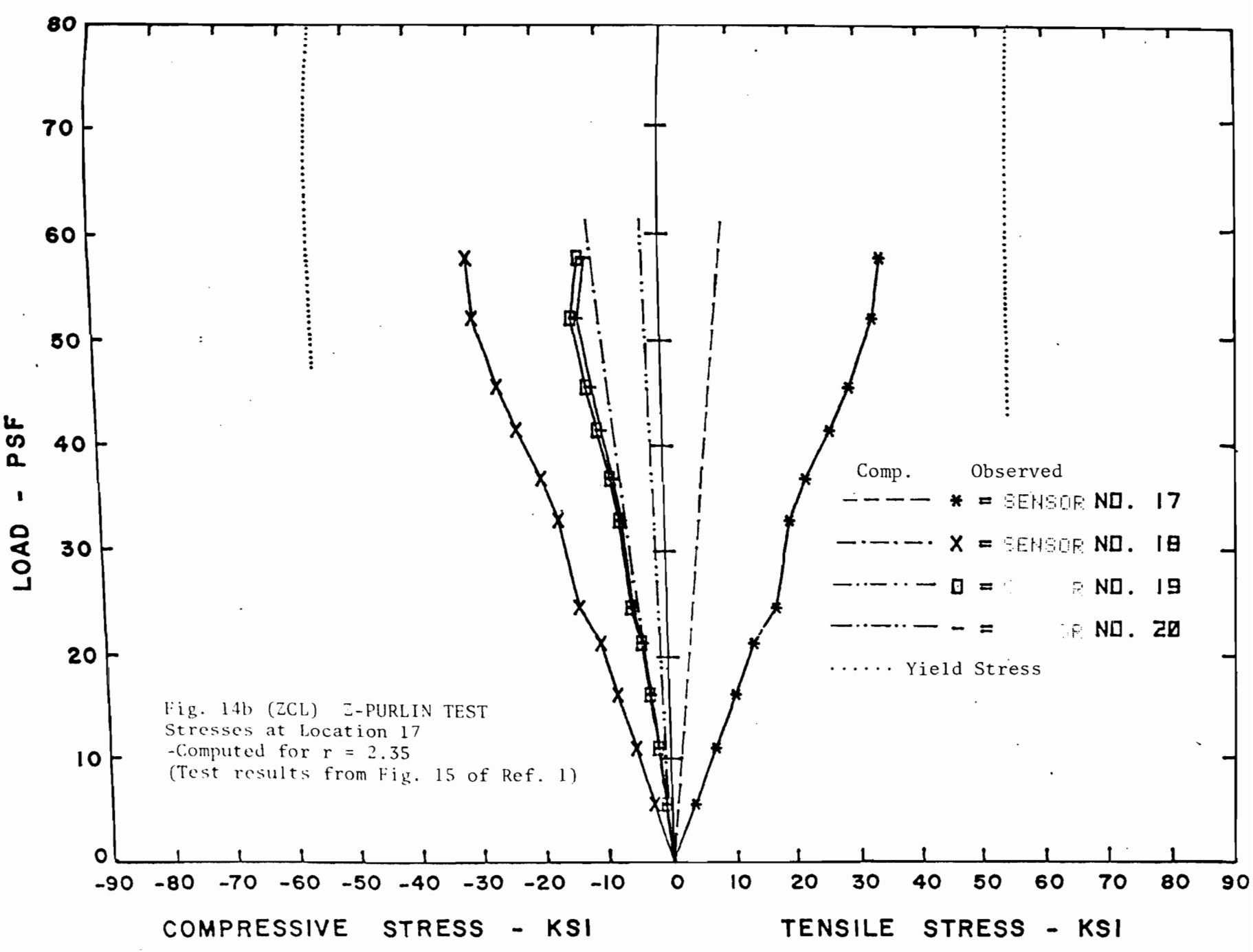

Fig. 14b (ZCL) Z-PURLIN TEST
Stresses at Location 17
-Computed for r = 2.35
(Test results from Fig. 15 of Ref. 1)

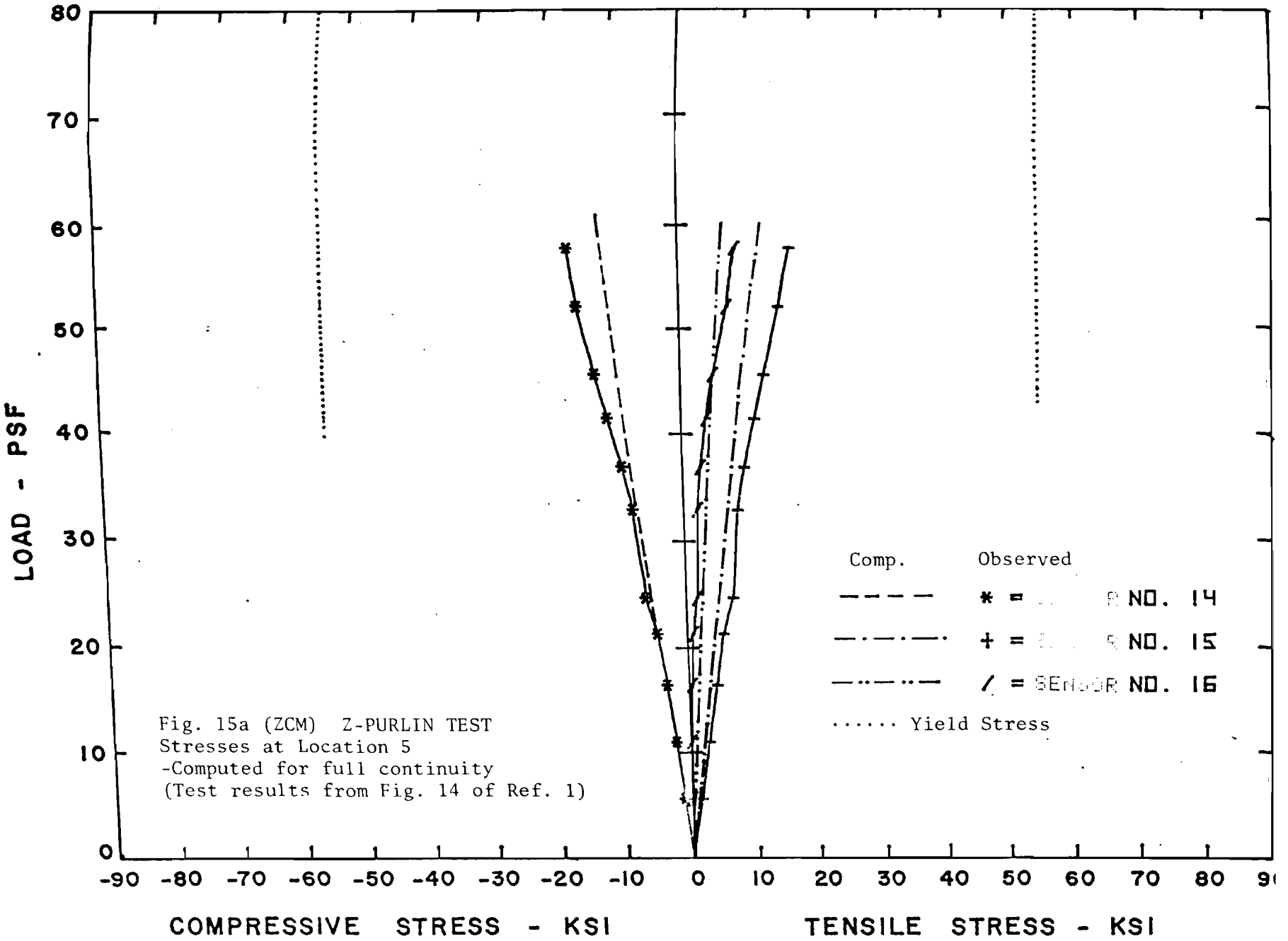

Fig. 15a (ZCM) Z-PURLIN TEST
Stresses at Location 5
-Computed for full continuity
(Test results from Fig. 14 of Ref. 1)

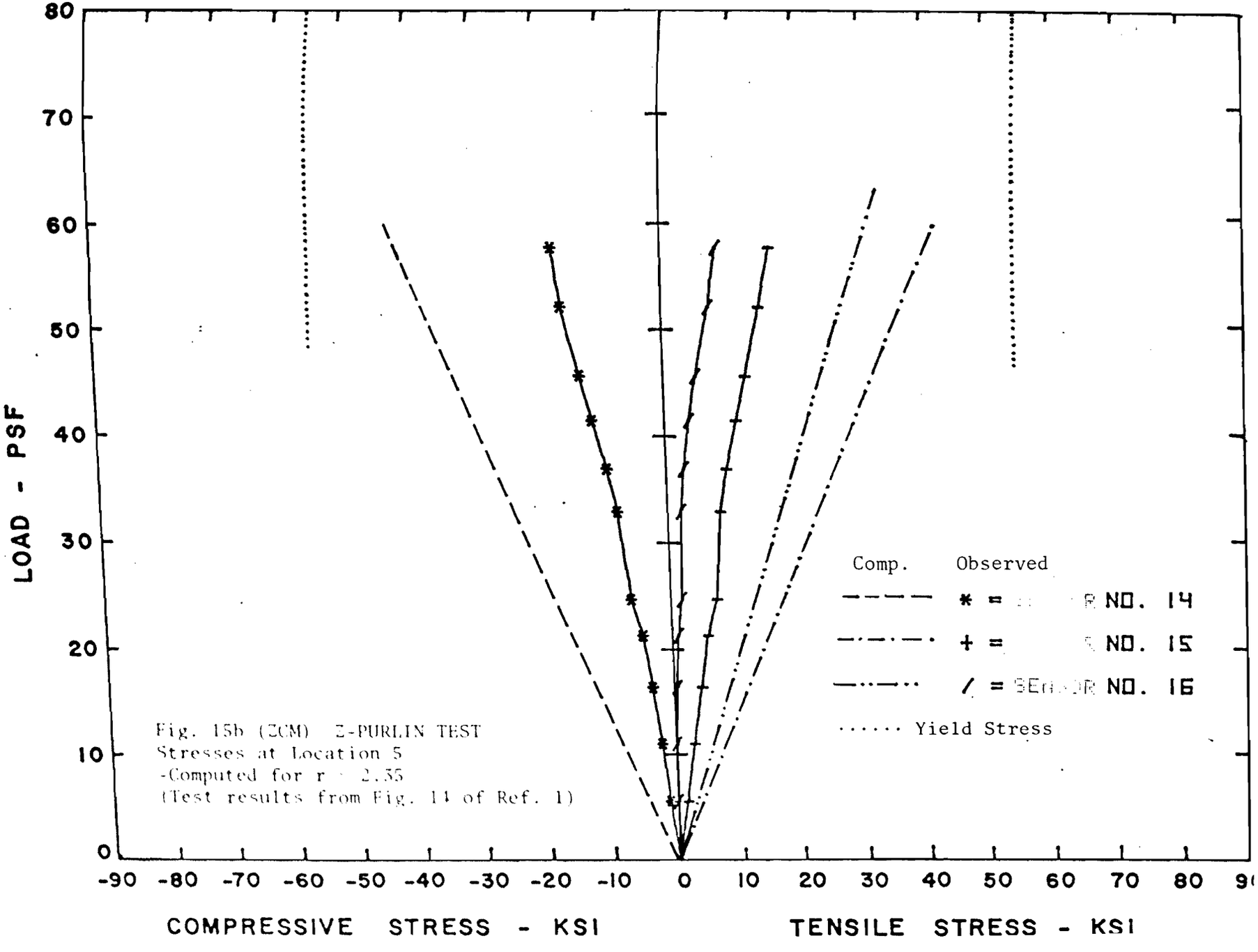

Fig. 15b (ZCM) Z-PURLIN TEST
Stresses at Location 5
-Computed for r = 2.35
(Test results from Fig. 11 of Ref. 1)

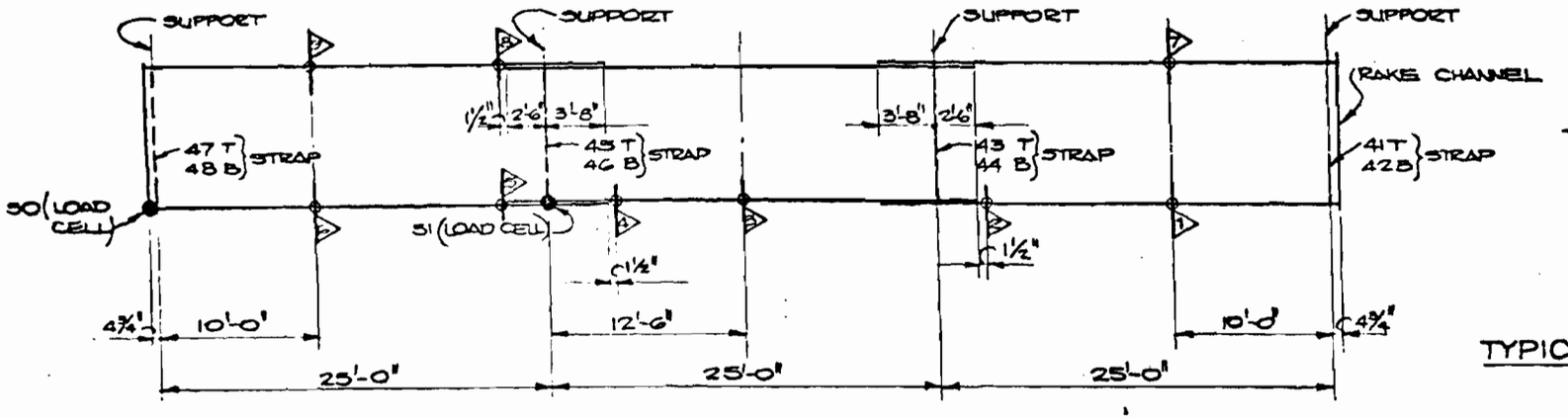

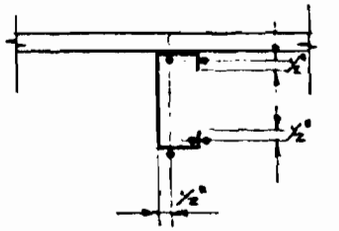

TYPICAL SECTION SHOWING GAGE LOCATION

PLAN VIEW OF 'C' PURLIN TEST

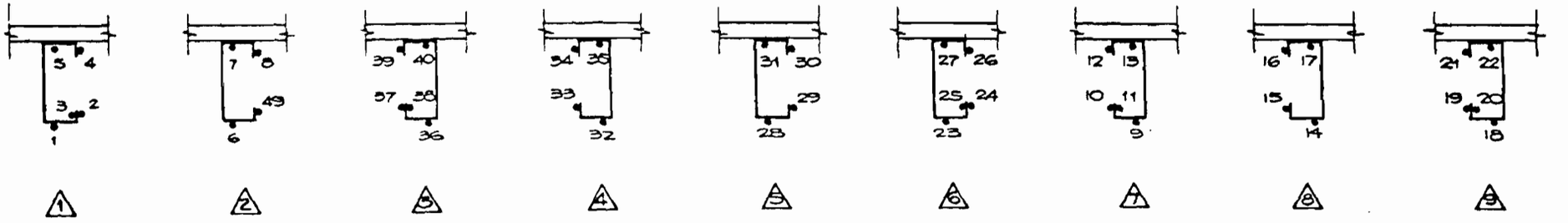

LOCATION FOR ARRAY POINTS 1 TO 51

WISS, JANNEY, ELSTNER AND ASSOCIATES
CONSULTING & RESEARCH ENGINEERS
330 PFINGSTEN ROAD, NORTHBROOK, ILL. 60062

DATE:	STRAIN GAGE LOCATIONS 'C' PURLIN TEST	SHEET NUMBER 5
DRAWN BY: RW		
CHECKED BY: CGS	CLIENT: MBMA	74565
SCALE: 1"=5		

Fig. 16a

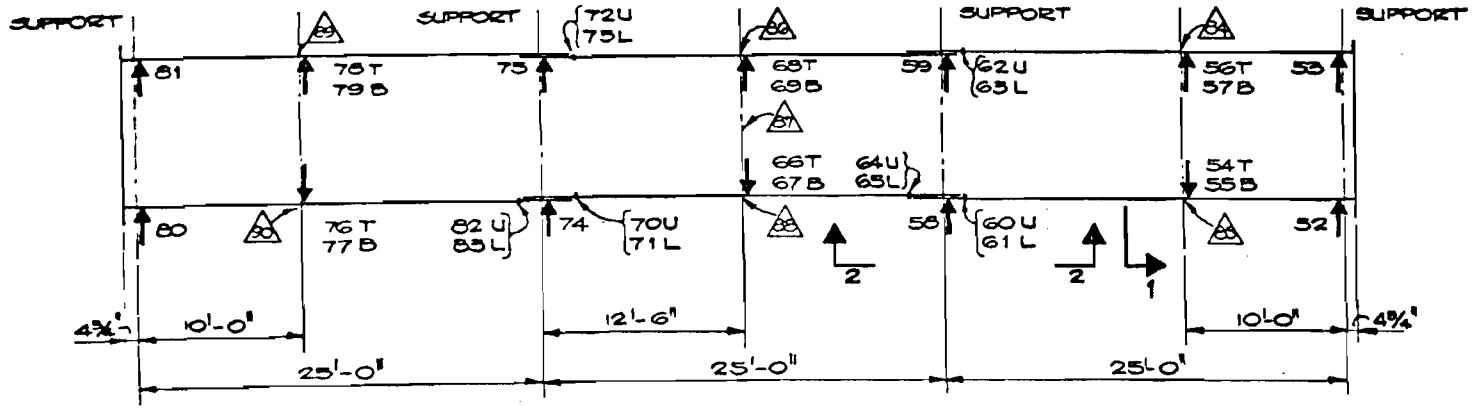

Sensor No.	Dimension A (in.)	B	Sensor No.	Dimension A (in.)	B
52	5.75	-	68T	5.00	-
53	5.375	-	69B	-	1.750
54T	5.50	-	70U	4.250	-
55B	-	2.00	71U	-	1.500
56T	5.50	-	72U	5.125	-
57B	-	2.50	73L	-	2.25
58	4.250	-	74	4.25	-
59	4.625	-	75	4.375	-
60U	5.75	-	76T	5.00	-
61L	-	2.625	77B	-	1.75
62U	5.00	-	78T	5.25	-
63L	-	2.00	79B	-	2.25
64	4.875	-	80	5.750	-
65L	-	2.25	81	5.750	-
66T	4.875	-	82U	4.625	-
67B	-	1.625	83L	-	1.50

PLAN VIEW OF 'C' PURLIN TEST

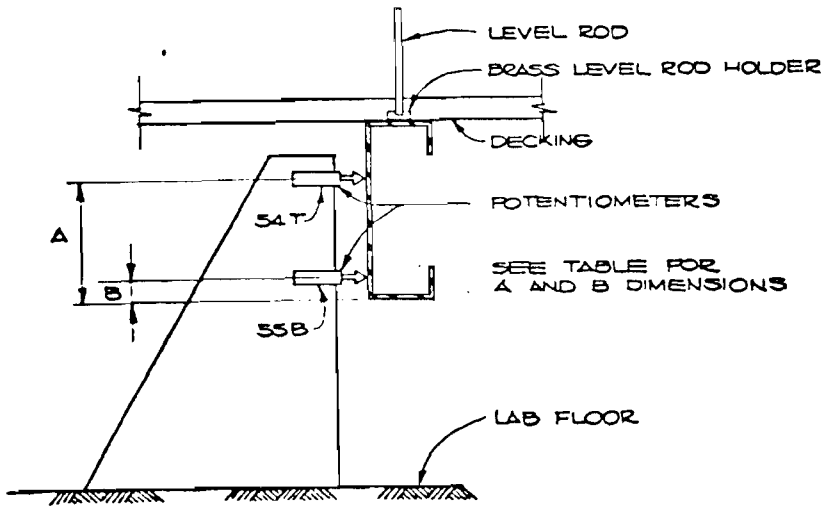

SECTION 1

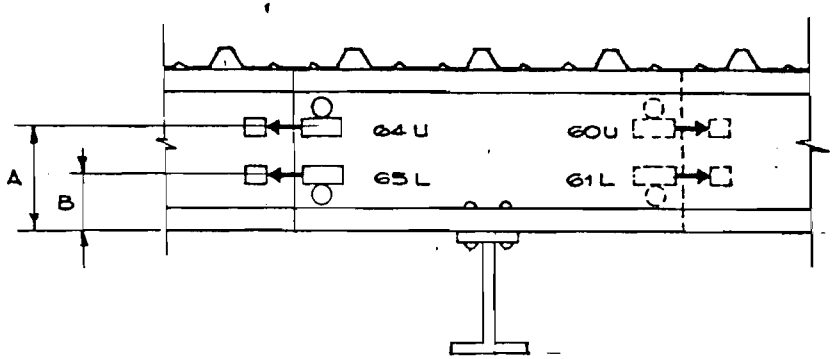

SECTION 2

LOCATION FOR ARRAY POINTS 52 TO 90

WISS, JANNEY, ELSTNER AND ASSOCIATES
CONSULTING & RESEARCH ENGINEERS
330 PFINGSTEN ROAD, NORTHBROOK, ILL. 60062

DATE:	DISPLACEMENT INSTRUMENTAT. 'C' PURLIN TEST	SHEET NUMBER 6
DRAWN BY: R.M.		
CHECKED BY: O.C.G.	CLIENT: MBMA	74565
SCALE: NTS		

Fig. 16b

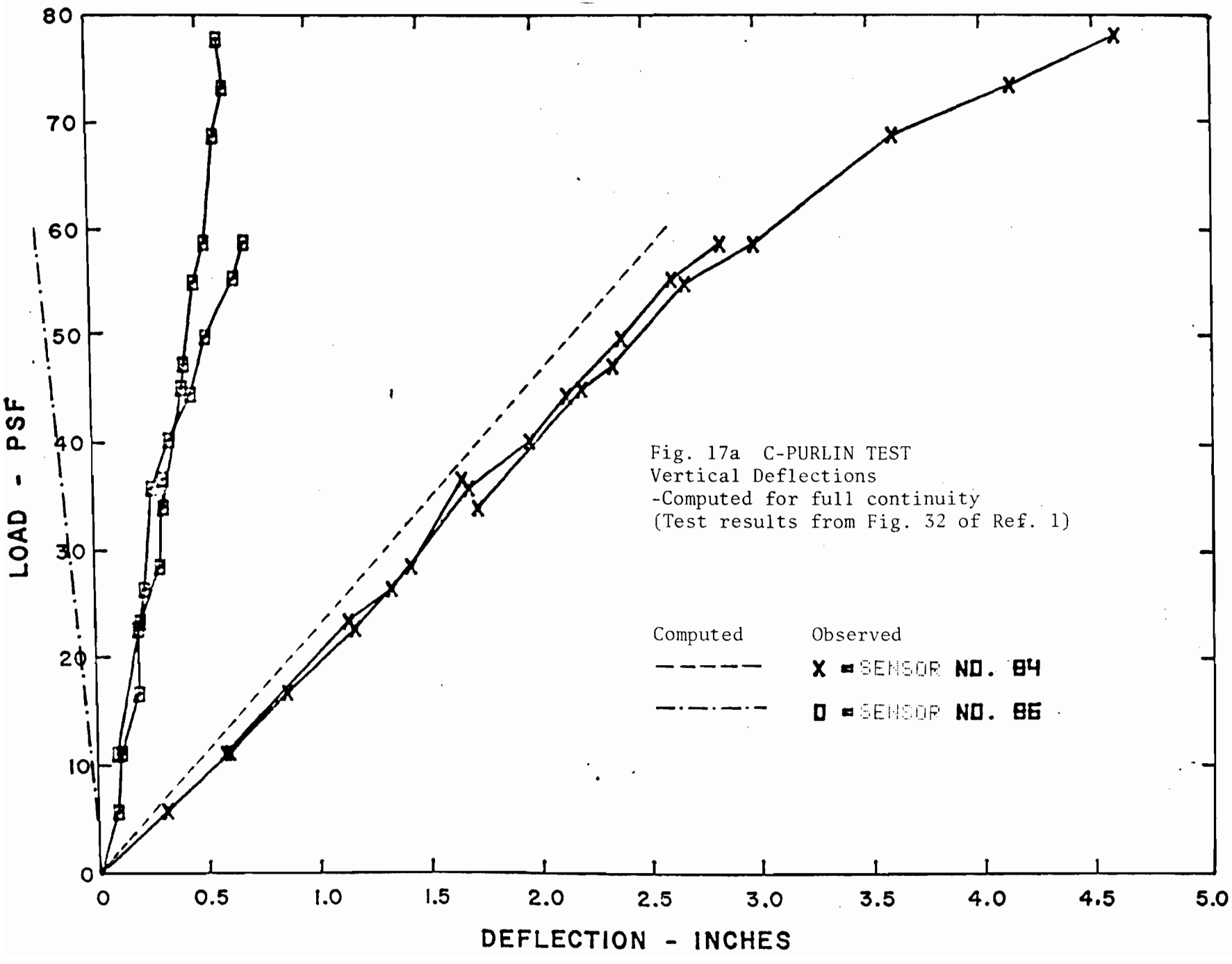

Fig. 17a C-PURLIN TEST
Vertical Deflections
-Computed for full continuity
(Test results from Fig. 32 of Ref. 1)

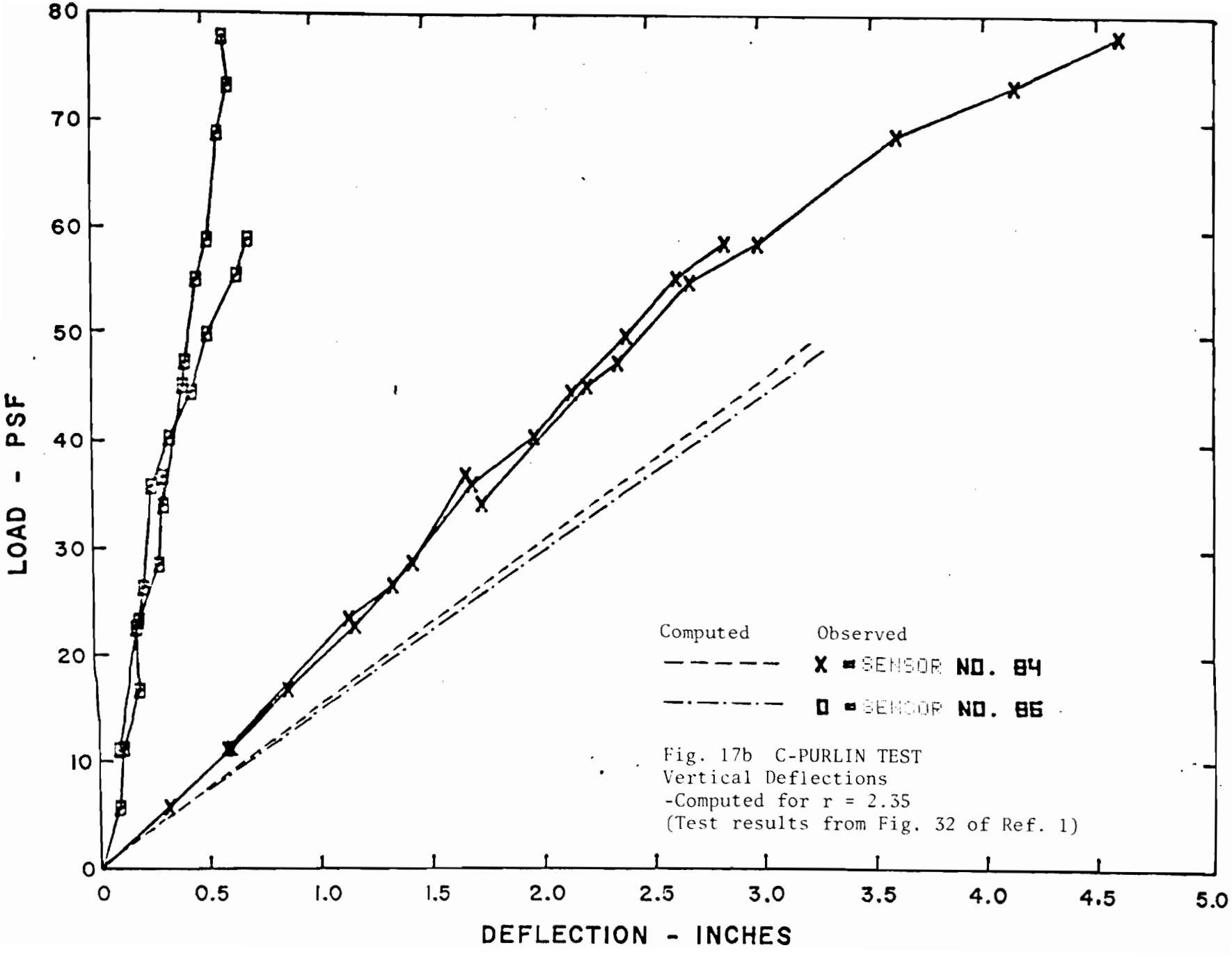

Fig. 17b C-PURLIN TEST
Vertical Deflections
-Computed for r = 2.35
(Test results from Fig. 32 of Ref. 1)

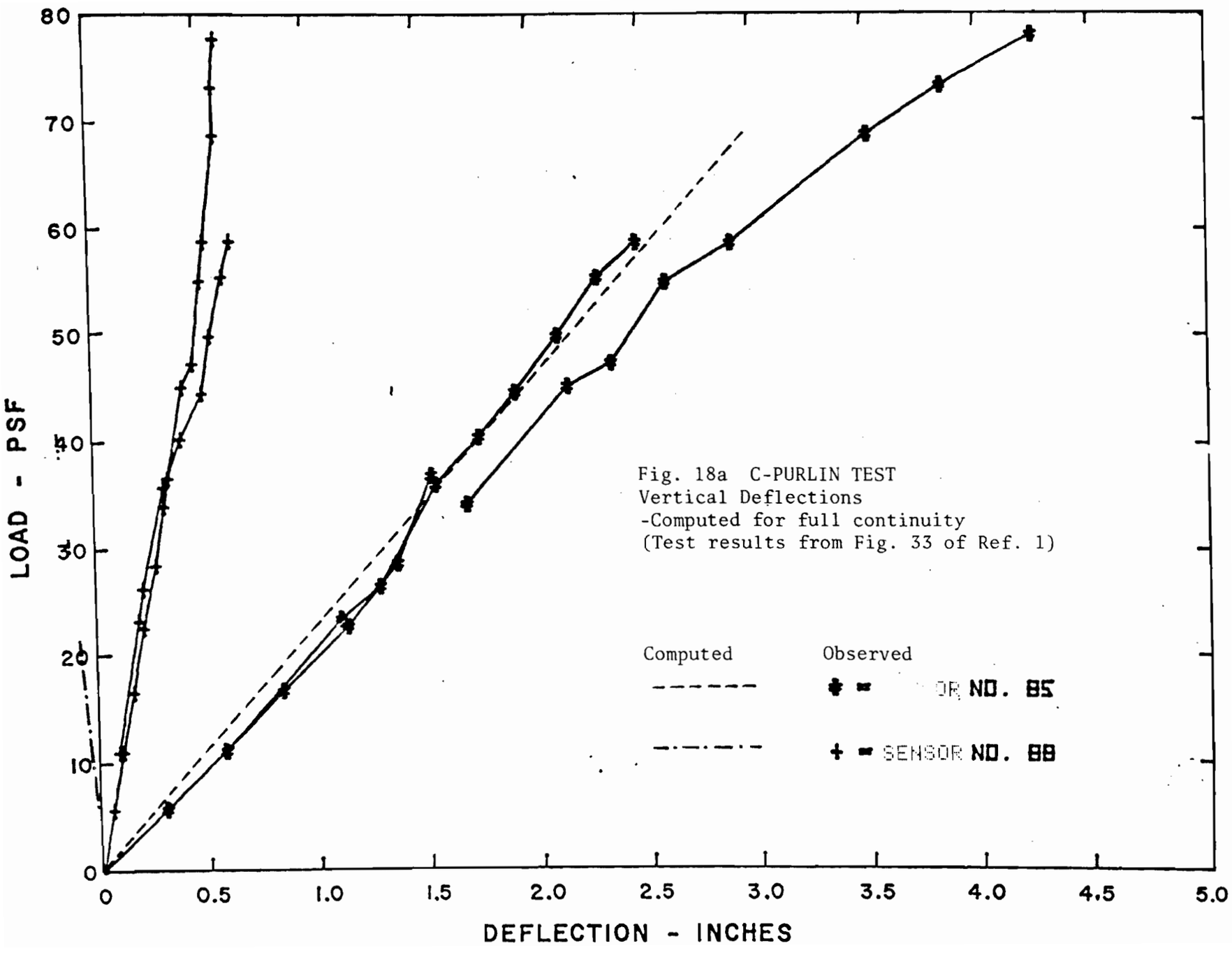

Fig. 18a C-PURLIN TEST
Vertical Deflections
-Computed for full continuity
(Test results from Fig. 33 of Ref. 1)

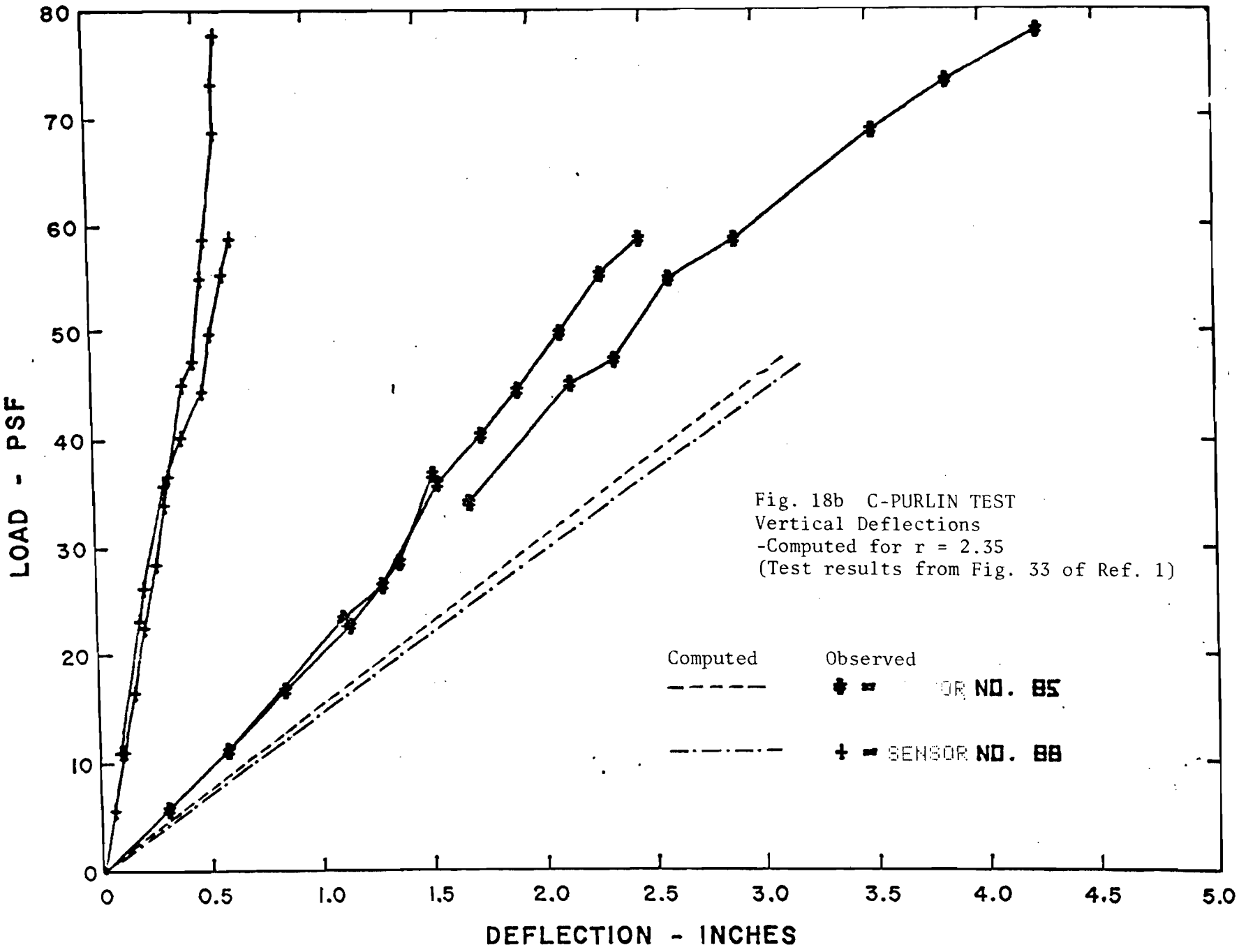

Fig. 18b C-PURLIN TEST
Vertical Deflections
-Computed for r = 2.35
(Test results from Fig. 33 of Ref. 1)

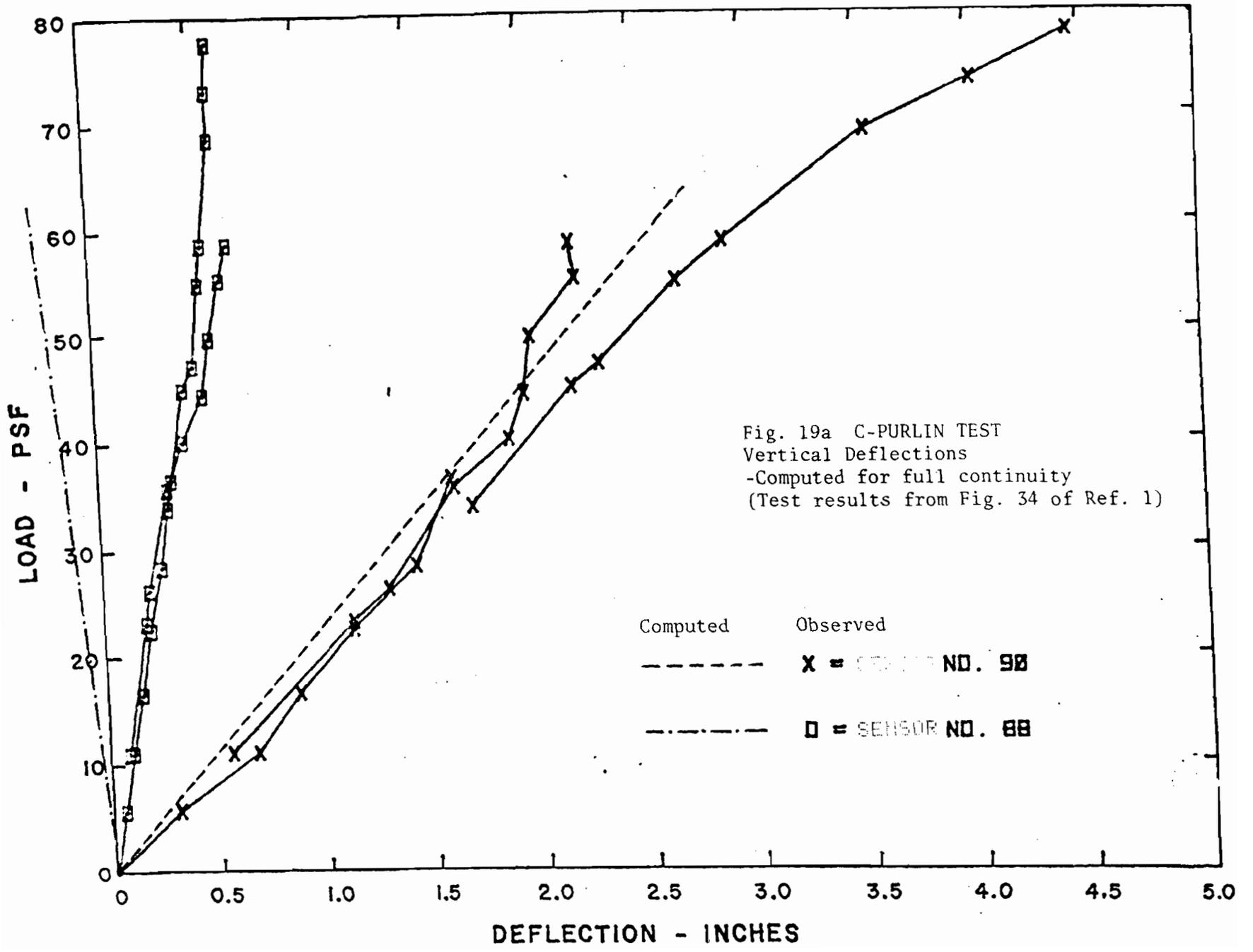

Fig. 19a C-PURLIN TEST
Vertical Deflections
-Computed for full continuity
(Test results from Fig. 34 of Ref. 1)

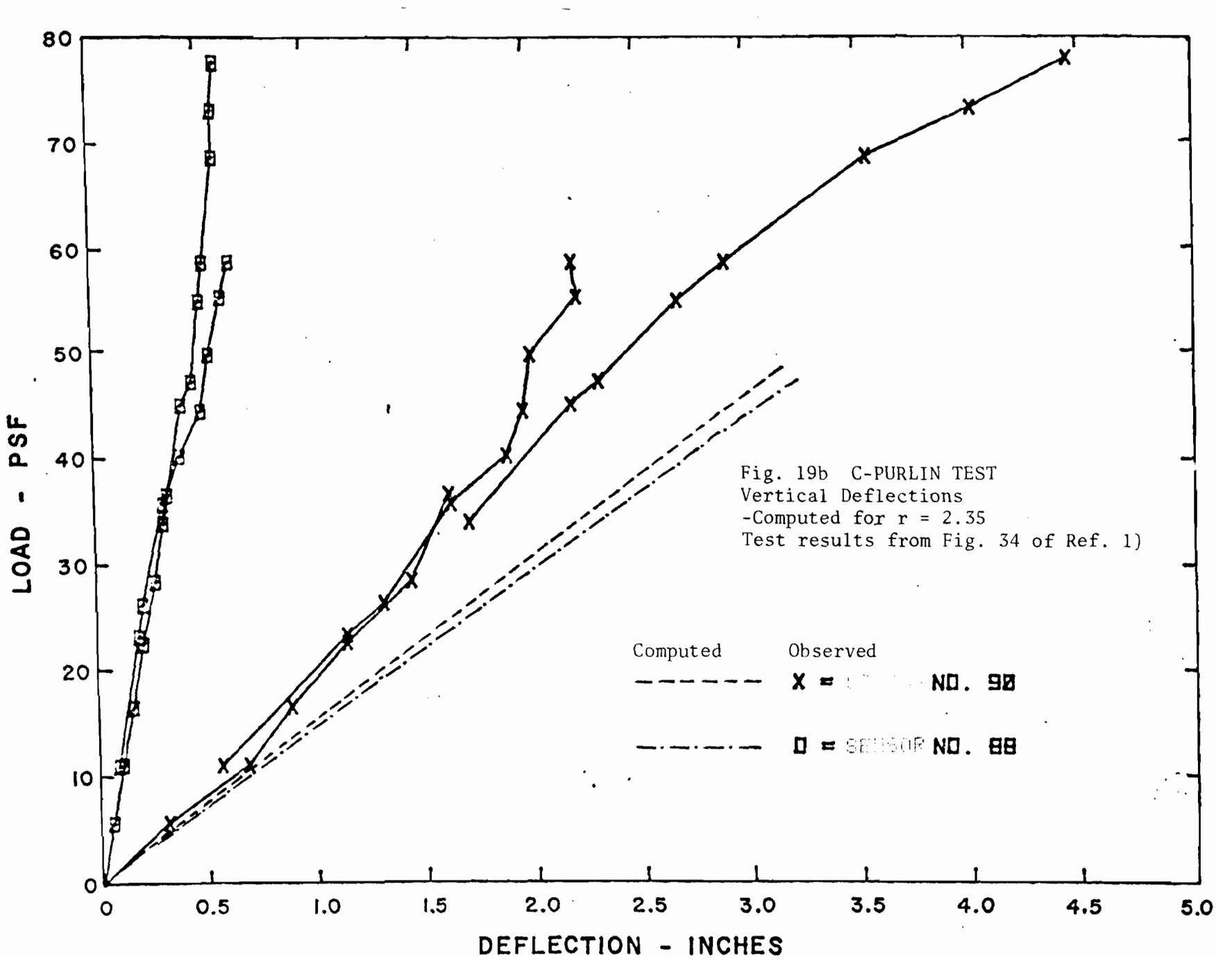

Fig. 19b C-PURLIN TEST
Vertical Deflections
-Computed for r = 2.35
Test results from Fig. 34 of Ref. 1)

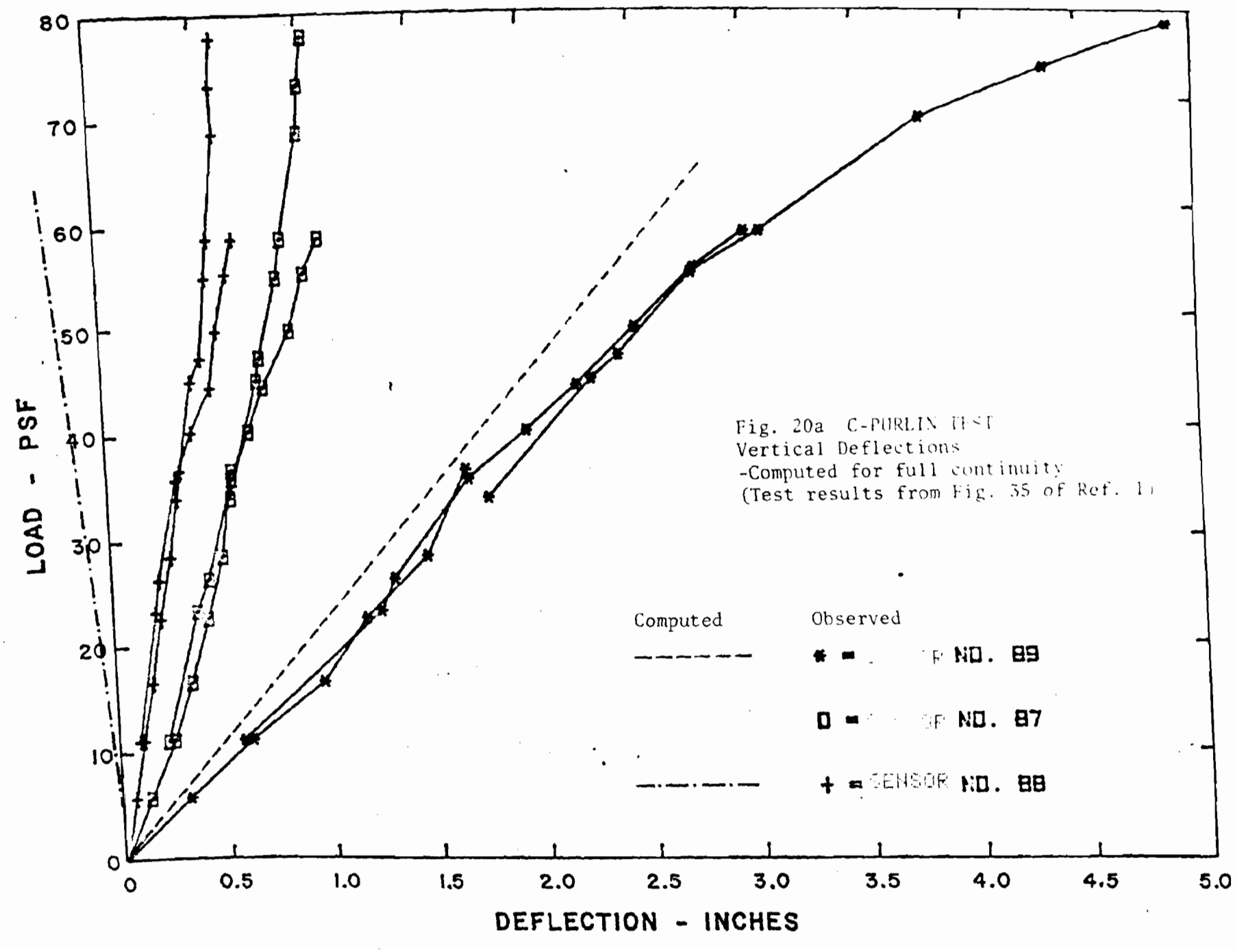

Fig. 20a C-PURLIN TEST
Vertical Deflections
-Computed for full continuity
(Test results from Fig. 35 of Ref. 1)

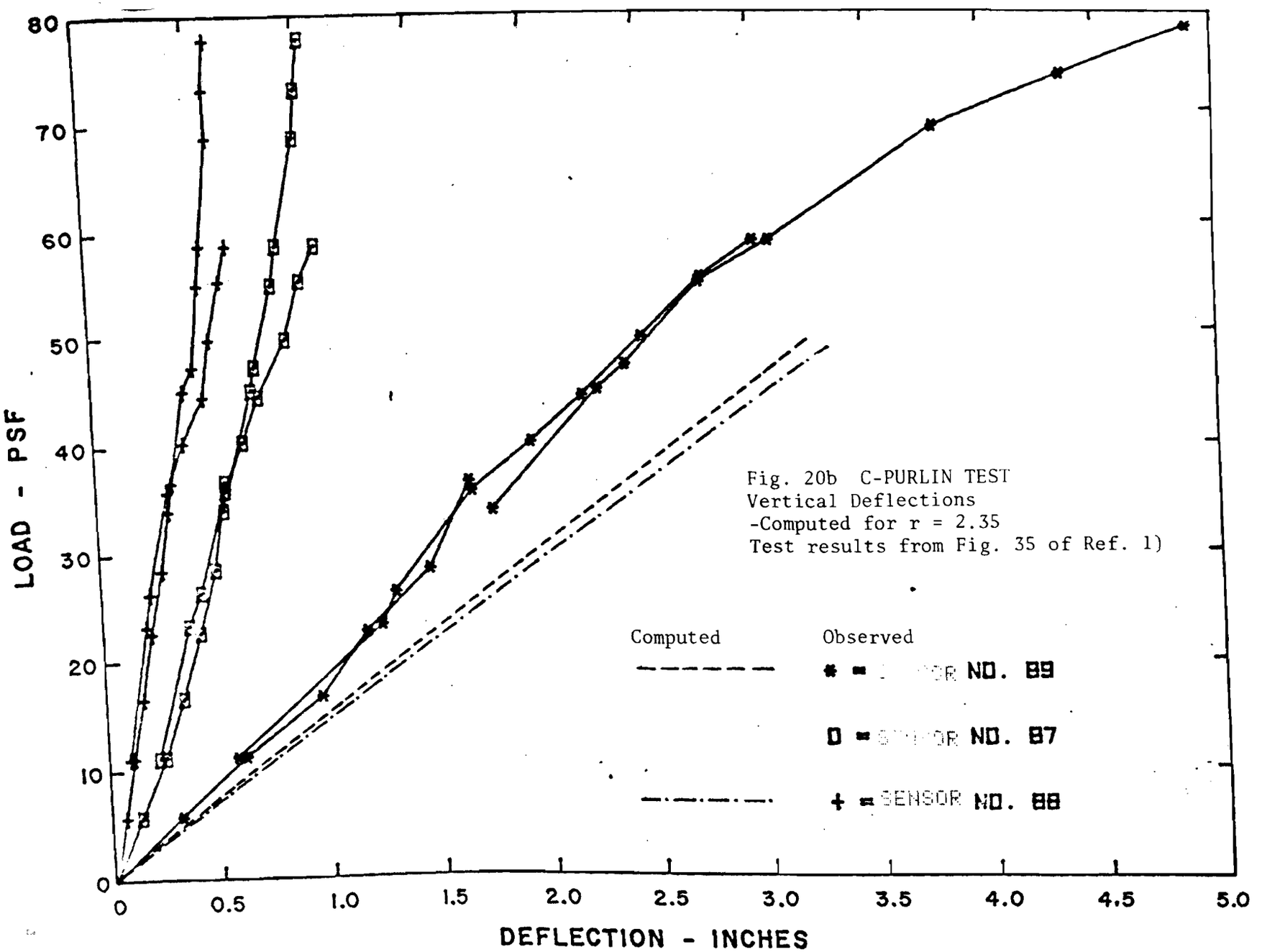

Fig. 20b C-PURLIN TEST
Vertical Deflections
-Computed for r = 2.35
Test results from Fig. 35 of Ref. 1)

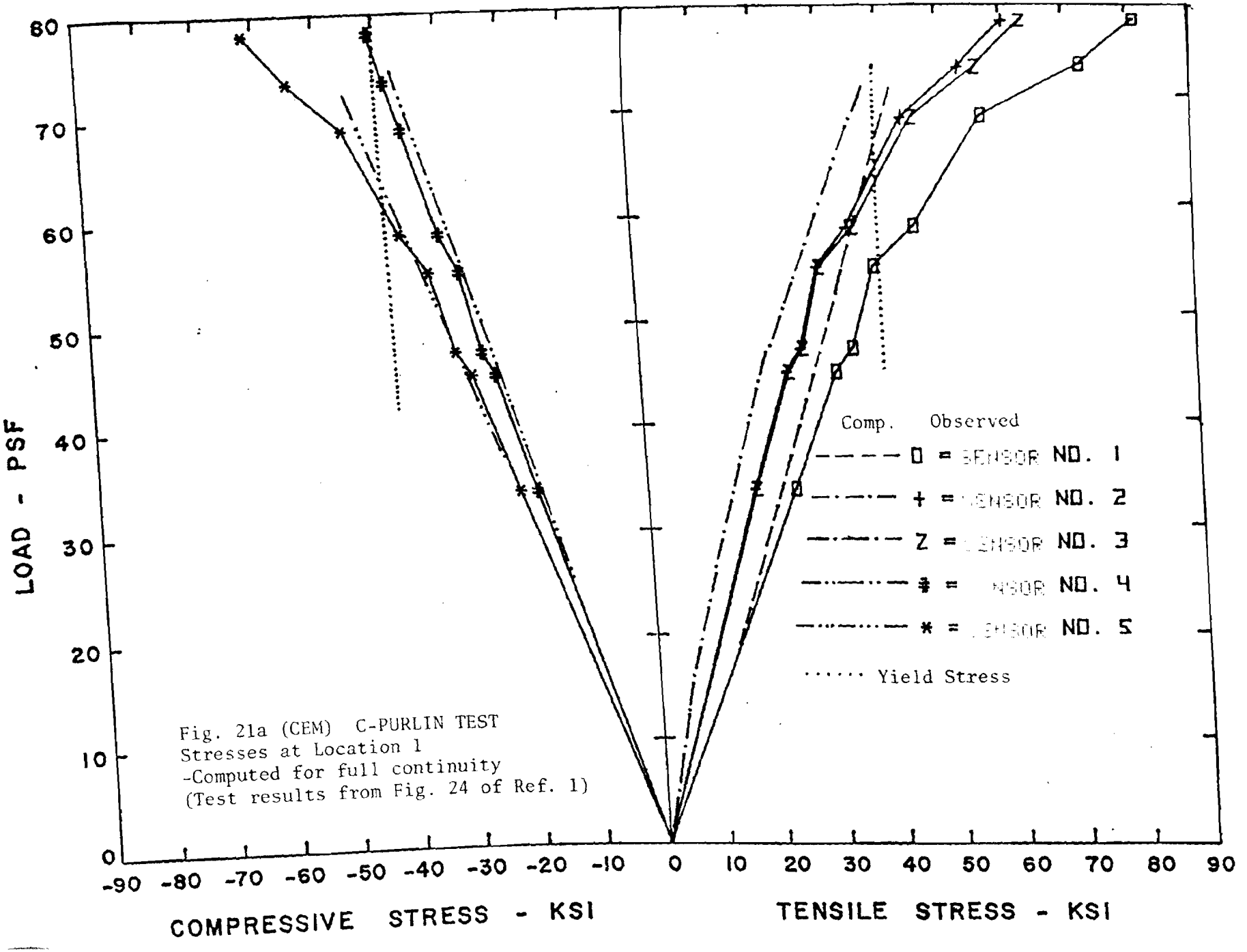

Fig. 21a (CEM) C-PURLIN TEST
Stresses at Location 1
-Computed for full continuity
(Test results from Fig. 24 of Ref. 1)

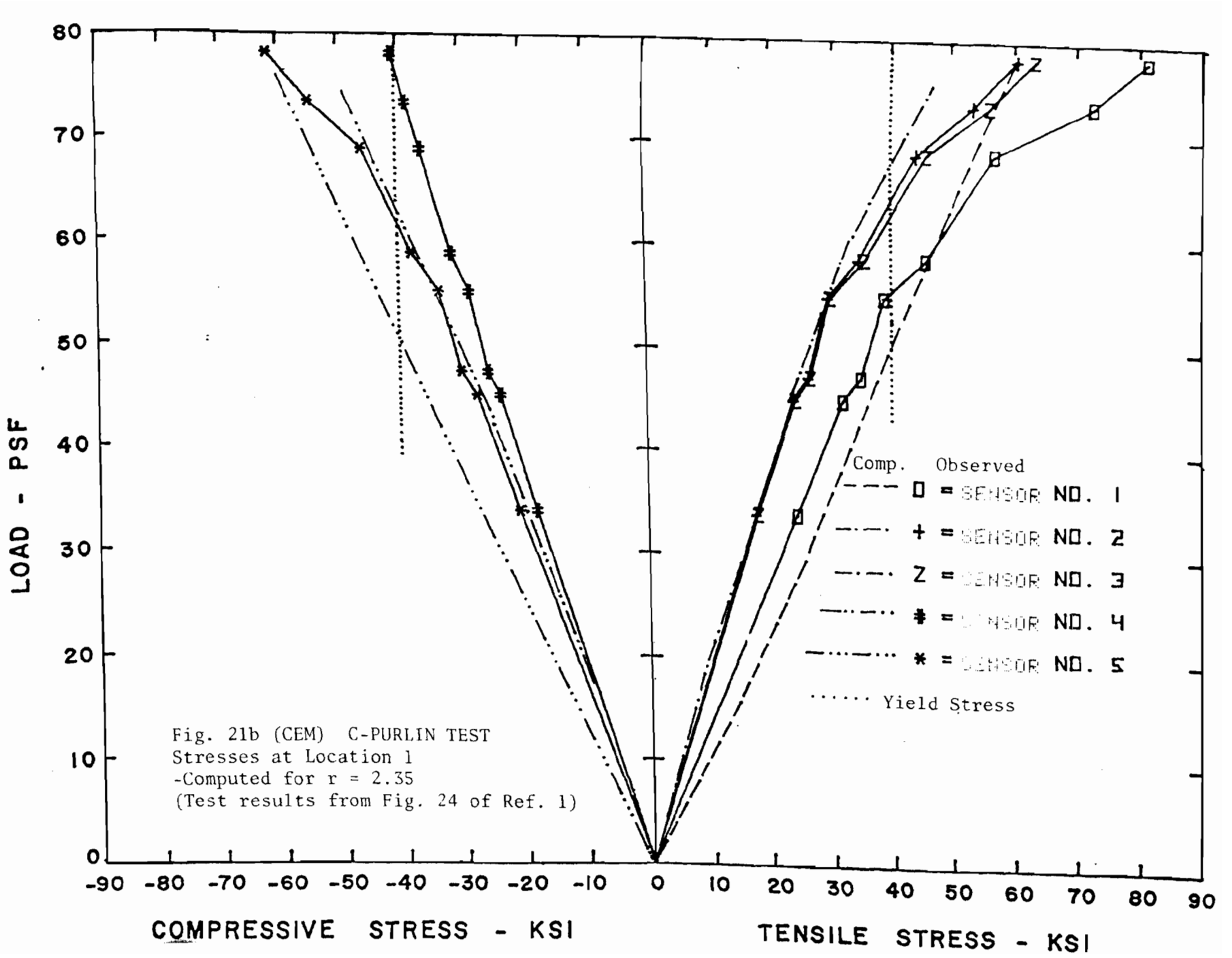

Fig. 21b (CEM) C-PURLIN TEST
Stresses at Location 1
-Computed for r = 2.35
(Test results from Fig. 24 of Ref. 1)

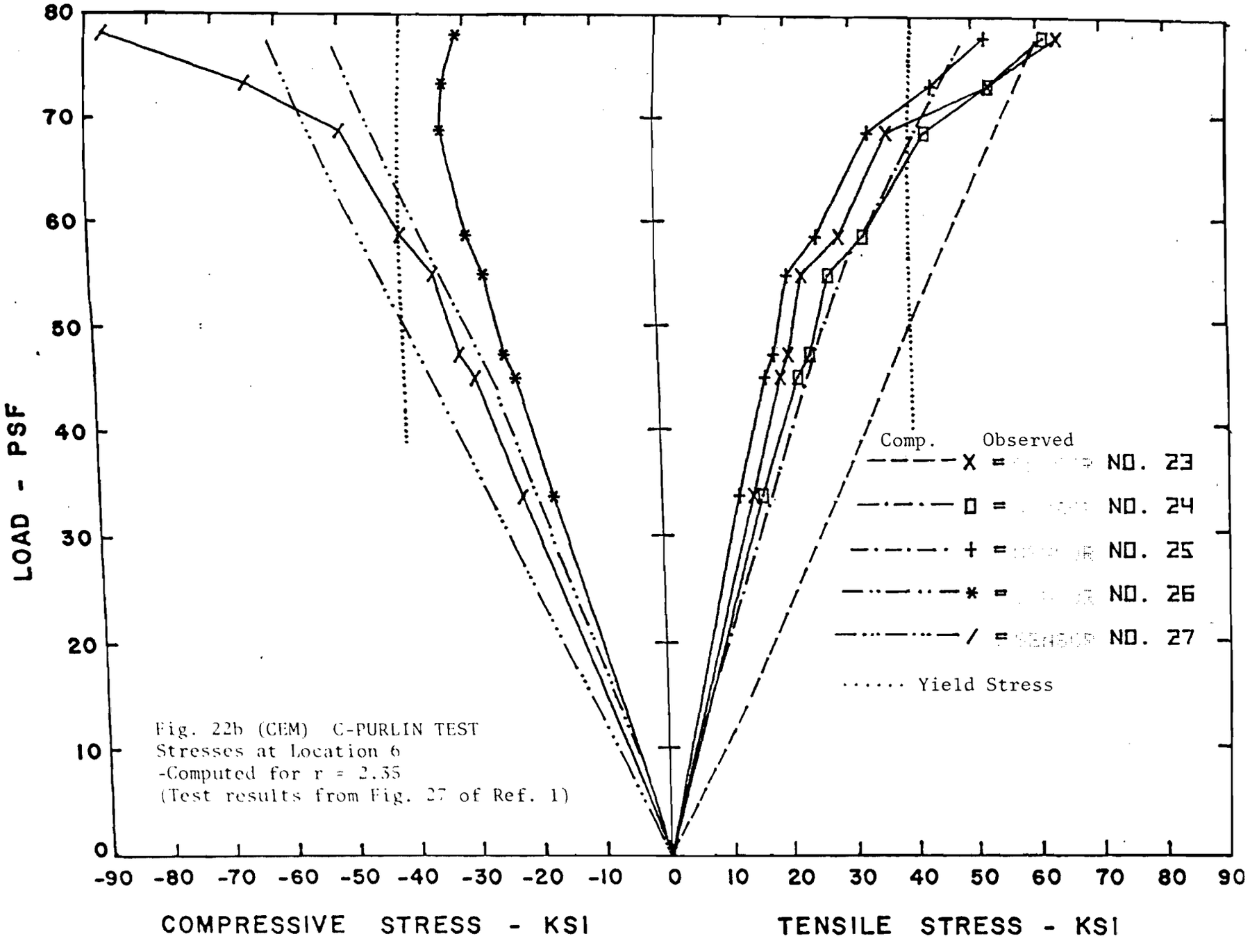
LOAD - PSF
80
70
60
50
40
30
20
10
0
-90 -80 -70 -60 -50 -40 -30 -20 -10 0 10 20 30 40 50 60 70 80 90
COMPRESSIVE STRESS - KSI
TENSILE STRESS - KSI
Comp. Observed
X = NO. 23
□ = NO. 24
+ = NO. 25
* = NO. 26
/ = NO. 27
Yield Stress
Fig. 22b (CEM) C-PURLIN TEST
Stresses at Location 6
-Computed for r = 2.35
(Test results from Fig. 27 of Ref. 1)

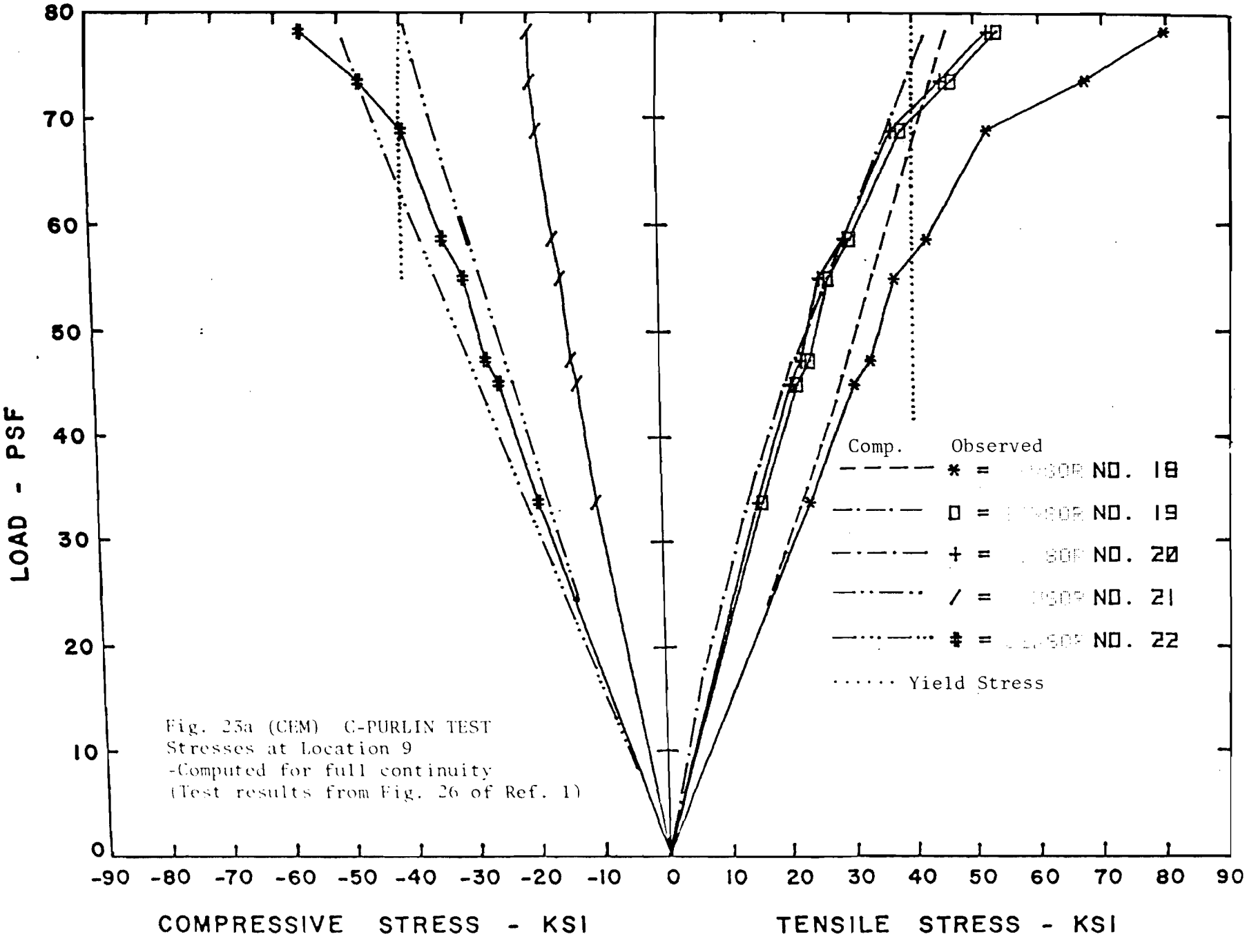

Fig. 23a (CEM) C-PURLIN TEST
Stresses at Location 9
-Computed for full continuity
(Test results from Fig. 26 of Ref. 1)

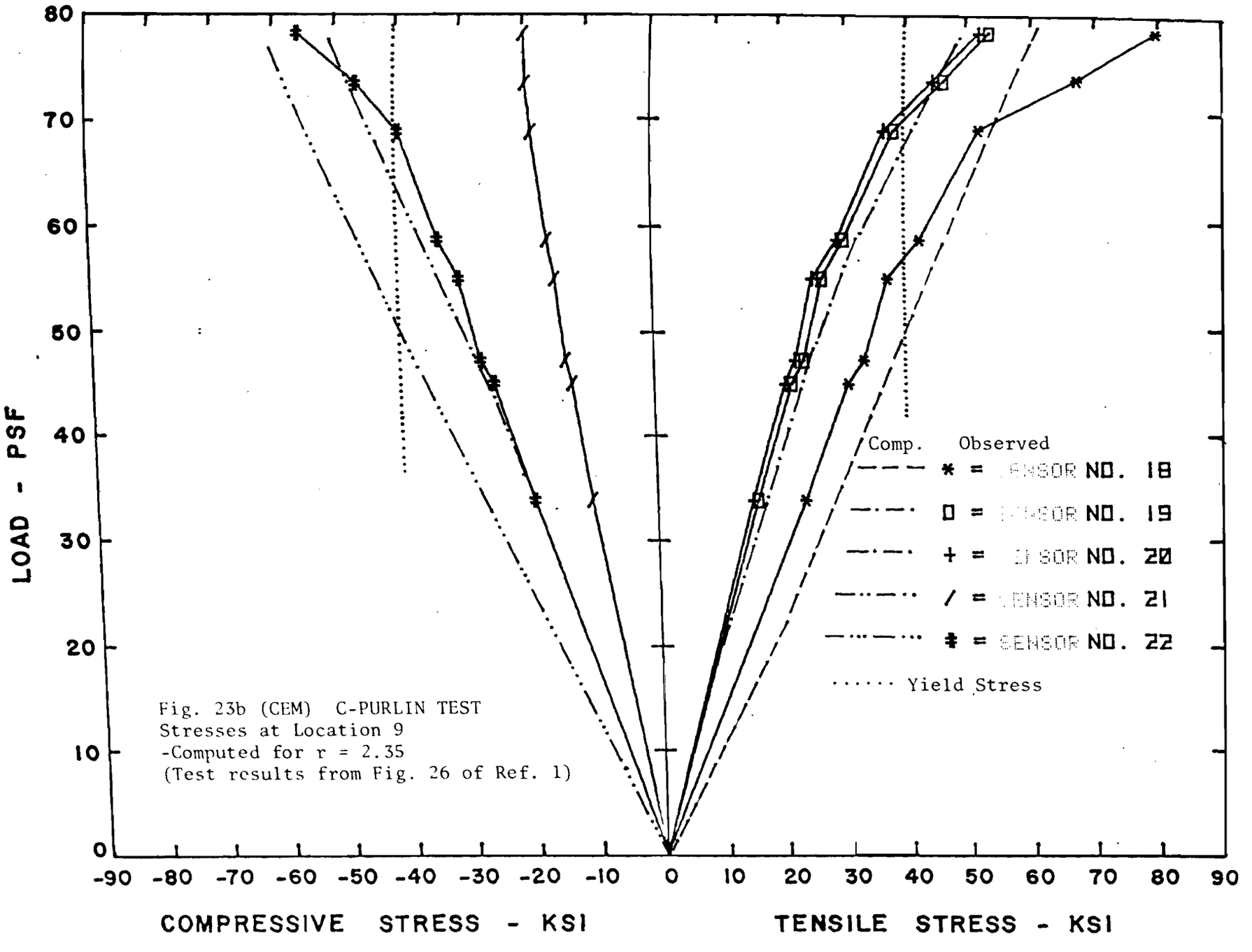

Fig. 23b (CEM) C-PURLIN TEST
Stresses at Location 9
-Computed for r = 2.35
(Test results from Fig. 26 of Ref. 1)

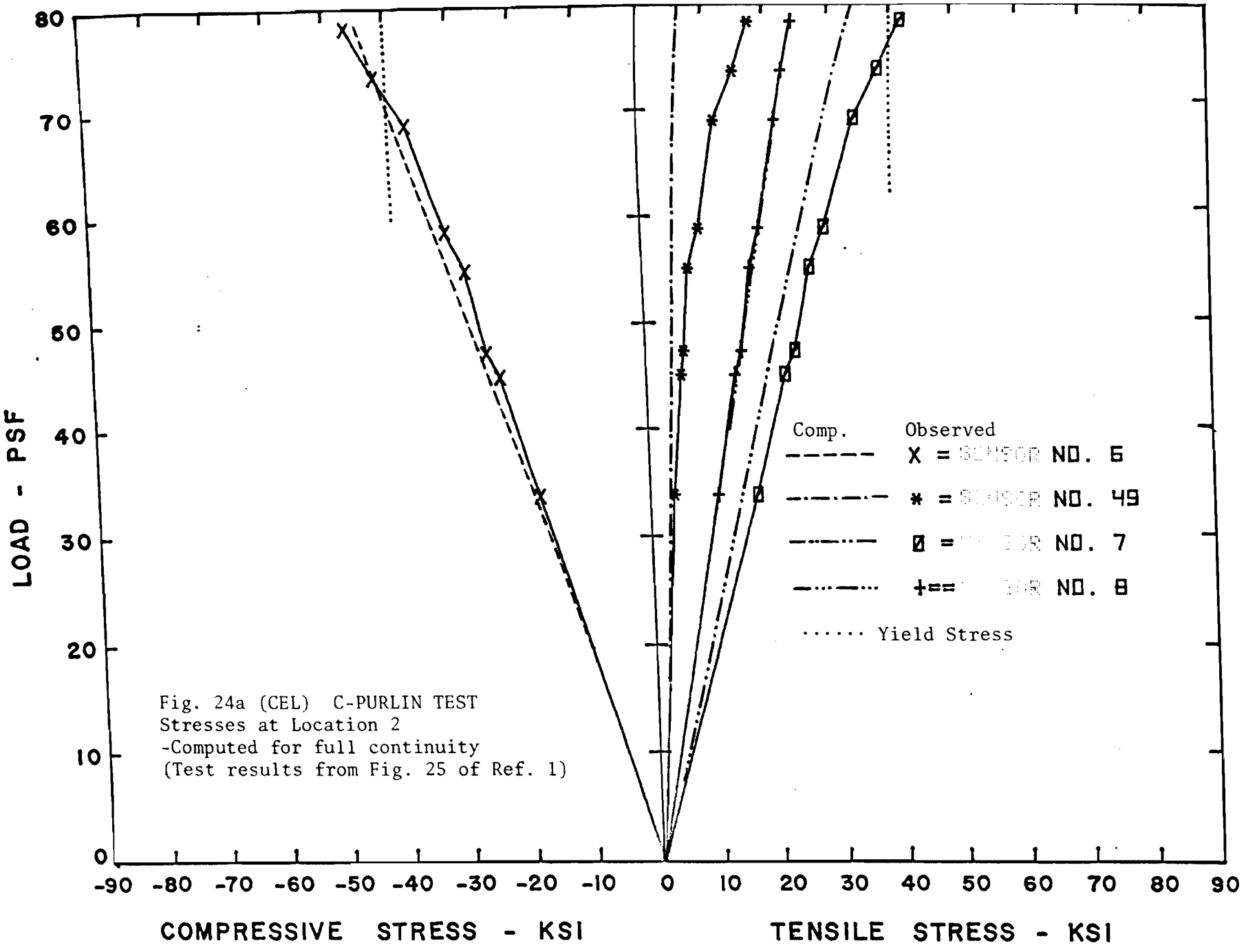

Fig. 24a (CEL) C-PURLIN TEST
Stresses at Location 2
-Computed for full continuity
(Test results from Fig. 25 of Ref. 1)

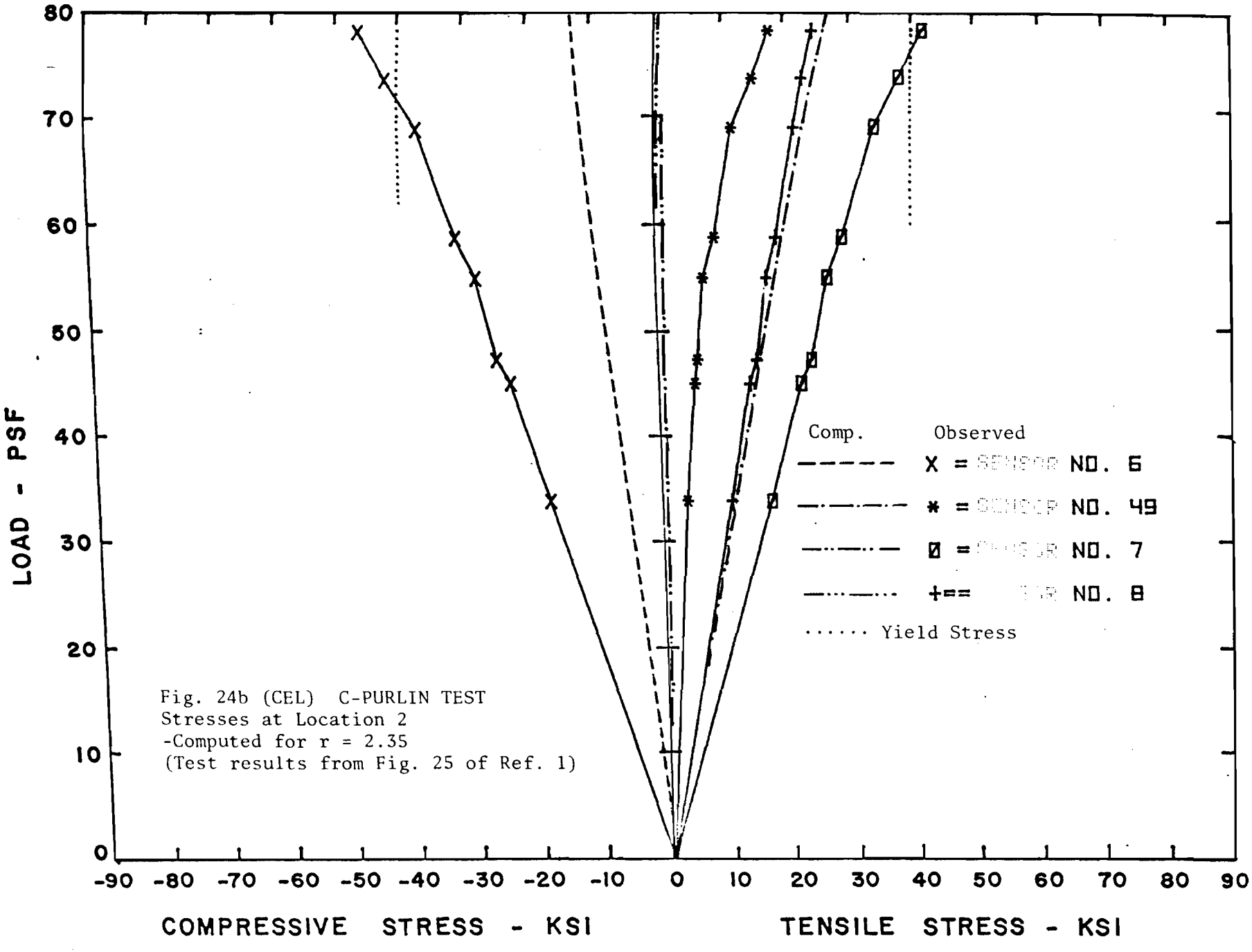

Fig. 24b (CEL) C-PURLIN TEST
Stresses at Location 2
-Computed for r = 2.35
(Test results from Fig. 25 of Ref. 1)

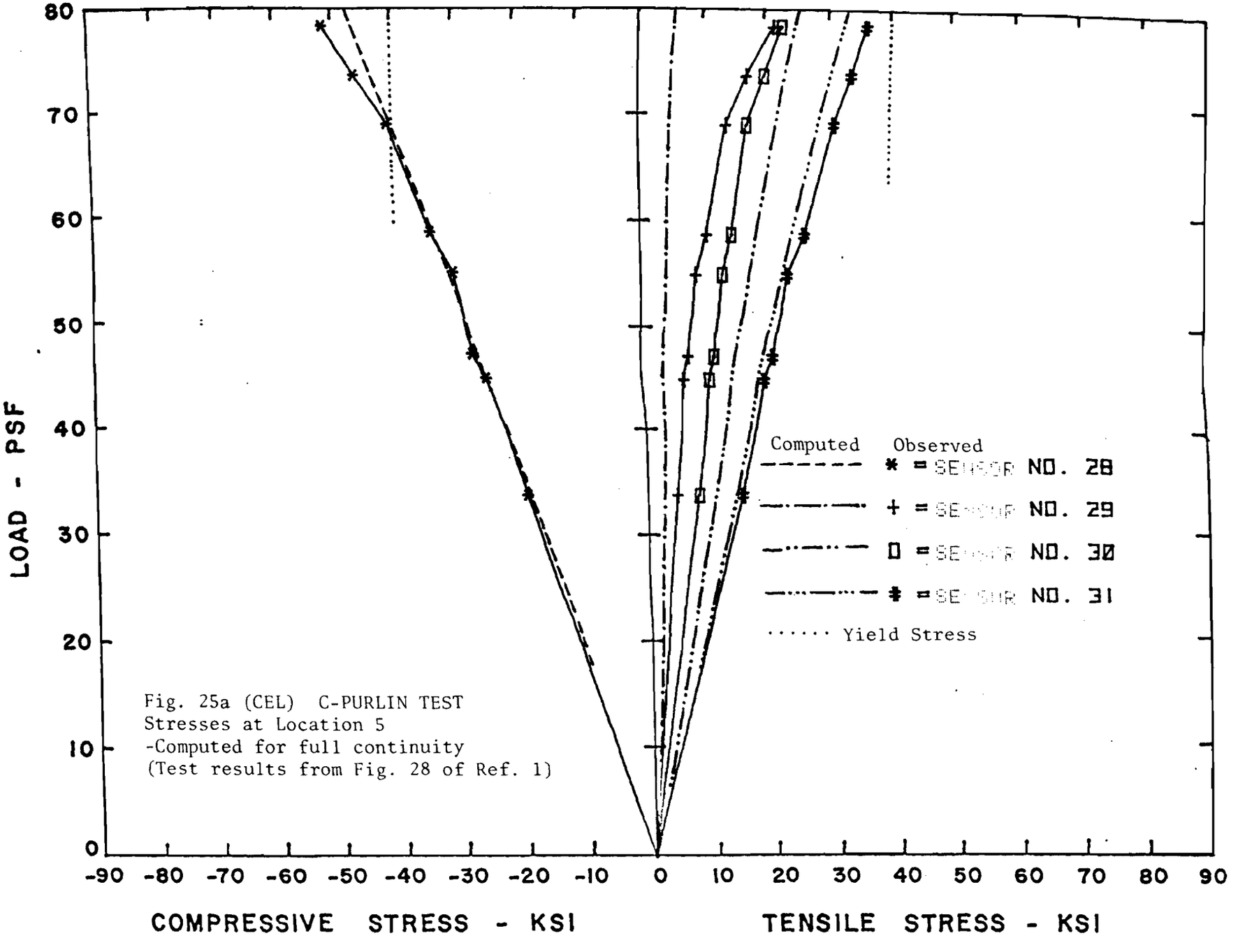

Fig. 25a (CEL) C-PURLIN TEST
Stresses at Location 5
-Computed for full continuity
(Test results from Fig. 28 of Ref. 1)

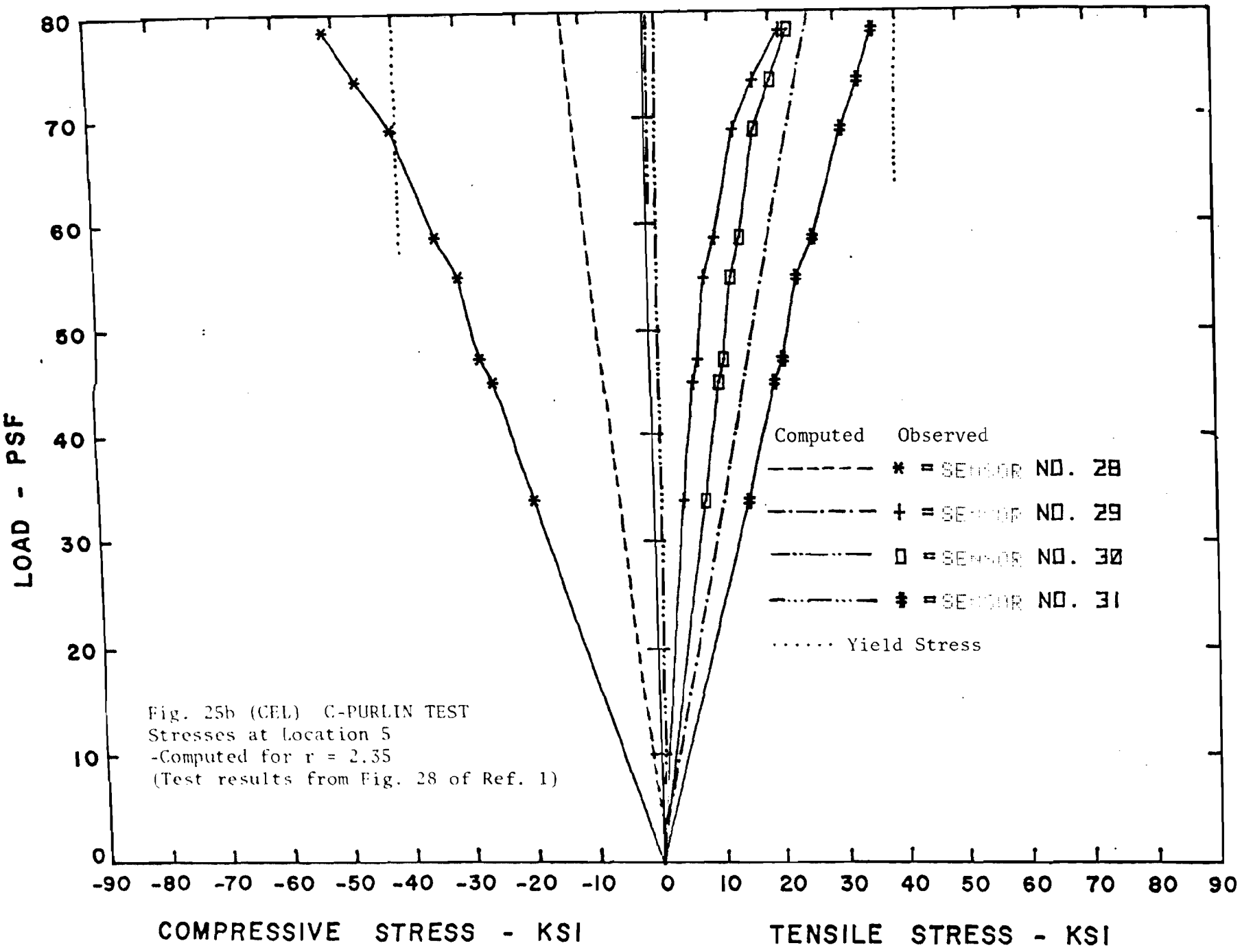

Fig. 25b (CEL) C-PURLIN TEST
Stresses at Location 5
-Computed for r = 2.35
(Test results from Fig. 28 of Ref. 1)

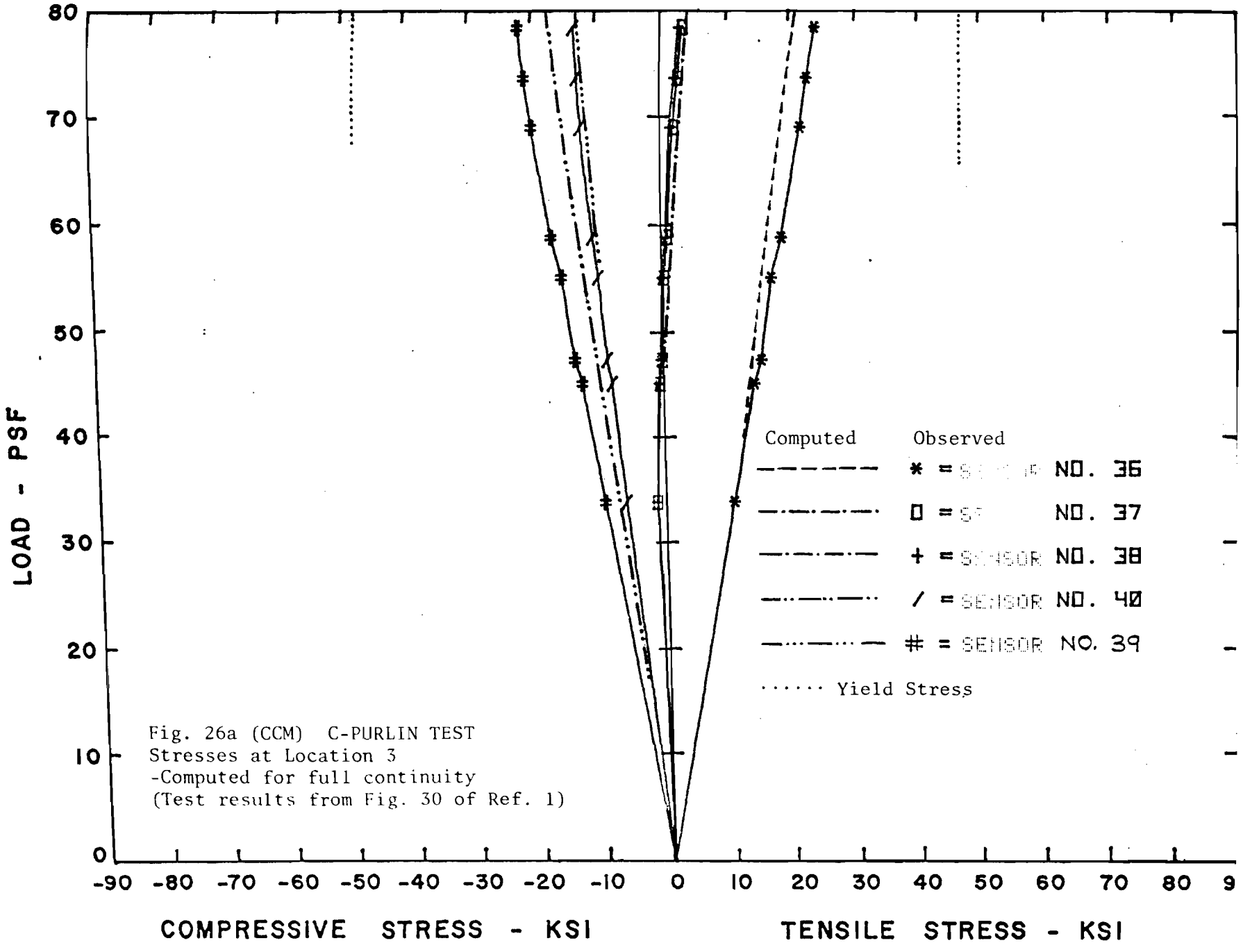

Fig. 26a (CCM) C-PURLIN TEST
Stresses at Location 3
-Computed for full continuity
(Test results from Fig. 30 of Ref. 1)

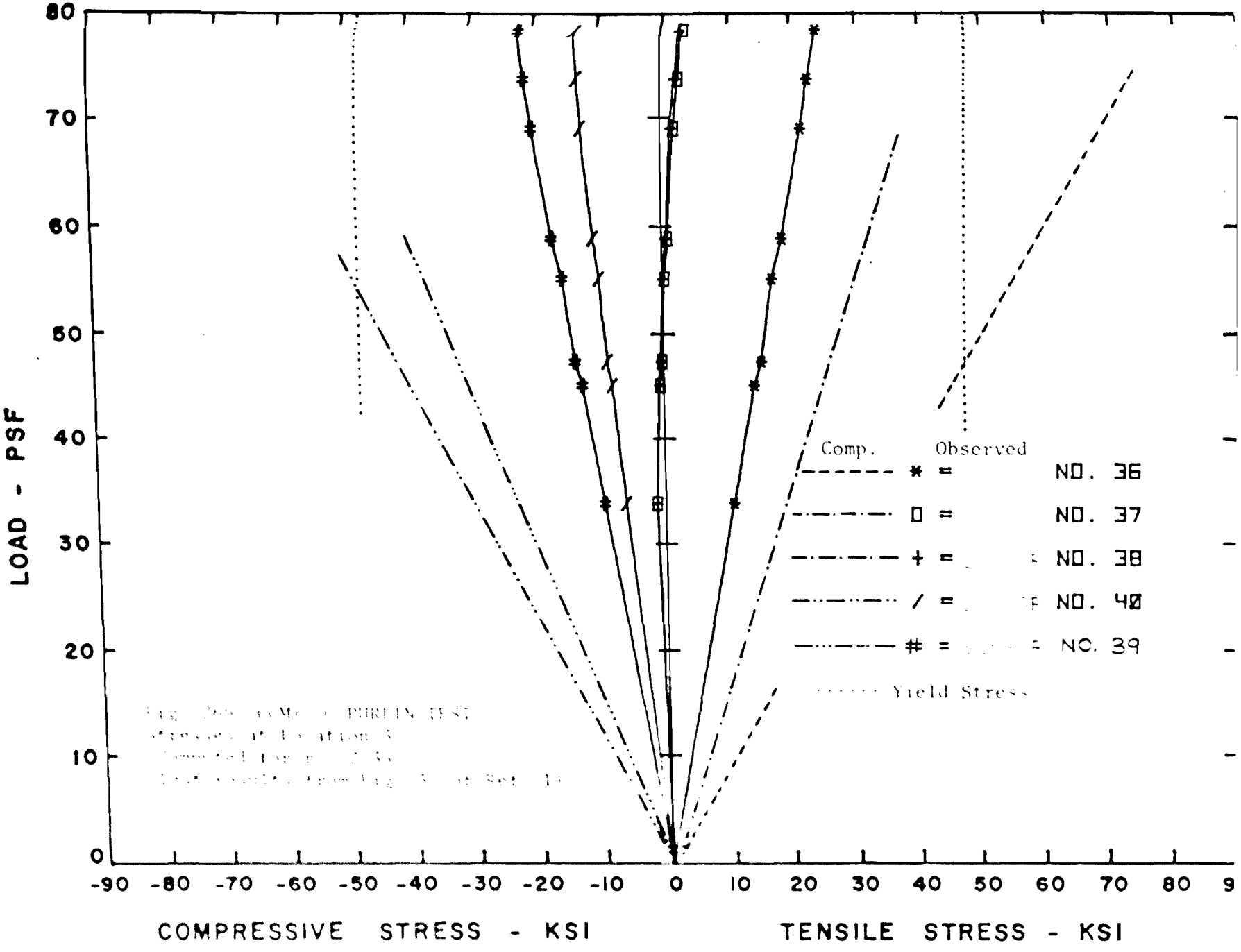
LOAD - PSF
80
70
60
50
40
30
20
10
0
-90 -80 -70 -60 -50 -40 -30 -20 -10 0 10 20 30 40 50 60 70 80 9
COMPRESSIVE STRESS - KSI
TENSILE STRESS - KSI
Comp. Observed
* = NO. 36
□ = NO. 37
+ = NO. 38
/ = NO. 40
= NO. 39
Yield Stress

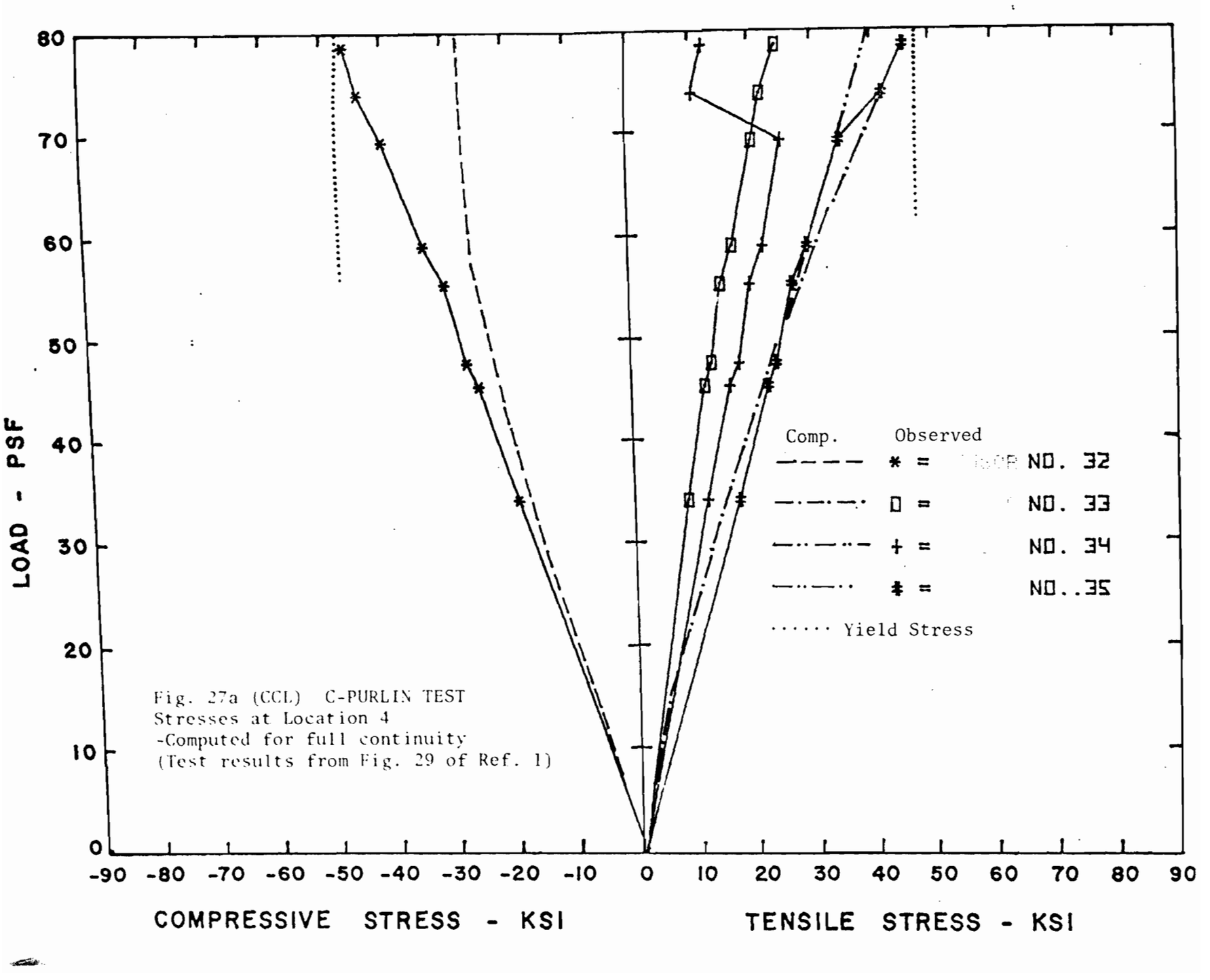

Fig. 27a (CCL) C-PURLIN TEST
Stresses at Location 4
-Computed for full continuity
(Test results from Fig. 29 of Ref. 1)

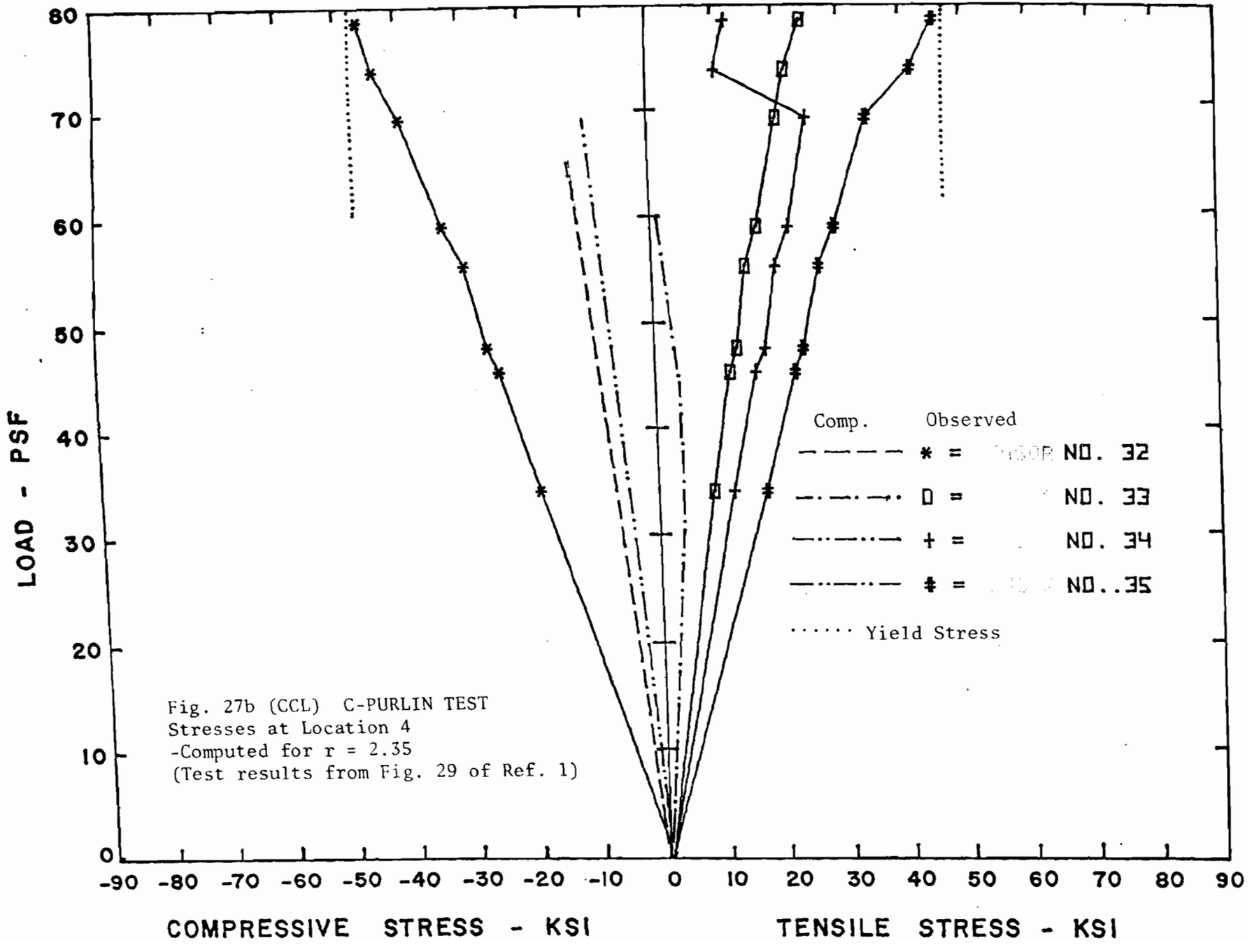

Fig. 27b (CCL) C-PURLIN TEST
Stresses at Location 4
-Computed for r = 2.35
(Test results from Fig. 29 of Ref. 1)